TRANSPORTATION RESEARCH RECORD 594

Photogrammetry, Water Quality, Safety Appurtenances, and Shoulder Design

TRANSPORTATION RESEARCH BOARD

COMMISSION ON SOCIOTECHNICAL SYSTEMS
NATIONAL RESEARCH COUNCIL

NATIONAL ACADEMY OF SCIENCES
WASHINGTON, D.C. 1976

Transportation Research Record 594
Price $2.80
Edited for TRB by Marianne Cox Wilburn

subject areas
21 photogrammetry
22 highway design
23 highway drainage
24 roadside development
40 general maintenance
51 highway safety

Transportation Research Board publications are available by ordering directly from the board. They may also be obtained on a regular basis through organizational or individual supporting membership in the board; members or library subscribers are eligible for substantial discounts. For further information, write to the Transportation Research Board, National Academy of Sciences, 2101 Constitution Avenue, N.W., Washington, D.C. 20418.

Notice

The project that is the subject of this report was approved by the Governing Board of the National Research Council, whose members are drawn from the councils of the National Academy of Sciences, the National Academy of Engineering, and the Institute of Medicine. The members of the committee responsible for the report were chosen for their special competence and with regard for appropriate balance.

This report has been reviewed by a group other than the authors according to procedures approved by a Report Review Committee consisting of members of the National Academy of Sciences, the National Academy of Engineering, and the Institute of Medicine.

The views expressed in this report are those of the authors and do not necessarily reflect the view of the committee, the Transportation Research Board, the National Academy of Sciences, or the sponsors of the project.

Library of Congress Cataloging in Publication Data
National Research Council. Transportation Research Board.
Photogrammetry, water quality, safety appurtenances, and shoulder design.

(Transportation research record; 594)
1. Roads–Safety measures–Addresses, essays, lectures. 2. Roads–Shoulders–Addresses, essays, lectures. 3. Road drainage–Addresses, essays, lectures. 4. Aerial photography in road surveying–Addresses, essays, lectures. I. Title. II. Series.
TE7.H5 no. 594 [TE228] 380.5'08s [625.7] 76-30779
ISBN 0-309-02563-X

Sponsorship of the Papers in This Transportation Research Record

GROUP 2–DESIGN AND CONSTRUCTION OF TRANSPORTATION FACILITIES
W. B. Drake, Kentucky Department of Transportation, chairman

General Design Section
F. W. Thorstenson, Minnesota Department of Highways, chairman

Committee on Photogrammetry and Aerial Surveys
Olin D. Bockes, U.S. Department of Agriculture, chairman
William T. Pryor, Federal Highway Administration, secretary
R. L. Alston, William T. Baker, Fred B. Bales, Roger R. Chamard, Jack E. Eades, Jesse E. Fant, L. O. Herd, Tommie F. Howell, Fred P. Jeter, George P. Katibah, Malcolm H. MacLeod, Charles E. McNoldy, Grover W. Parrott, William T. Pryor, Harold T. Rib, Vernon H. Schultz, James I. Taylor, A. Keith Turner, Robert J. Warren, James I. Webster, Donald E. Wilbur, Marshall S. Wright, Jr.

Committee on Hydrology, Hydraulics, and Water Quality
Samuel V. Fox, Texas State Department of Highways and Public Transportation, chairman
Frank L. Johnson, Federal Highway Administration, secretary
Charles J. Allen, John J. Bailey, Jr., Harry H. Barnes, Jr., Lawrence D. Bruesch, Darwin L. Christensen, Earl C. Cochran, Jr., Allen L. Cox, Richey S. Dickson, John Joseph Duffy, Kenneth S. Eff, Gene R. Fiala, Philip F. Frandina, John L. Grace, Jr., Lester A. Herr, J. Sterling Jones, Neil J. McMillen, William O. Ree, Brian M. Reich, August R. Robinson, John E. Sandahl, William P. Somers, A. Mainard Wacker

Committee on Safety Appurtenances
Eric F. Nordlin, California Department of Transportation, chairman
Gordon A. Alison, Dennis W. Babin, William E. Behm, W. C. Burnett, Duane F. Dunlap, Malcolm D. Graham, Wayne Henneberger, Jack E. Leisch, Edwin C. Lokken, Bruce F. McCollom, Jarvis D. Michie, Roy J. Mohler, Roger J. Murray, Robert M. Olson, William L. Raymond, Jr., Edmund R. Ricker, Neilon J. Rowan, F. G. Schlosser, Richard A. Strizki, Flory J. Tamanini, James A. Thompson, John G. Viner, Charles Y. Warner, M. A. Warnes, Earl C. Williams, Jr.

Committee on Shoulder Design
John F. Nixon, Texas State Department of Highways and Public Transportation, chairman
W. E. Baumann, P. B. Coldiron, A. C. Estep, Wade L. Gramling, Roger L. Hatton, R. G. Hicks, Robert N. Hunter, John W. Hutchinson, Theodore Koch, Edwin C. Lokken, D. W. Loutzenheiser, Richard A. McComb, Lloyd S. McKenzie, W. Grigg Mullen, Leon M. Noel, Josette M. Portigo, James A. Scherocman, F. W. Thorstenson, John S. Urban, Graeme D. Weaver, W. A. Wilson, Jr.

Lawrence F. Spaine, Transportation Research Board staff

Sponsorship is indicated by a footnote on the first page of each report. The organizational units and the officers and members are as of December 31, 1975.

Contents

OBLIQUE AIRPHOTOS FOR MAPPING, EDUCATING USERS, AND ENHANCING PUBLIC PARTICIPATION IN ENVIRONMENTAL PLANNING
Harry W. Smedes, A. Keith Turner, and John C. Reed, Jr. 1

REMOTE SENSING OF ATMOSPHERIC POLLUTANTS TO ASSESS ENVIRONMENTAL IMPACT OF HIGHWAY PROJECTS (Abridgment)
John H. Davies 6

SEDIMENT TRAPPING EFFICIENCY OF STRAW AND HAY BALE BARRIERS AND GABIONS
David J. Poché and W. Cullen Sherwood 10

IMPACT PERFORMANCE OF THE MINNESOTA 1.5-m-RADIUS PLATE BEAM GUARDRAIL (Abridgment)
Eugene Buth, Joe W. Button, and Paul J. Diethelm 15

CONCRETE SAFETY SHAPE RESEARCH (Abridgment)
Maurice E. Bronstad and C. E. Kimball, Jr. 17

CRASH TEST AND EVALUATION OF A PRECAST CONCRETE MEDIAN BARRIER
T. J. Hirsch, E. L. Marquis, John F. Nixon, and David Hustace 21

IMPACT DESIGN OF CRASH CUSHIONS FOR NONSTATIONARY BARRIERS (Abridgment)
F. W. Jung and A. M. Billing 26

FULL-SCALE TESTS OF A MODIFIED COLLAPSING-RING BRIDGE RAIL SYSTEM (Abridgment)
C. E. Kimball, M. E. Bronstad, J. D. Michie, J. A. Wentworth, and J. G. Viner 27

TEST EVALUATION OF TUBULAR THRIE BEAM FOR UPGRADING CONCRETE BRIDGE RAILING (Abridgment)
C. E. Kimball, E. O. Wiles, and J. D. Michie 32

DYNAMIC TESTS OF BREAKAWAY LIGHTING STANDARDS BY USING SMALL AUTOMOBILES (Abridgment)
R. F. Prodoehl, J. P. Dusel, Jr., and J. R. Stoker 36

SIMPLIFIED ANALYSIS OF CHANGE IN VEHICLE MOMENTUM DURING IMPACT WITH A BREAKAWAY SUPPORT
Raymond P. Owings and Clarence Cantor 39

LABORATORY ACCEPTANCE TESTING OF BREAKAWAY SUPPORTS FOR SIGNS AND LUMINAIRES (Abridgment)
Raymond P. Owings, Clarence Cantor, and James W. Adair 45

DESIGN PRACTICES FOR PAVED SHOULDERS
R. G. Hicks, Richard D. Barksdale, and Donald K. Emery 48

STATE-OF-THE-ART REVIEW OF PAVED SHOULDERS
Josette M. Portigo 57

Oblique Airphotos for Mapping, Educating Users, and Enhancing Public Participation in Environmental Planning

Harry W. Smedes, U.S. Geological Survey, Denver, Colorado
A. Keith Turner, Colorado School of Mines, Golden
John C. Reed, Jr., U.S. Geological Survey, Reston, Virginia

Low-altitude oblique color airphotographs were used in a case study of land use planning in Jefferson County, Colorado. Because these photographs help bridge the gap from the real world to maps, they readily enabled the authors to communicate information traditionally available only in map format to the general public, county planners, and a citizens' open space advisory committee. The photographs helped educate citizens in the county about current land use conditions and trends and the degree and rate of land use changes. They documented the impact of urban sprawl and the demands on the land made by competing activities such as resource extraction and housing development. The photographs were used in studies that included siting of open space, landfills, septic tanks, and housing developments; making excavation easier; extracting resources; selecting corridors; and determining optimum sequential patterns of development. In these studies, the photographs helped explain the meaning of technical terms, illustrated the difference and significance of various classes of land use and land cover, and aided in compiling maps and in teaching users how to interpret the maps and establish criteria and guidelines that define suitable lands for different uses. These photographs provide graphic documentation of environmental conditions at specific times and greatly facilitate the evaluation of the impact of changes due to various land use activities and natural processes.

Low-altitude oblique color airphotographs have proved to be a highly effective communications medium for environmental planning. They provide a familiar but more encompassing view of our environment, similar to views from a mountain ridge or a tall building. This similarity allows most people to readily grasp what is portrayed by these photograph.

Traditionally, maps are relied on heavily in attempts to communicate data to intended users. Most people who use maps in their professions take maps for granted because they readily understand them. Some now realize, though, that important classes of users, including many politicians, other decision makers, and much of the general public, do not understand maps. Yet, recent legislation, such as the National Environmental Policy Act of 1969, requires the public to participate in a decision-making process that should be based in large part on maps. To transfer information from the scientists and engineers to lay public users, one needs to portray conventional map data by alternate means. Vertical airphotographs have been used for this purpose. Our experience indicates that the average person finds the conventional vertical airphotograph to be nearly as difficult to understand as a map. For a product to be used by the decision maker and other users, it must be understood by them. Otherwise, it has no credibility. Therefore, in this study we taught map reading to users by letting oblique color airphotographs serve as an intermediate and familiar link to relate the conditions on the ground to the way these features are shown on a map in generalized or abstract form.

Lay people have difficulty in relating to maps because they lack an understanding of the complex and subtle reasoning used by the mapmaker in grouping certain assemblages of terrain conditions as a single map class. Maps use a uniform color, patterns, or symbol to define what appears to be a heterogeneous terrain unit. The real world does not appear so simple and as neatly subdivided as it is portrayed on maps. By means of oblique airphotographs, we can illustrate the kinds of complex assemblages that are mapped as a unit and explain the rationale of why we drew the boundary locations. We can point to places on a low-altitude oblique color airphotograph to show what the green color on the map represents. The impression that a uniform green color on the map is akin to a well-kept golf green gives way to an understanding that it connotes instead an assemblage of residual soil interrupted by outcrops of bedrock and covered by scattered stands of brush and grass (for example, the dissected hills in the middle ground of Figure 1). The map then begins to change from something abstract into something that has meaning to nontechnical people. Lines and points on it are understood as describing specific conditions as well as location.

In addition to being a useful and effective means of illustrating and clarifying the information contained in maps, the oblique color airphotographs can provide an inexpensive documentation of environmental conditions at specific times. Any good-quality 35-mm camera hand held in a light aircraft can do the job well. Photographs taken several seconds apart, centered on the

Publication of this paper sponsored by Committee on Photogrammetry and Aerial Surveys.

same object, provide excellent stereoscopic views, which add more depth, realism, and information when viewed with a stereoscope (13). Any of these photographs may be used later to evaluate and document the consequences of land use changes. For best results, the photographs should be taken through an open window or door of the airplane rather than through the Plexiglas of the window. In addition, the film speed should be considered as about 1½ times normal. For example, if the film speed listed by the manufacturer is 64, the light meter should be set for a film speed (revised) of about 100 to prevent overexposure.

Our experience over the past 3 years in Jefferson County, Colorado, serves as a case study. During this period, oblique color airphotographs were effectively used in a sequence of tasks that included (a) educating the voters about the need for legislation for open space, (b) educating lay persons on advisory boards and in civic groups about the means of implementing the legislation, (c) compiling maps, (d) explaining the maps to the users, and (e) documenting both objective and subjective features of the terrain. The oblique airphotographs were especially useful in mapping vegetation assemblages because they permitted us to interpret the understory or substratum by allowing us to see beneath the canopy of evergreens in the mountains and uplands.

JEFFERSON COUNTY CASE STUDY

The Need

Initially the need was to educate the voters about the problem of accelerating depletion of open space lands in Jefferson County (11). In 1972, concerned citizens formed an action group called PLAN Jeffco to determine the best way to get an official open space program, with sufficient funds to acquire and maintain land suitable for preserving as open space. This group decided to attempt to have an additional sales tax enacted as the source of funds, even though this traditionally is the most difficult kind of legislation to get voters to agree to. A detailed account of how this citizen group was formed and how it operated and succeeded in getting open space legislation passed for the entire county is given by Ward (14).

A resolution calling for planning for, developing necessary access to, acquiring, maintaining, administering, and preserving open space real property and developing paths and trails thereon was adopted by unanimous vote of the Board of County Commissioners of Jefferson County, Colorado, September 26, 1972. The resolution passed during the election of November 7, 1972.

Many individuals and civic groups rallied behind the PLAN Jeffco campaign to get the open space legislation passed. John C. Reed and Harry W. Smedes were among those who helped design the lecture program that served to alert the county voters about current land use conditions and trends that threatened the vital open space lands. Color slides were an integral part of the lectures; they included oblique airphotographs that provided enlightening views of the terrain. Repeated low-altitude color airphotographs powerfully illustrated changing land use. For example, a present-day oblique airphotograph (Figure 2), which closely duplicates the camera position and angle of an airphoto taken 38 years earlier (Figure 3), demonstrates the degree and rate of land use changes and effectively documents the impact of urban sprawl on the land. Such photographic comparison has sparked much interest by the lay public.

Oblique airphotographs were used to explain the significance of technical terms and to illustrate specific problems such as development in uniquely scenic areas (Figure 4) or in potentially hazardous areas (Figure 5). No maps were used at this stage.

In Figure 4, the following codes are used:

Code	Term	Code	Term
hr	Hogback ridges	mf	Mountain front
hv	Hogback valleys	mu	Mountains and uplands
tl	Tablelands		

Approximately 200 hm^2 (500 acres) of the area shown in Figure 4 were purchased on November 3, 1975, by the Colorado State Parks and Recreation Board to be set aside as the state's sixth park. This purchase provides one more link on the Colorado Trail, which leads from metropolitan Denver into the Pike National Forest. The area shown in Figure 5 is one of rapidly expanding housing development on landslide-prone deposits and slopes.

Implementation of Open Space Act of 1972

The open space legislation passed by a wide margin in the county election of November 1972. Key items included were (a) 0.5 percent increase in sales tax to be used to acquire suitable lands for open space and (b) formation of a citizens' open space advisory committee of 10 persons to advise the 3 county commissioners on what constituted suitable lands. Thus the immediate goal was to educate the advisory committee and, through them, the commissioners, on the rationale needed to objectively define "suitable." The first step in this education was to compile maps, teach the users how to interpret the maps, and assist them in establishing criteria and formulating logical and objective guidelines or strategies that define suitable lands for open space.

Continuing their initiative and involvement, private citizens with a wide variety of backgrounds and technical expertise made several maps that portrayed attributes important for any strategy of selecting land for open space. Because environmental impact studies involve a consideration of the consequences of a change in land use, a map showing current land use was of prime importance. Such a map did not exist for the county but was prepared by two of the authors (Reed and Smedes) from National Aeronautics and Space Administration high-altitude color photographs in about 1 man-week.

Oblique color airphotographs were used in public hearings, symposia, and meetings of smaller groups to illustrate the differences and significance of the various classes of current land use and land cover. Without a comprehension of this single land use map, citizens would not have been able to go on to more complex concepts, such as cartographic overlay of two or more maps and the use of maps portraying rock, soil, vegetation, and the like, to arrive at concepts of land capability, which is quite a different concept than current land use.

At public meetings we presented our ideas concerning the data that would be useful and that also existed or could be compiled readily on the basis of objective criteria. We also suggested and demonstrated—through manual techniques at first and later by computer—a rationale for putting together strategies for selection of optimum land for open space. Throughout all this, effective use was made of oblique color airphotographs as an aid in assisting lay persons to bridge the gap from real-world conditions to maps. The advisory committee responded enthusiastically to these ideas and began to assume leadership in making decisions about data and strategies or guidelines.

User Groups

Clearly, the immediate user was the advisory committee, a group of 10 citizens representing a cross section of the public. The county commissioners to whom the advisory committee made recommendations composed a second user group, and the citizens of the county formed a third. Through a series of regional meetings, the advisory committee, the director of the open space program, and the Jefferson County Planning Department presented the program to the citizens of the county. These regional meetings served to educate the citizens about the open space program and to encourage citizens to give their views on open space priorities. Oblique color airphotographs again played an important role as an alternate for or supplement to maps in the transfer of technical information to the general public. As a result of the citizens' comments and recommendations, the criteria to be used for selecting open space were modified and expanded.

Because open space planning fits into and should be in harmony rather than in conflict with master planning, the Jefferson County Planning Department became a user group. Subsequently, the Jefferson County Planning Department adopted our approach for use in long-range planning and master planning (6).

Approach

There is an urgent need to devise a system of combining and manipulating new and existing data, to reformat the data into products that are understandable, and to educate the public and decision makers by aids such as oblique airphotographs.

There are many competitive demands on the land. Our approach is that no one demand should be considered out of the context of all the others (7). Land use planning (including open space selection), land management, and evaluations of the environmental impact of specific changes in land use require a consideration of the total environment. Wise management will ensure proper balance of these competitive demands and will reduce the likelihood of thoughtless foreclosures of fundamental options. This requires map, point, and tabular data of such varied attributes as types of land cover and terrain; surface and subsurface natural physical features such as slope, landform, type of rock, thickness and nature of surficial deposits, surface and subsurface hydrology, vegetation, soils, wildlife habitat, and rangeland quality; ecology; socioeconomic features such as income, ethnic concentrations, and available labor skills; and locations of key facilities.

It is true that we need to accelerate the acquisition of pertinent data. However, many of the data that already exist are not being used because they are peer-oriented rather than user-oriented. In this study a means was developed for combining and analyzing the diverse types of environmental data in a common format by way of a cellular composite computer mapping system. The approach was to select those data that already existed or that were inexpensive and easy to acquire, and that would eliminate the maximum amount of county land that really was not suitable for open space. This meant that the places selected had a high statistical likelihood of meeting all the criteria. After having reached a level of understanding of individual maps, the users were then shown how two or three maps could be cartographically overlaid to portray those places where optimum features on the several maps coincided. These places were of higher rating than others. The oblique airphotographs served as an aid in this step also. At this time, it became clear to us, and to the users, that cartographic overlays were largely subjective and that, if more than four or five maps were overlaid, the result was a hopeless scramble of lines and colors. Objective, manually prepared overlays were time consuming and costly. This awareness prepared the way for objective weighting and overlaying by computer, as described by Smedes and others (7).

The next step in selecting optimum sites was to use data that were more difficult and expensive to acquire. Although those were more costly per hectometer^2, far less area was being considered. Hence this was a cost-effective approach to problem solving. The lay person group now had a good understanding of maps, composites of maps, and formulation of rational objective criteria or strategies for selection of open space tracts.

The next stage was to demonstrate how the computer could accomplish the same steps faster and more accurately. Without having systematically built up to this level of understanding through numerous short briefings supported by color oblique airphotographs, the group could not have envisaged how the computer could accomplish the job of weighting and overlaying numerous maps according to specified strategies and alternatives.

After computer-selected sites were printed, the oblique color airphotographs were helpful documentations of what the preliminary selected sites really looked like. Some attributes that were not covered by any of the basic maps could be detected and were portrayed by these photographs. In addition, subjective features such as scenic beauty could be evaluated and used in further eliminations to finally zero in on the most desirable, available tracts. For example, a unique combination of features produced the striking landscape shown in Figure 4. This can be readily compared with other areas such as the undeveloped area of Figure 1 and part of Figure 5.

Although other computer mapping experiments have been made (1, 2, 3, 4, 5, 10, 12), some considered only physical features and others considered only social or economic conditions. This Jefferson County study is the only one that we know of in which (a) both the natural and socioeconomic conditions (the total environment) were considered, (b) users were actively involved in the design and conduct of the study, (c) users were taught how maps are made and interpreted and how planning strategies can be objectively formulated, (d) users made the decisions involving attributes (maps) and weights (priorities), and (e) users adopted the complete system and concept as an ongoing operational procedure, including periodic taking of oblique color photographs from aircraft.

Although we started by addressing only the open space problem, we were able at the last moment to expand the study to include commonly occurring land use problems such as selecting optimum sites for sanitary landfill, septic tanks, and housing developments; making excavation easier; selecting corridors; and determining optimum sequential patterns of development of the land. Starting with 20 maps of basic data (8, 9), we created an additional 23 derivative maps from them.

For a test of corridor selection, the county planners requested a map showing places suitable for hiking trails according to priorities they selected (9). Oblique airphotographs will aid in the final selection among the alternatives.

There are two other corridor applications. First, a proposed Interstate highway (I-470) will pass near the lakes shown in Figure 6. This photograph provides useful information on natural features (the lakes and associated ecosystems) and aesthetically pleasing areas that should be preserved or on which there should be

Figure 1. Northeastward look of Lakewood, Colorado, showing complexity of natural terrain surface features, 1974.

Figure 2. West-southwestward look at part of Lakewood, Colorado, 1972.

Figure 3. West-southwestward look at part of Lakewood, Colorado, 1934.

Figure 4. Southward look of Roxborough Park, 1972.

Figure 5. Westward look of Green Mountain, 1972.

Figure 6. Westward look of Soda Lakes, 1972.

Figure 7. Westward look toward the Front Range of the valley of Bear Creek, 1972.

minimum impact. In addition, the ridge immediately beyond the lakes forms a wind barrier that may be of consequence in subduing dispersal of air polluted by exhaust fumes. Second, a dam is currently being built across Bear Creek valley, shown in Figure 7, which is subject to flooding. Patterns of relocation can be visualized readily by maps accompanied by oblique airphotographs. Sand and gravel quarrying on top of the butte in the foreground (Mt. Carbon) is largely concealed from view at present. In planning the location of new roads required because of the dam and future reservoir, an attempt should be made to maintain this visual concealment at least until the deposit has been mined out and the hilltop reclaimed.

This expansion of the original open space study demonstrates how a bank of basic data can be weighted and combined in different ways to solve a wide variety of land use problems.

Cost

The cost of acquiring about 100 low-altitude oblique color airphotographs was $59. This included $35 for charter of airplane and pilot plus $24 for the purchase and processing of 3 rolls of 35-mm color slide film.

CONCLUSIONS

As far as we know, the Jefferson County study is the only one in which the users actively participated and made the decisions on appropriate attributes and weights. Furthermore, the users were a group of citizens with no training in planning, map reading, or formulating of decision strategies. An important aspect of this study—perhaps the most important—was to instill in these users an understanding of the complex techniques and concepts employed in the study. To judge from the results, this was successful. Use of oblique color airphotographs played a key role in this endeavor. The following summarizes the planning steps for which the oblique airphotographs were used:

1. Environmental planning, which involved mapping, educating, and public participation in the problem (areas in which oblique airphotographs were helpful);
2. Recognizing what is needed;
3. Campaigning for open space legistation to let voters know what was happening to their county so that they would want to vote for additional tax;
4. Implementing legislation by aiding the advisory board in (a) defining and selecting suitable land, (b) understanding maps and overlays, (c) adopting guidelines or strategies, (d) selecting lands by visualizing results of weighting and overlaying many basic maps, first manually and then by computer, and (e) showing photographs of what selected sites look like and making final selection on a visual basis of scenic beauty and the like; and
5. Documenting display areas selected for environmental conditions at specific times and evaluating impact of changes due to various land use activities and natural processes.

ACKNOWLEDGMENTS

This paper is based on a cooperative project of the U.S. Geological Survey, Colorado School of Mines, Federation of Rocky Mountain States, and Jefferson County Open Space Program under the initiative and direction of the Resource and Land Investigations Program, U.S. Department of the Interior. The project is an outgrowth of informal activity by a number of technical specialists as part of a citizens' group, PLAN Jeffco (14).

REFERENCES

1. G. M. Clark and W. B. Ashton. Development of a Computer System for Spatial Analysis of Geographic Attributes (SAGA). Department of Industrial and Systems Engineering, Ohio State Univ., Technical Rept. 4, 1975.
2. Colorado Environmental Data Systems. College of Forestry and Natural Resources, Colorado State Univ., 1973, 435 pp.
3. K. H. Ferris and J. G. Fabos. The Utility of Computers in Landscape Planning. Massachusetts Agricultural Experiment Station, Univ., of Massachusetts, Amherst, Research Bulletin 617, 1974, 116 pp.
4. F. C. Hachman, C. Bigler, and R. Weaver. Report on the Implementation of Composite Computer Mapping. Bureau for Economic and Business Research, Univ. of Utah, Salt Lake City, 1971, 227 pp.
5. G. Nez. Capabilities of Computerizing Composite Mapping for Simulating Location Zones for Selected Economic Activities and Public Services. HRB, Highway Research Record 399, 1972, pp. 99-103.
6. G. Schalman and others. Jefferson County Mountain Area Research Project. Univ. of Colorado, Denver, and Jefferson County, Colorado, Planning Department, Sept. 1974, 5 Vols.
7. H. W. Smedes, G. Nez, L. Salmon, A. K. Turner, E. E. Lutzen, and J. C. Reed, Jr. Land-Use Planning Aided by Computer Cellular Modelling/Mapping System to Combine Remote Sensing, Natural Resources, Social and Economic Data. Proc., 9th International Symposium on Remote Sensing of Environment, Ann Arbor, Mich., Vol. 1, 1974, pp. 289-298.
8. H. W. Smedes and A. K. Turner. Environmental Map Atlas of the Northern Part of Jefferson County, Colorado. U.S. Geological Survey, Open-File Rept. 75-608, 1975.
9. H. W. Smedes and A. K. Turner. Cooperative Development of an Environmental Information System for Jefferson County, Colorado. International Symposium on Land Use, Phoenix, Arizona, Oct. 26 to 31, American Society of Photogrammetry, Falls Church, Va., 1975.
10. S. E. Tilmann, S. B. Upchurch, and G. Ryder. Land Use Site Reconnaissance by Computer-Assisted Derivative Mapping. Bulletin of Geological Society of America, Vol. 86, 1975, pp. 23-34.
11. A. K. Turner and H. W. Smedes. Environment, Computers, and Planning—The Jefferson County Experience. Mines, April 1974.
12. Illinois Resources Information System (IRIS)—Feasibility Study, Final Report. Center for Advanced Computation, Univ. of Illinois, Urbana, 1972, 204 pp.
13. T. H. Walsh and W. B. Hall. Pocket Guide for Making Color Oblique Stereo Aerial (COSA) Photographs With 35 mm Cameras. Idaho Bureau of Mines and Geology, Dec. 1975, 10 pp.
14. V. J. Ward. Open Space Lands—Vote Yes. PLAN Jeffco, Jefferson County Citizens for Planned Growth With Open Space, Golden, Colorado, 1974, 84 pp.

Abridgment

Remote Sensing of Atmospheric Pollutants to Assess Environmental Impact of Highway Projects

John H. Davies, Research and Development Division, Barringer Research Limited, Toronto, Ontario

Remote sensing techniques provide a powerful and effective tool for monitoring atmospheric pollutants to assess their environmental impact. Because of the mounting concern for the health hazards involved in living close to highways, environmental studies have become an increasingly important aspect in highway planning.

Conventional pollution monitoring devices use point sampling techniques to sense the presence of pollutants in ambient air. This method is costly because of the large number of units required, and it does not provide the continuum of data that can be obtained by remote sensing of an area from an airplane or from a moving vehicle. Remote measurements can include not only the nature and concentrations of the pollutant gases, but also the mass flow and mass transport of pollutants from one area to the next.

The majority of gaseous pollutants exhibit characteristic absorption bands in the ultraviolet, visible, or infrared regions of the spectrum. Radiation passing through an atmosphere containing these gases will have the characteristic absorption fingerprint of these vapors superimposed on it. Analysis of this radiation allows identification and concentration path length product measurements to be made of environmental pollutants associated with industrial activity, urban developments, and transportation. Both dispersive and nondispersive correlation sensors can be used for these measurements.

CORRELATION SPECTROSCOPY

A simple technique to measure gas correlation compares the absorption obtained at one wavelength corresponding to a strong absorption band in the gas with an absorption at an adjacent wavelength where the gas does not absorb. Although absorption bands are unique, interference problems occur from other gases present whose absorption bands overlap in one of the chosen spectral areas of measurement. This interference can be effectively resolved by correlating a substantial portion of the absorption spectrum of a gas being measured against a stored replica or mask of the spectrum. This technique has been named correlation spectroscopy and the method and applications are summarized in several publications (1, 2, 3).

COSPEC

In the Barringer Cospec group of instruments, the stored masks are a series of exit slits concentrically inscribed on a circular disk rotating in the exit plane of a conventional folded Ebert spectrometer. The mask line positions match the peak and trough absorption bands of sulfur dioxide (SO_2) and nitrogen dioxide (NO_2); the spectrum is shown in Figure 1. The rotational position of the masks is monitored by logic diodes, and a photomultiplier (PM) tube is used for signal detection. Calibration references are provided by positioning internal calibration cells containing sealed known amounts of SO_2 gas in front of the PM tubes. This single gas instrument is known as the Cospec IV. The Cospec IV provides increased sensitivity for single gas monitoring by fully using a single grating for one gas without any time shared multiplexing. For dual gas operation, a Cospec II instrument has been developed in which half the grating is used for SO_2, the other half is used for NO_2, and the rotating disk is divided into two halves—one for each gas. This instrument has enjoyed worldwide use for high-sensitivity measurements of SO_2 and, more recently, NO_2. Figure 2 shows an overview of the Cospec optical layout.

Cospec has been frequently used to remotely sense the total vertical burden of pollution, that is, the amount of gas in a column above a unit area of ground, usually expressed in milligrams of gas per meter^2. Mobile vertical burdens can be measured by using ground mobile and low-flying airborne platforms looking vertically upward where Rayleigh backscattered daylight from the overhead hemisphere is used. Mobile vertical burdens can also be measured from an airborne, vertical, downward-looking mode where sunlight reflected upward from the earth is used. A third application is the airborne closed path mode where the Cospec views horizontally along an optical path beamed around the aircraft

Publication of this paper sponsored by Committee on Photogrammetry and Aerial Surveys.

from an active light source. Optical paths of 20 to 30 m can be practically achieved by employing wing-tip and tail-stabilizer retroreflectors. Of these platforms, the ground mobile method is most widely used. Mass transportation of a pollutant can be estimated from the vertical burden measurements along a traverse line. When this is coupled with wind velocity and direction information, the mass of gas transported across the traverse line can be estimated in terms of mass per linear distance of traverse line. This concept can be used on both large and small scales and clearly provides a picture of the resulting diffusion of pollutants from smoke plumes, an entire industrial complex, or highway. Figure 3 shows the current single-gas Cospec IV high-sensitivity SO_2 instrument.

Figure 1. SO_2 absorbance versus wavelength.

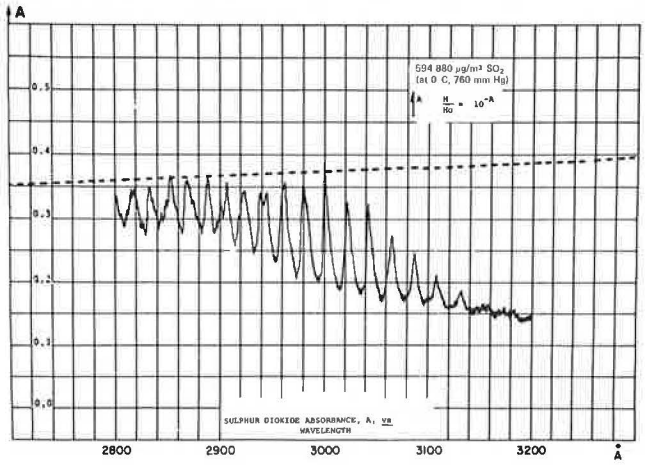

Figure 2. Cospec optical layout.

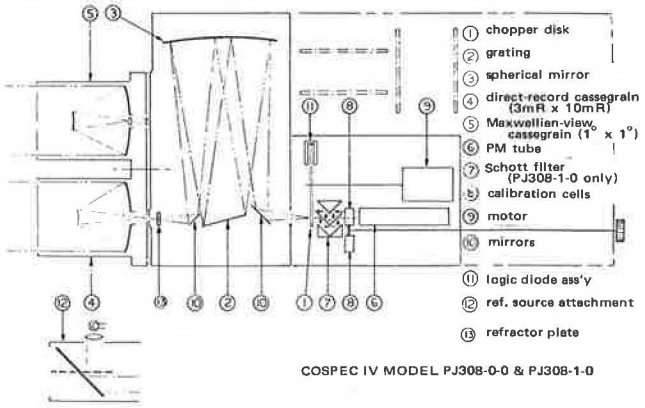

Figure 3. Cospec IV high-sensitivity SO_2 layout.

GASPEC

The Barringer Gaspec, or gas filter correlation spectrometer, operates by employing the differential measurement of characteristic absorption of the gas of interest by using the gas itself as a very selective filter as shown in Figure 4. A pair of gas cells are employed. A reference cell contains a spectrally inactive gas, and the filter gas cell contains the target gas to be sensed in a quantity such that the optical depth of the gas is optimized for a maximum product of the modulation of target gas energy and high average transmission. Incoming radiation characteristic of the target gas is selectively filtered by being absorbed in the sample cell but is readily transmitted through the reference cell. Thus

Figure 4. Gaspec optical layout.

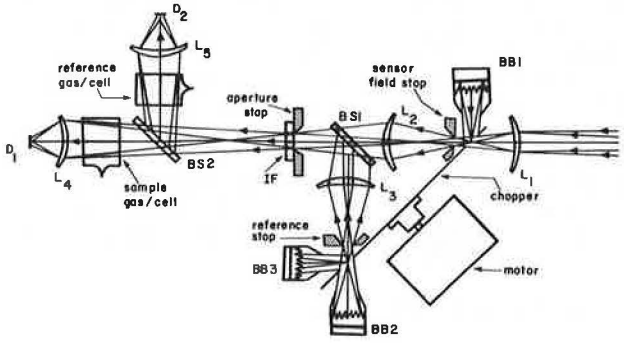

Figure 5. Method of operation of Gaspec system.

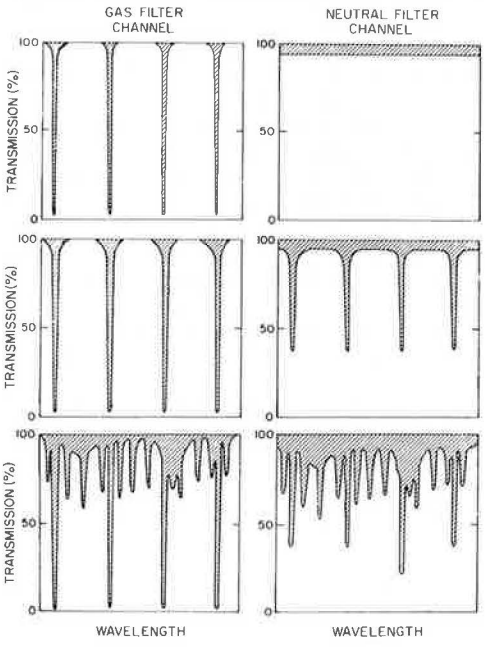

the transmitted radiance through the sample cell is largely independent of the target gas signatures, and the transmitted radiance of the reference cell is strongly dependent on the presence of target gas. The differential spectral transmittance between the cells provides a sensitive indicator for the amount of target gas present in the incoming radiation.

The principle of operation of this system is best described by the consideration of two channels as shown in Figure 5. In one, the absorption line spectrum of the target gas is present with almost zero transmission occuring at these band positions while the other channel contains a neutral filter adjusted to yield the same total absorption as in the first channel. Thus, as the detection system alternates between the two channels, it sees constant intensity. When matching spectral lines characteristic of the target gas appear in the incident radiation, the transmission in the first channel will not change appreciably because it is already at almost full absorption; however, a decreased intensity is transmitted through the second channel and the detection system now sees unequal intensities appearing at the channel switching frequency. If an interfering gas is also present, the transmitted light will be reduced equally in both channels, and, because the alternating signal is not changed, the interfering gas will be observed by the instrument.

To overcome the problems of spatial responsiveness difference at the detector that is produced by chopper changes and to avoid scene radiance changes as the sensor footprint moves, a two-detector system was developed. The detectors receive amplitude-shared source signals at the source chopping frequency. Another feature of the Gaspec design is a further adjustable reference blackbody that may be adjusted to have comparable radiance to the source and thereby facilitate electronic signal processing by minimizing the chopped radiance. Gaspec is further described elsewhere (4, 5). The most recently built Gaspec is now capable of sensing two different gases simultaneously.

METHODOLOGY AND MODELS

The application of these remote sensing instruments to highway and transportation environmental problems and studies is now possible. Pioneering work in these applications has already taken place, and further developments are envisaged.

One initial application is to the validation and verification of mathematical computer models of local and regional pollution and air-shed movements. There are of course in the generalized area of environmental input studies two major sources, fixed and mobile. Essentially the moving automotive sources provide the carbon monoxide (CO) oxidents, oxides of nitrogen, and hydrocarbon pollutants. The fixed sources, such as industrial plants, petrochemical complexes, and power stations, chiefly provide particulates, oxides of sulfur, and oxides of nitrogen. Selection of the appropriate mathematical model then depends on short- and long-term reaction rates and time-distance domain requirements.

For modeling transportation sources in urban areas, almost all CO is emitted from mobile sources. Thus, in Washington, D.C., 98 percent of all CO emissions are from transportation sources. Several types of models are possible, including synoptic, climatological, and grid-point models.

1. The synoptic model computes hourly concentrations as a function of time for operational applications.
2. The climatological model computes the frequency distribution of concentrations for statistical predictions of specified high concentrations for planning needs.
3. The grid-point model computes concentrations at different locations in a geographical grid for horizontal isopleth patterns for both operational and planning needs. Such a model assumes all emissions to be at ground level because they are from transportation sources.

In considering the running of a grid-point model, emission data are inputted from (a) emissions from vehicles traveling the major thoroughfares, streets, and freeways and (b) secondary background emissions from vehicles on less densely traveled local and feeder streets and roads. This model also requires essential traffic data such as

1. Coordinates of ground-level ambient receptors;
2. Gasoline consumption rates;
3. Vehicle speeds for the various types of roads;
4. Daily traffic fraction within each 24-h period by type of road and day of week for workdays versus weekends;
5. Day and hour to be modeled;
6. Associated projected air temperature and air pressure for the day and hour;
7. Associated hourly surface data such as type of cloud cover, temperature, wind speed, and direction.

A similar methodology allows the development of a fixed-source SO_2 model by using point and area source inputs such as geographical location of source, stack height, stack diameter, stack gas exit velocity and temperature, and source emission rate. The SO_2 model also requires, in addition to the above point and source inputs, the following:

1. Mean morning and afternoon mixing height;
2. SO_2 decay constant;
3. Day and hour to be modeled;
4. Meteorological inputs for wind field profiles for stable, neutral, or unstable atmospheres;
5. Background level concentrations;
6. Surface data for ceiling heights, sky conditions, air temperature, wind speed and direction, and the like;
7. Coordinates of ground-level ambient receptors.

CO MODEL

The models previously described have been run for assessing the CO emissions from transportable sources. For example, they have been used in Washington, D.C., where the basis for CO emission was a network of 737 road segments or links each assigned a daily traffic volume generated from historical, current, or projected data obtained from U.S. Department of Transportation sources. Growth factors have to be extrapolated into the model conditions. The CO model can generate the ground-level ambient CO for 625 chosen receptor points. From these projected readouts, projected isopleths can be plotted. Because the minimum detectable sensitivity for continuous CO ambient monitors is 0.565 mg/m^3 (0.5 ppm), this is the lower bound for the isopleths. However many assumptions are made with regard to the input data when such models are generated. Errors in assumption relate to both the pollution source data and the associated meteorology. The net result is a model prediction that needs validation. The remote sensing Gaspec and Cospec technology then becomes most valuable in the validation of these models. The Cospec-Gaspec technique takes total vertical burden measurements through the atmosphere and in effect sounds the isopleth. These rapid, mobile Cospec-Gaspec surveys enable a complete veri-

fication of the model to be undertaken and the model to be adjusted through iterative fine tuning.

REFERENCES

1. A. R. Barringer. Chemical Analysis by Remote Sensing. Paper presented at 23rd Annual Instrument Automation Conference, Instrument Society of America, Oct. 1968.
2. A. R. Barringer and J. H. Davies. Applications of Correlation Interferometry and Spectroscopy to Aerospace Monitoring of Earth Resources and Pollution. Paper presented at 7th International Aerospace Instrumentation Symposium, Cranfield, U.K., March 1972.
3. A. R. Barringer, J. H. Davies, and A. J. Moffatt. The Problems and Potential in Monitoring Pollution From Satellites. American Institute of Aeronautics and Astronautics, New York, Paper 70-305, March 1970.
4. J. H. Davies, T. V. Ward, and H. H. Zwick. Latest Developments With an Airborne Gas Filter Correlation Spectrometer. Canadian Journal of Remote Sensing, Nov. 1975.
5. T. V. Ward and H. H. Zwick. Gas Cell Correlation Spectrometer—Gaspec. Applied Optics, Vol. 14, No. 12, Dec. 1975.

Sediment Trapping Efficiency of Straw and Hay Bale Barriers and Gabions

David J. Poché, Virginia Highway and Transportation Research Council
W. Cullen Sherwood, Virginia Highway and Transportation Research Council and Madison College

Laboratory and field investigations were undertaken to determine the sediment-trapping efficiency of straw and hay bale filter barriers and gabions. A flume was designed and built for the laboratory portion of the study and 21 bales were tested. Trapping efficiencies varied from 46 to 88 percent; the overall average was 68 percent. No significant differences were noted in the efficiencies of straw and hay, and the bulk density and porosity of the bales correlated poorly with the trapping efficiencies. Field observations of contractor-placed bale barriers showed a high percentage of failures. Most failures were due to undercutting, end flow, and washouts. Experimental field barriers with numbers and positions based on the universal soil loss equation were installed in place of the unmodified barriers. To minimize barrier failures, loose straw was wedged under and between the bales making up the barrier, the barrier length was extended so that the bottoms of the end bales were higher than the top of the lowest middle bale, and loose straw was scattered behind each barrier. Trapping efficiencies approximating laboratory efficiencies were obtained with the experimental barriers. Gabions filled with crushed stone yielded significantly lower trapping efficiencies than straw and hay bales yielded. However, a layer of straw in the bottom of the gabion increased the efficiency to levels comparable to those of straw bales.

Because of the possible degradation of water quality in streams from sediment and the resulting adverse effects on downstream ecology, the Virginia Department of Highways and Transportation has placed a high priority on improving erosion and sedimentation controls on highway construction sites. The purpose of these controls is to provide an effective temporary means of controlling construction-generated sediment before the establishment of a permanent vegetative cover.

In Virginia, the ultimate aim of the control program is good vegetative cover, and the program includes provisions for early, staged, and temporary seeding aimed at establishing a strong stand of vegetation as early as possible in the construction cycle. Even with this maximum effort at vegetation establishment, experience has shown that significant numbers of temporary erosion and sediment control measures are required particularly during early construction activity (1). Temporary measures include various types of barriers and retention structures designed to filter and impede the flow of runoff waters. Although a number of measures have been found to be valuable, the single most commonly used measure is the straw or hay bale filter barrier (usually referred to indiscriminately as straw barrier). One can judge from visits to other agencies, field observations, and personal communications that these barriers appear to be widely used.

Despite the widespread use of straw barriers little appears to be known about their sediment-trapping efficiency. Field observations of trapped sediment and impeded storm water flow in Virginia and other states have indicated that these barriers can be effective. The level of effectiveness, however, seems to be unknown. A search of the literature turned up neither data on straw barrier trapping efficiency nor a rational method for determining the number of barriers or distribution. The purpose of this paper is to report on laboratory and field tests of the trapping efficiencies of straw and hay bale barriers. Included are discussions of common problems resulting from improper field placement and maintenance. A secondary purpose was to test stone and stone-and-straw-filled gabions in a similar manner.

The first priority in the study was to determine the level of efficiency that could be expected of bale barriers under ideal conditions. Also of interest were the relative efficiencies of straw and hay. Answers to these basic questions were pursued under controlled conditions in the laboratory.

METHOD

A test flume was designed so that sediment-laden water could be filtered through either one or two bales. The flume was constructed of 1.9-cm-thick (¾-in-thick) plywood and coated with a waterproof paint (Figure 1). For most of the comparative tests, only a single bale was used. The test followed a set procedure.

1. The bale was mounted securely in the flume and flushed several times with clear water.
2. A total of 250 liters (65 gal) of 10 000-ppm and 400 liters (104 gal) of 20 000-ppm water-soil mixtures

Publication of this paper sponsored by Committee on Hydrology, Hydraulics, and Water Quality.

were prepared and kept in suspension by mechanical agitation.

3. A 50-liter (13-gal) volume of 10 000-ppm water-soil mixture was poured rapidly into the flume, allowed to flow through the bale, and caught in a 114-liter (30-gal) container.

4. The effluent was mechanically agitated and a depth-integrated sample was withdrawn by using a DH48 hand sampler.

5. Steps 3 and 4 were repeated 5 times with the 10 000-ppm mixture.

6. Eight runs were then made with the 20 000-ppm mixture according to steps 3 and 4.

7. The 13 effluent samples were oven dried in preweighed evaporating dishes and weighed to the nearest 0.01 g.

8. The average parts per million of suspended sediment for each of the 13 samples was then computed and a grand average was calculated.

With these data, the trapping efficiency of each bale was computed from the formula

$$\text{Percent efficiency} = \frac{SS_{in} - SS_{out}}{SS_{in}} \times 100 \quad (1)$$

where SS = average suspended solids concentration.

Twenty-one bales were tested for trapping efficiency. At the same time, the porosity of each bale was determined by using measurements of bulk density (grams per centimeter^3 of the whole bale) and fiber density (grams per centimeter^3 determined by pycnometer). Porosity E of each bale was found from

$$E = 1 - \frac{\text{bulk density}}{\text{fiber density}} \quad (2)$$

Table 1 gives the bulk density, fiber density, porosity, and percentage of sediment trapping efficiency for all bales tested. As shown by the data given in Table 1, the single bale filtering efficiency ranged from 46 to 88 percent with an overall average value of 68 percent. Double thicknesses (2 bales) were found to be approximately two-thirds more efficient in filtering than single bales. A t-test showed that no significant difference in the relative filtering efficiency of straw and hay could be ascertained from the data. Porosity appears to have a low correlation with filtering efficiency. Thus any scheme to pretest the efficiency of bales by using porosity or bulk density would likely meet with little success.

Other potentially useful observations were made during the bale tests. First, a linear decrease in the portion of the bale wetted by the water and sediment mixture was noted as the mixture went through the bale. It appears that, as the lower portion of the bale becomes clogged with mud, flow corridors are found in the higher, cleaner portions of the bale. The suspended solids retention was found to be nearly constant with each succeeding test.

Second, bales prewet and allowed to stand for several days were observed to show marked improvement in trapping efficiencies. A prewet bale was first tested in the normal way. After several weeks, it was tested again and its efficiency had increased from 74 to 98 percent. Prewetting apparently swells the individual fibers and promotes growth of fungi within the bale (if the temperature is not too low), which significantly increases trapping efficiency.

Finally, suspended sediment was noted to be removed in two ways: (a) by the filtering action of the bale and (b) by the settling out of the coarsest particles in the pond area behind the bale. This dual mechanism of sediment removal is similar to that observed many times in the field.

FIELD OBSERVATIONS

The widespread use of straw bale filter barriers in Virginia allowed observations to be made on a large number of barriers placed under a variety of field conditions. Although some barriers were observed to be quite effective, a high percentage showed a significant degree of failure due to improper initial placement or improper maintenance.

Barrier failures were noted to be mainly of three types.

1. Undercutting, shown in Figure 2, is a placement problem. It is caused by improper bale-to-soil contact, which allows storm water to run under the bale. The resulting concentrated flow tends to cut a channel under the bale. The process of channelization mobilizes sediment in addition to that generated upstream from the bale. Elimination of undercutting can be accomplished by entrenching and backfilling the bales to a depth of 5 to 8 cm (2 to 3 in) before staking or by wedging loose straw from a broken bale under the bale after staking.

2. End flow, also shown in Figure 2, occurs when storm waters flow around the end of the barrier. As in the case of undercutting, end flow can result in a higher concentration of suspended sediment downstream from a barrier than that reaching the barrier from upstream. Elimination of end flow can best be ensured by extending the barrier where possible so that the bottoms of the end bales are higher than the top of the lowest center bale. This placement forces water to pond and flow over rather than around the lower bale or bales.

3. Washouts, a third common type of failure, occur when bales are moved by high-velocity storm waters. Movement may vary from a few centimeters to distances far downstream. In either case the integrity of the barrier is destroyed and its effectiveness impaired or eliminated. Washouts can be eliminated by careful staking and limiting the use of straw barriers to low-energy flow situations.

The data given in the following tabulation provide percentage figures for the efficiency of one series of contractor-placed straw barriers:

Flow Barrier	Efficiency	Flow Barrier	Efficiency
A	+56	E	+1
B	-35	F	+25
C	-83	Average	-7
D	-1		

Flow was from barrier F to barrier A in the ditch line. Barriers were 61 m (200 ft) apart and were constructed of wheat straw. Rainfall occurred on August 4, 1974. The trapping efficiency was determined by sampling storm water downstream and upstream from a barrier by using a large plastic syringe to obtain a depth-integrated sample and by computing the percentage of efficiency as in the laboratory tests. The presence of negative numbers indicates that in some cases suspended sediment was actually higher downstream from the bales than it was in storm water reaching the barrier from upstream. In every case, high downstream concentrations were correlated with one or more of the barrier failures previously listed. Field observations indicated the presence of a few barriers partially or wholly buried by sediment. Improper maintenance is clearly indicated in these cases.

Figure 1. Apparatus for testing the trapping efficiency of a bale.

Figure 2. Improperly constructed and maintained filter barrier.

Table 1. Summary of laboratory bale tests.

Type of Bale	Bulk Density (g/cm^3)	Fiber Density (g/cm^3)	Porosity	Efficiency (%)
Hay, orchard grass	0.087	1.43	0.838	78
	0.086	1.43	0.838	78
	0.127	1.30	0.902	56
	0.124	1.19	0.894	–
	0.153	1.35	0.887	66
	0.120	1.43	0.916	64
	0.183	1.16	0.842	64
Straw, barley	0.104	1.45	0.928	46
Straw, wheat	0.094	1.20	0.921	65
	0.104	1.31	0.921	65
	0.071	1.37	0.948	62
	0.087	1.47	0.941	62
Hay, fescue	0.111	1.45	0.923	56
	0.101	1.59	0.936	71
	0.103	1.35	0.942	74
Hay, timothy, orchard mixed	0.130	1.24	0.895	88
	0.137	1.33	0.897	–
	0.125	1.15	0.891	83
Straw, oats	0.078	1.07	0.927	76
	0.089	1.16	0.924	72
	0.079	1.12	0.929	–

Figure 3. Location of field tests.

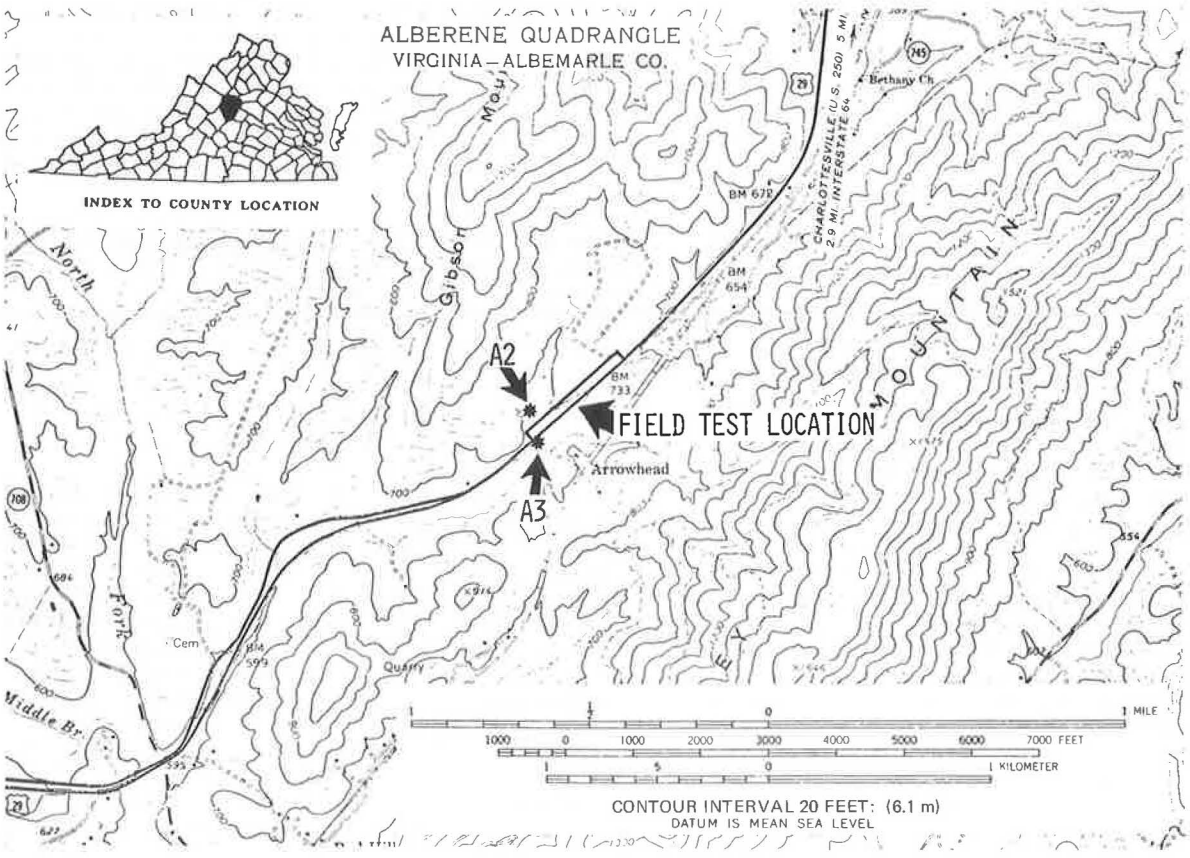

FIELD EXPERIMENTS

After observations were made of the relatively high efficiencies of straw bales in the flume experiments in the laboratory and the low efficiencies measured for straw barriers in the field, the question immediately arose, Could barriers be placed in the field that would match or nearly match the sediment-trapping efficiencies observed in the laboratory? To attempt to answer this question, we selected a test site on a project in central Virginia (Figure 3). Here, US-29 was undergoing conversion from a 2-lane to a 4-lane facility. The project proved to be ideal because it traversed moderately erosive Piedmont soils and was located close enough to the Virginia Highway and Transportation Research Council laboratories so that frequent and detailed observations of the field experiments were possible.

The efficiency measurements given in the tabulation on contractor-placed straw barriers were taken on a series of unmodified barriers placed on the project by the contractor. Figure 2 shows a barrier located on this project. Before the experimental barriers were placed, all of the old barriers were removed.

The number of experimental barriers to be placed per 30.5 m (100 ft) of roadway was determined by using a computer program developed by Poché and based on the soil loss equation (2). Each barrier was placed by using the criteria discussed in the section on field observations. That is, (a) straw was wedged under each bale after staking (subsequent field investigations in Virginia have indicated that a small amount of loose soil placed by shovel and lightly compacted along the upstream edge of a bale barrier eliminates undercutting and significantly aids barrier efficiency), and (b) the bottoms of the end bales were higher than the top of the lowest center bale. In addition, loose straw was scattered on the upstream side of each barrier to provide an increased filter travel length. Field observations indicate that subsequent movement of the loose straw tends to seal any undetected openings in the barrier. A typical experimental barrier is shown in Figure 4. The following tabulation gives percentage figures for trapping efficiency of barriers for storm events subsequent to placement of the experimental barriers:

	Efficiency	
Flow Barrier	Rainfall on Nov. 6, 1974	Rainfall on Dec. 1, 1974
A	67	-11
B	76	30
C	79	-5
D	98	46
E	35	37
F	64	50
G	34	19
H	28	-38
I	32	–
Average	57	16

Flow was from barrier I to barrier A in the ditch line. Barriers were 30.5 m (100 ft) apart and were constructed of wheat straw. The data from the storm of November 6 clearly indicate that the sediment-trapping efficiency of field barriers can approximate that obtained under laboratory conditions. Unfortunately, the average trapping efficiency for the storm of December 1 dropped significantly because of the failures of barriers A, C, and H. These failures vividly point out the need for constant surveillance and close attention to maintenance.

Figure 4. Experimental barriers in place.

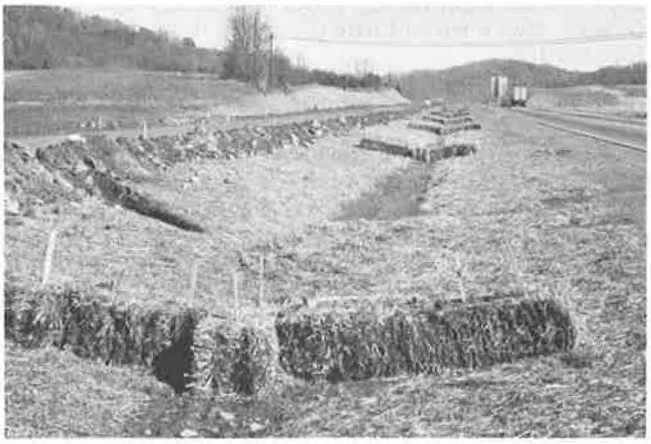

GABIONS

Four laboratory tests were performed by using bale-sized gabions filled with crushed stone and crushed stone and straw mixtures. Two sizes of crushed stone were used: a fine mix of stone approximately 0.9 to 1.9 cm (3/8 to 3/4 in) in diameter, and a coarse mix of stone 3.8 to 6.3 cm (1 1/2 to 2 1/2 in) in diameter. The results are given in the following tabulation:

Stone Size	Without Straw	With Straw
Fine mix	32	62
Coarse mix	29	58

The straw added to the stone was placed as a 2.5-cm (1-in) layer of compressed straw in the bottom of the gabion, and crushed stone was placed on top.

Based on these experiments, stone alone apparently will yield low trapping efficiencies even at relatively small sizes. However, the efficiency approximately doubled with the introduction of a bottom layer of straw and approached the efficiency of straw and hay bales. It should be noted that relatively low flows of simulated storm water were generated in the laboratory so that much of the filtering action involved the thin straw layer. Field flows would be expected to be greater during high-intensity storm events.

Field observations of stone-filled gabions indicate a high permeability and probably a low filter efficiency. However, use in or along live streams, where straw bales are discouraged, appears to be a beneficial one for stone-filled gabions. Placement downstream from in-stream construction retards stream velocity and bank erosion and traps streambed load that may be injurious to downstream benthic communities.

CONCLUSIONS

Laboratory and field investigations were undertaken to determine the sediment-trapping efficiency of straw and hay bale filter barriers and gabions. Based on a combination of laboratory and field experimental results and field observations, seven conclusions appear to be justified.

1. Laboratory tests of a series of straw and hay bales performed in a specially designed flume yielded sediment-trapping efficiencies ranging from 46 to 88 percent and averaged 68 percent.
2. Use of the t-test showed no significant differences in trapping efficiencies between straw and hay bales.

3. A bale prewetted and allowed to stand for several days yielded significantly better sediment-trapping efficiency than a normal bale prewetted immediately before testing.
4. Normal field placement of straw filter barriers often results in failure because of undercutting, end flow, and washouts.
5. The efficiency of field barriers can approximate that measured in the laboratory if barriers are placed in accordance with the criteria used to place the experimental barriers on US-29. These criteria are (a) entrenching or wedging loose straw under staked bales, (b) extending barrier so that the bottoms of the end bales are higher than the top of one of the center bales, and (c) breaking up a bale and scattering loose straw behind each barrier.
6. Laboratory tests of stone-filled gabions showed relatively low (29 and 32 percent) filter efficiencies that were approximately doubled with the addition of a 2.5-cm (1-in) layer of compressed straw at the bottom.
7. Based on field observations, gabions appear to be well suited to in-stream use to slow stream velocity and trap bed load.

ACKNOWLEDGMENT

The opinions, findings, and conclusions expressed in this report are ours and not necessarily those of the sponsoring agencies.

REFERENCES

1. Manual on Erosion and Sedimentation Control. Virginia Department of Highways and Transportation, Richmond, 1975.
2. D. J. Poché. A Design Program for the Estimation and Abatement of Soil Losses From Highway Slopes. Virginia Highway and Transportation Research Council, Charlottesville, VHRC 73-R51, 1974.

Abridgment

Impact Performance of the Minnesota 1.5-m-Radius Plate Beam Guardrail

Eugene Buth and Joe W. Button, Texas Transportation Institute, Texas A&M University
Paul J. Diethelm, Minnesota Department of Transportation

The Minnesota Department of Transportation employs a 1.5-m-radius (5-ft-radius) plate beam end treatment for median rails at twin bridges and piers or divided roadways. The crashworthiness of this end treatment was evaluated in a program that included two full-scale vehicle crash tests. A small-size and a full-size test vehicle were towed head-on into the median rail system at 96.6 km/h (60 mph). Performance of the system was excellent in both tests.

DESCRIPTION OF GUARDRAIL

The hardware components and geometrics of the end treatment are described in Minnesota Department of Transportation standard drawings. The department uses 15.2 × 20.3 × 183-cm (6 × 8 × 72-in) wooden posts spaced 1.9 m (6 ft, 3 in) apart. In the test installation, which is shown in Figure 1, the posts were set approximately 114 cm (45 in) in oversized holes backfilled with lean concrete to simulate frozen ground conditions. Standard 12-gauge plate beam was used for the rail. Two 56-cm-diameter (22-in-diameter) concrete posts (simulated piers) were placed 10.7 m (35 ft) behind the nose of the guardrail.

DESCRIPTION AND RESULTS OF TESTS

Test B1

A 1971 Chevrolet Vega weighing 1039 kg (2290 lb) impacted the guardrail head-on at 99 km/h (61.5 mph) (Figure 2). On impact, the foremost post failed at ground level. As the vehicle advanced into the attenuator, the guardrail buckled and wrapped around the front of the vehicle, and posts on each side of the installation were successively broken at ground level. Significant yaw displacement of the vehicle occurred, but pitching and rolling motions were negligible. After failure of five wooden posts and partial failure of four others, the vehicle came to rest with a yaw angle of 33 deg. The vehicle center of mass penetrated 7.1 m (23.2 ft) into the barrier.

The average deceleration of the test vehicle computed from the impact velocity and the stopping distance of the vehicle center of gravity was 5.3 *g* (1). The highest average deceleration determined over a 200-ms interval was 6.1 *g*, and over 50 ms was 9.1 *g*.

The vehicle received moderate damage in the form of distortion of front frame members and considerable sheet metal deformation. Based on the TAD scale (2), the vehicle damage rating was FD-5. The Society of Automotive Engineers (SAE) collision deformation classification was 12FDEW3 (3).

Test B2

A 1969 Chrysler weighing 2041 kg (4500 lb) impacted the guardrail head-on at 100.26 km/h (62.3 mph) (Figure 3). On impact, the foremost post was broken, and the vehicle began to yaw counterclockwise as it advanced. The rail wrapped around the vehicle, and posts on each side of the installation were successively broken as the vehicle advanced. In the final stages of the collision, the rearward force on the steel guardrail caused the remaining three posts supporting the left side to split, and the guardrail fell to the ground. The test vehicle continued to advance

Figure 1. Installation at test site.

Publication of this paper sponsored by Committee on Safety Appurtenances.

Figure 2. Test B1.

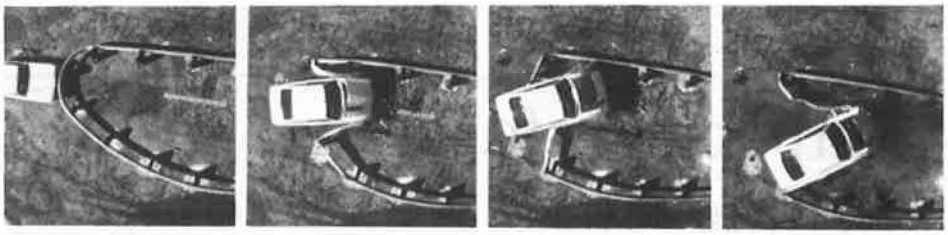

t = 0 ms t = 274 ms t = 370 ms t = 959 ms

Figure 3. Test B2.

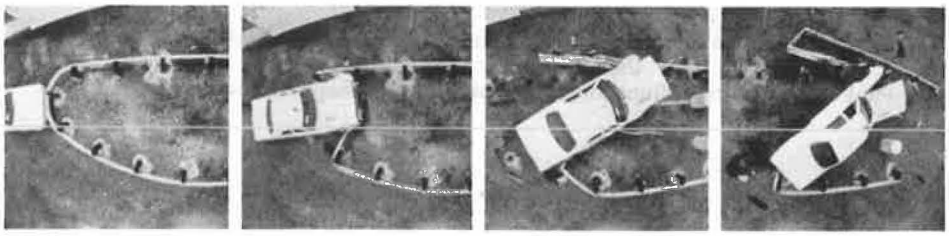

t = 0 ms t = 147 ms t = 441 ms t = 1029 ms

and yaw counterclockwise until the right front corner impacted one of the simulated concrete piers. During contact with the pier, the vehicle roll displacement reached about 45 deg. The vehicle rebounded approximately 0.61 m (2 ft) and came to rest with a yaw angle of 43 deg. The vehicle center of mass penetrated 11.83 m (38.8 ft) during impact.

Average deceleration of the vehicle computed from the impact speed and stopping distance was 3.8 *g*, which is well below the acceptable limit. The highest average longitudinal deceleration over a 200-ms interval, obtained from the accelerometer traces, was 3.4 *g*; the highest over 50 ms was 4.7 *g*.

At the time of impact with the simulated pier, the forward velocity of the vehicle had been reduced to such a level that the impact was entirely acceptable. Damage to the front of the vehicle consisted of severely deformed sheet metal and somewhat distorted front frame members. Damage to the right rear consisted of minor dents in the sheet metal. The vehicle damage rating was FD-5 and RBQ-3 (2), and the SAE collision deformation classification was 12FDEW1 (3).

CONCLUSIONS

The Minnesota 1.5-m-radius (5-ft-radius) plate beam guardrail performed satisfactorily under full-scale 96.6-km/h (60-mph), head-on impacts with 1039-kg (2290-lb) and 2041-kg (4500-lb) vehicles. The values of average deceleration are well below the Federal Highway Administration design criteria of 12 *g* (4) for vehicles within the weight category tested. Accelerometer data for test B1 indicate that vehicle occupants may have received some minor injuries, but accelerometer data from test B2 place the occupants in the zone of safety (5).

The passenger compartments of the test vehicles remained intact and were not penetrated by any foreign objects.

Significant but acceptable transverse accelerations were imposed on the test vehicles as a result of the yaw displacement during impact.

The system, as constructed and tested, performs adequately when struck head-on by both large and small automobiles. The W-section experienced severe local damage in each case. Although tensile load in this element was not measured, vehicle condition after impact indicated that it was loaded near ultimate capacity and that not much reserve strength existed, especially in test B2.

REFERENCES

1. M. E. Bronstad and J. D. Michie. Recommended Procedures for Vehicle Crash Testing of Highway Appurtenances. NCHRP, Rept. 153, 1974.
2. Vehicle Damage Scale for Traffic Accident Investigators. Traffic Accident Data Project, National Safety Council, 1968.
3. Collision Deformation Classification. Automotive Safety Committee, Society of Automotive Engineers, New York, SAE J224a, 1972.
4. Use of Crash Cushions on Federal-Aid Highways. Federal Highway Administration, Instructional Memorandum 40-5-72, HNG-32, Nov. 8, 1972.
5. A. S. Hyde. Biodynamics and the Crashworthiness of Vehicle Structures. Research Staff, Wyle Laboratories, Huntsville, Ala., Vol. 3, Rept. WR 68-3, March 1968.

Abridgment

Concrete Safety Shape Research

Maurice E. Bronstad and C. E. Kimball, Jr., Southwest Research Institute, San Antonio, Texas

Use of the concrete safety shape, which is a widely specified traffic barrier, is greatly on the increase. Recognizing the need for research on concrete safety shapes, 21 transportation agencies entered into a Highway Planning and Research pooled-funds study administered by the Federal Highway Administration (FHWA) Office of Research.

BACKGROUND

As reported in an FHWA notice (1) in 1971, 36 states employed a concrete safety shape to some extent. Of these 36 states, 19 specified the shape first used by New Jersey [denoted as MB5 by Michie and Bronstad (2)]; 8 specified a shape developed by General Motors [denoted as MB6 by Michie and Bronstad (2)]; and the remaining states used some variation of these two shapes. Although crash test investigations had been conducted on both the MB5 and MB6 shapes (3, 4, 5, 6), tests of the two shapes were not comparable because of wide variation in test conditions.

Accordingly, one of the early tasks of the concrete barrier research was to conduct base-line tests by using identical test conditions on the two widely used shapes. In addition, in recognition of the increasing number of small cars in today's traffic, subcompact baseline tests were subsequently added to the program. An added stimulus to this investigation was an accident report from an FHWA region (7) that indicated a high incidence of rollover when subcompact vehicles impacted the MB6 shape.

Mathematical simulations (when compared with crash tests) permit low-cost examination of barrier performance. The highway-vehicle-object simulation model (HVOSM) (8, 9) program was used to investigate several variations of the MB5 shape as shown in Figure 1. Based on the results of these investigations, configuration F was determined to offer potential improvement in performance, and base-line crash tests were programmed for this shape. This program used the same types of vehicles as were used in the previous base-line tests.

OBJECTIVE

The objective of the research discussed in this paper was to obtain comparable information on three different concrete safety shapes impacted by both standard sedans and subcompact sedans at 96.6 km/h (60 mph) and at angles of 7 and 15 deg.

TEST RESULTS

Standard Sedan Base-Line Tests

All standard sedan tests were conducted with 1972 Ford Galaxie sedans weighing 1982 kg (4370 lb). Because these vehicles were from a police fleet, they were in similar condition. Table 1 gives a summary of standard sedan test data. Figures 2 and 3 illustrate performance of the shapes.

Subcompact Vehicle Baseline Tests

All subcompact tests were conducted with 1971 Chevrolet Vegas weighing 1021 kg (2250 lb). Table 2 gives a summary of subcompact vehicle test data. Figures 4 and 5 illustrate performance of the shapes.

DISCUSSION OF RESULTS

Based on results of the base-line crash tests, four conclusions can be stated:

1. Vehicle roll angles in all tests were greatest for the MB6 shape and the smallest for the new configuration F. An exception was the 15-deg test 12 with configuration F. A higher roll angle was observed in this test although vehicle climb was less. The higher roll angle may be attributed to the higher speed of this configuration F test.
2. Vehicle rollover occurred with the MB6 shape during a subcompact crash at 91.9 km/h (57.1 mph) and angle of 16.5 deg.

Publication of this paper sponsored by Committee on Safety Appurtenances.

Figure 1. Barrier profiles, parametric studies.

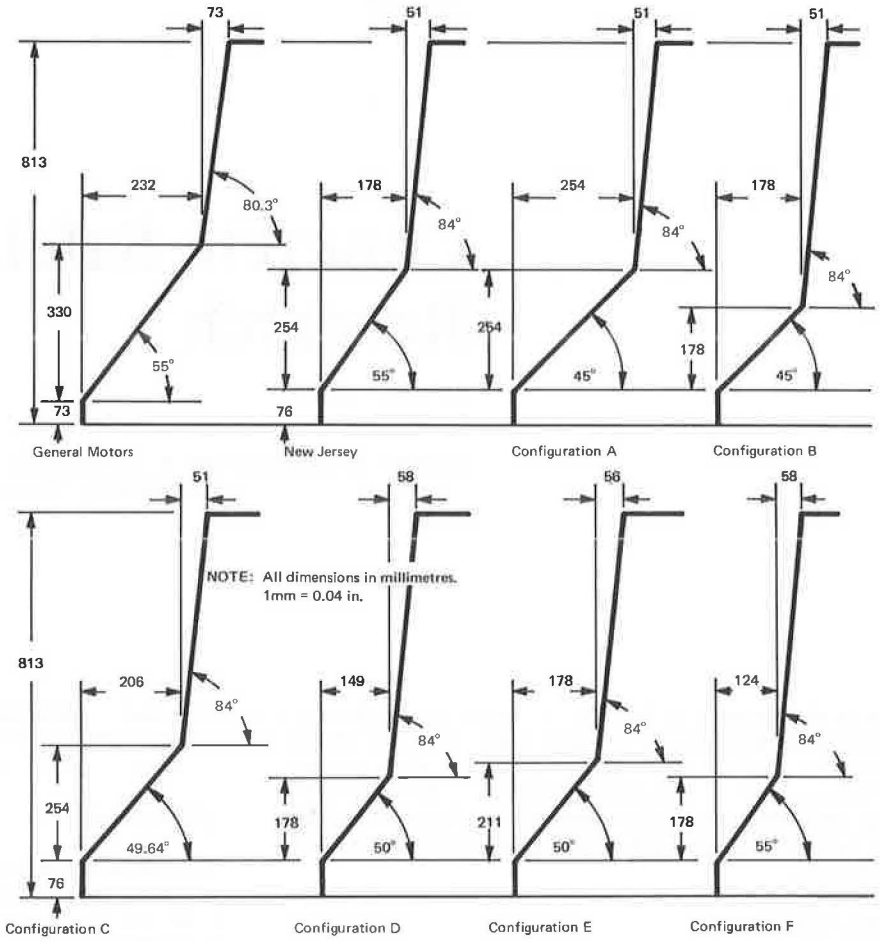

Figure 2. Standard vehicle, 7-deg tests.

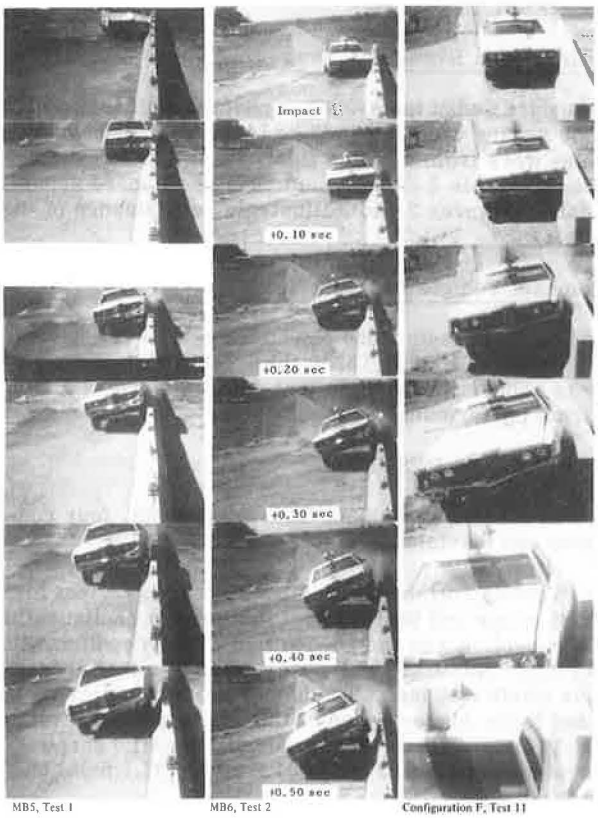

Figure 3. Standard vehicle, 15-deg tests.

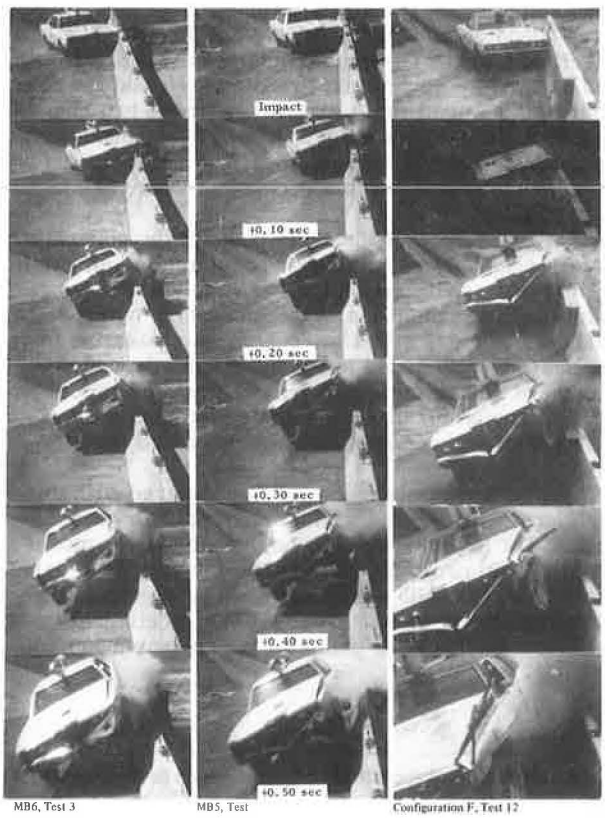

Table 1. Summary of standard vehicle base-line crash tests.

Test Angle (deg)	Test Number	Barrier Shape	Impact Speed (km/h)	Impact Angle (deg)	Maximum Roll Angle (deg)		Maximum Acceleration[a] (g)				Maximum Vertical Acceleration (g)	Duration of Peak g (ms)
							Film		Accelerometer			
					Test	HVOSM	Longitudinal	Lateral	Longitudinal	Lateral		
7	1	MB5	97.0	7.5	15	2	-1.7	-5.0	-0.9	-2.0	14	12.5
	2	MB6	99.1	7.3	20	5	-1.5	-3.6	-2.2	-2.8	11	12.5
	11	Configuration F	93.3	8.0	11		-1.4	-3.4	-3.0	-3.9		
15	3	MB5	90.9	15.5	20	26	-3.3	-10.1	-1.6	-5.2	28	10.9
	4	MB6	89.9	15.9	20	17	-5.0	-10.1	-1.6	-5.5	32	13.4
	12	Configuration F	98.8	15.2	21	6	-5.1	-6.6	—[b]	-6.7		

Notes: 1 km/h = 0.621 mph.
All vehicles tested were 1982-kg (4370-lb) 1972 Ford Galaxies.
[a]50-ms average. [b]Not applicable.

Table 2. Summary of subcompact base-line crash tests.

Test Angle (deg)	Test Number	Barrier Shape	Impact Speed (km/h)	Impact Angle (deg)	Maximum Roll Angle (deg)		Maximum Acceleration[a] (g)				Maximum Vertical Acceleration (g)	Duration of Peak g (ms)
							Film		Accelerometer			
					Test	HVOSM	Longitudinal	Lateral	Longitudinal	Lateral		
7	5	MB6	86.7	8.4	31	20	-2.4	-4.3	-1.4	-2.0	18	12
	6	MB6	87.9	9.2	21	20	-2.7	-5.3	-1.9	-2.4	21	5
	8	MB5	89.96	8.0	20	14	—	—	-1.0	-3.2	22.0	9
	10	Configuration F	95.4	6.8	10		-3.4	-4.6	-3.3	—[b]		
15	7	MB6	91.9	16.5	—[c]	—[c]	-5.3	-8.3	-3.4	-4.6	19	6
	9	MB5	94.8	15.5	20	27	-3.6	-5.1	-0.9	-6.0	27.6	11
	13	Configuration F	91.2	14.6	13		-3.9	-4.6	—[b]	-7.3		

Notes: 1 km/h = 0.621 mph.
All vehicles tested were 1021-kg (2250-lb) 1971 Chevrolet Vegas.
[a]50-ms average. [b]Not applicable. [c]Rollover.

Figure 4. Subcompact vehicle, 7-deg tests.

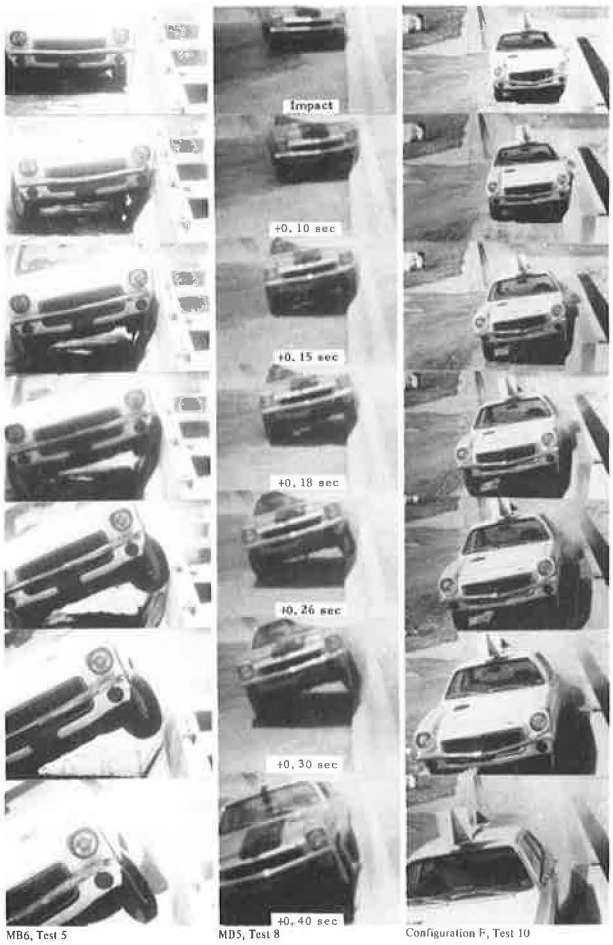

MB6, Test 5 MB5, Test 8 Configuration F, Test 10

Figure 5. Subcompact vehicle, 15-deg tests.

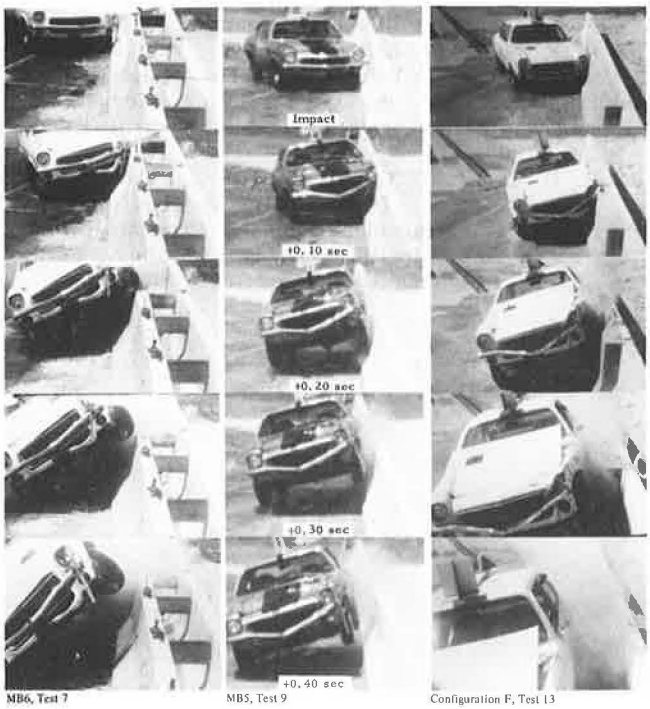

MB6, Test 7 MB5, Test 9 Configuration F, Test 13

3. Vehicle damage was generally less with the MB6 shape except for the rollover. Large-vehicle damage was less with the new configuration F, but small-vehicle damage was greater with the MB5 shape.
4. Average vehicle decelerations indicate that similar performance can be expected with the three shapes, but the new configuration F shape appears to provide the lower values.

REFERENCES

1. Concrete Median Barriers and Parapets. Federal Highway Administration, Notice EN-20, March 1971.
2. J. D. Michie and M. E. Bronstad. Location, Selection, and Maintenance of Highway Traffic Barriers. NCHRP, Rept. 118, 1971.
3. E. F. Nordlin and N. F. Field. Dynamic Tests of Steel Box Beam and Concrete Median Barriers. California Division of Highways, Research Rept. M&R 636392-3, Jan. 1968.
4. L. C. Lundstrom, P. C. Skeels, B. R. Englund, and R. A. Rogers. A Bridge Parapet Designed for Safety: General Motors Proving Ground Circular Test Track Project. HRB, Highway Research Record 83, 1965, pp. 169-187.
5. E. R. Post, T. J. Hirsch, and J. F. Nixon. Truck Tests on Texas Concrete Median Barrier. HRB, Highway Research Record 460, 1973, pp. 73-81.
6. E. F. Nordlin, J. H. Woodstrom, R. P. Hackett, and J. Jay Folsom. Dynamic Tests of the California Type 20 Bridge Barrier Rail. HRB, Highway Research Record 343, 1971, pp. 57-74.
7. P. Schlosser. Report on Accident Experience—Concrete Median Barrier. Wisconsin Division, Federal Highway Administration, Dec. 1973.
8. R. R. McHenry and N. H. Deleys. Vehicle Dynamics in Single Vehicle Accidents: Validation and Extensions of a Computer Simulation. Cornell Aeronautical Laboratory, Buffalo, VJ-2251-V-3, Dec. 1968.
9. R. D. Young, T. C. Edwards, R. J. Bridwell, and H. E. Ross, Jr. Documentation of Input for the Single Vehicle Accident Computer Program. Texas Transportation Institute, Texas A&M Univ., College Station, Research Rept. 140-1, July 1969.

Crash Test and Evaluation of a Precast Concrete Median Barrier

T. J. Hirsch and E. L. Marquis, Texas Transportation Institute
John F. Nixon and David Hustace, Texas Department of Highways and Public Transportation

Median barriers are used on high-volume, high-speed traffic facilities to prevent errant vehicles from crossing a median and conflicting with the opposing traffic stream. A secondary function for some designs of median barriers is to minimize the glare of opposing headlights. The cast-in-place concrete median barrier has proved to be an effective and economical barrier in Texas and other states. Investigation of the use of a precast concrete median barrier (PCMB) stemmed from the interest in using a barrier to be prefabricated concurrently with roadway construction. This more effective usage of work force as well as early project completion and acceptance could provide measurable potential savings to both the contractor and the state. In addition, when this barrier is installed on existing facilities, the traffic may be disrupted for a considerable period of time if it is cast in place. Consequently, PCMB that can be quickly installed on active facilities with a minimum period of traffic disruption is needed. For a precast concrete median barrier to function properly in redirecting vehicles, the relatively short precast sections must be adequately connected after they are placed in the highway median. Engineers of the Texas Department of Highways and Public Transportation and the Texas Transportation Institute developed working drawings for precast sections of a PCMB and two connection details. Full-scale crash tests were conducted on the PCMB and connections in order to verify the stability and strength of the installation.

Median barriers are used on high-volume, high-speed traffic facilities to prevent errant vehicles from crossing a median and conflicting with the opposing traffic stream. Current warrants proposed by the National Cooperative Highway Research Program for the installation of median barriers are based on a 2-year traffic projection and median width (1). In a typical case, the warrants state that, for a median width of 6.1 m (20 ft) or less and a predicted average daily traffic (ADT) of 20 000 or more, a median barrier should be installed. Facilities with less traffic than this frequently do not have median barriers. If the ADT increases to 20 000 or more, installation of a median barrier on an existing facility will often become necessary.

Texas median barrier warrants are based on the width of the median. In brief, the Texas warrants require that for medians up to 7.3 m (24 ft) in width a concrete barrier should be used. For medians from 5.5 to 7.3 m (18 to 24 ft) in width, either the concrete or the double steel type of beam should be used. For medians from 7.3 to 9.1 m (24 to 30 ft), the double steel type of beam should be used.

The cast-in-place concrete median barrier (CMB) has proved to be an effective and economical barrier in Texas and other states. Investigation into the use of a precast concrete median barrier stemmed from the interest in using a barrier to be prefabricated concurrently with roadway construction. This more effective usage of work force as well as early project completion and acceptance could provide measurable potential savings to both the contractor and the state. However, when this barrier is installed on existing facilities, the traffic may be disrupted for a considerable period of time if it is cast in place. As a consequence, a precast concrete median barrier (PCMB) that can be quickly installed on active facilities with a minimum period of traffic disruption is needed. In addition, sections of a PCMB can also be used as a temporary barrier during construction of a new facility since the precast sections are portable and can be moved after the need no longer exists.

For a PCMB to function properly in redirecting a vehicle, the relatively short precast sections must be adequately connected after they are placed in the desired location. Engineers of the Texas Department of Highways and Public Transportation (DHPT) and the Texas Transportation Institute (TTI) developed working drawings for 9.1-m-long (30-ft-long) precast concrete sections of a PCMB and two different connection details. Three sections of the PCMB were precast, hauled to the Texas A&M University Research Annex, and installed by using the two different connection details. Full-scale crash tests were conducted on each of the connections to verify the stability and the strength of the installation.

DESIGN AND INSTALLATION

Design

The cross section used for the PCMB is shown in Figure 1. This shape is standard in Texas and is essentially the New Jersey cross section with minor modifications. The

Publication of this paper sponsored by Committee on Safety Appurtenances.

concrete median barrier of the New Jersey cross section has been extensively tested to determine the adequacy of the shape and redirection capabilities. Since these tests, the CMB has been subjected to testing by numerous organizations including TTI (3, 4, 5). These reports attested to the sufficiency of the CMB particularly for narrow medians and shallow impact angles. In all of the successful tests, the CMB was attached to a simulated bridge parapet (2) or the barrier was long, massive, and rigid.

The Texas DHPT has used precast CMB sections on bridges for some time. These precast sections varied from 4.6 to 9.1 m (15 to 30 ft) in length and were rigidly attached to the bridge deck with anchor bolts at 0.6 m (2 ft) maximum spacing.

California had tested twelve 3.8-m-long (12.5-ft-long) precast sections approximately 2268 kg (5000 lb) each pinned together with a steel rod inserted into eyebolts cast in the ends of the sections to form a 45.7-m (150-ft) barrier free standing on asphalt concrete. Two tests were conducted with a 2177-kg (4800-lb) vehicle at a nominal speed of 104.6 km/h (65 mph). In the first test, which was moderately successful, the vehicle impacted the barrier at 7 deg. The second test was at a 25-deg-impact angle and was less than successful. The barrier rotated and displaced laterally, and the vehicle snagged. A second barrier of five 6.1-m (20-ft) sections of approximately 3629 kg (8000 lb) was constructed and tested at 104.6 km/h (65 mph) and 35 deg, that is, more than the normal 25 deg. This test was even less successful than test 2. The barrier segments rotated, displaced laterally, and the vehicle rolled over.

In view of the California experience, engineers with the Texas DHPT elected to test 9.1-m-long (30-ft-long) precast sections approximately 6804 kg (15 000 lb) in mass (Figure 2). This length and mass appeared to be the maximum that could be readily transported and handled.

Two slightly different dowel-joint details were used to connect the 9.1-m (30-ft) precast sections together (Figure 3). The male-female dowel connection used three No. 8 dowels [2.54 cm (1 in) in diameter] 0.46 m (18 in) long precast in one end and three mating 5.08-cm-diameter (2-in-diameter) tapered holes cast in the opposite end as shown in Figure 2. A pressure grout hole was cast vertically behind the tapered female holes. The second connection used was the grooved connection, which also used three No. 8 dowels [2.54 cm (1 in) in diameter] 46 cm (18 in) long as shown in Figure 3. The grooved connection was believed to be more desirable when the precast sections would be used as a temporary barrier. It was believed that the grout and dowels could be chipped out of the grooved blockouts and the precast sections more readily reused. This latter connection detail was arrived at after the PCMB sections were cast; therefore these grooves were sawed instead of being precast in as would be desirable.

The lower slope dimension on the PCMB sections was increased from 7.6 to 10 cm (3 to 4 in) so that the section would maintain the standard 81-cm (32-in) height after the 2.54 cm (1 in) of asphalt concrete fill is placed on the pavement (Figure 1). This asphalt concrete pavement (ACP) fill is an integral and necessary part of the barrier design for permanent installation because it prevents lateral displacement and cracking at the connections during vehicle impact.

Engineers and precast concrete contractors first indicated that the PCMB units would be cast right side up and lifted at the 1/6 points from each end. An analysis of the section indicated that the maximum concrete stress to be expected in tension was 393 kPa T (57 lbf/in^2) for an uncracked section. This value was well within the limits suggested by ACI-318-71. The recommended safe ultimate concrete stress in tension is $f_t = \sqrt{7.5f'_c}$ or 2827 kPa (410 lbf/in^2) for 20 684-kPa (3000-lbf/in^2) concrete. A cracked section analysis was made by using No. 4 bars [1.27 cm (0.5 in) in diameter] in each corner of the section. The steel stress would be approximately 7584 kPa T (1100 lbf/in^2) with the concrete compressive stress less than 827 kPa (120 lbf/in^2). All of these values are well within limits published by the American Association of State Highway and Transportation Officials and the American Concrete Institute.

Installation

Three 9.1-m (30-ft) precast sections were installed on the concrete parking apron at the Texas A&M University Research Annex as shown by Figure 2. An asphalt concrete leveling course was applied; each section, the mass of which was approximately 6804 kg (15 000 lb), was set in place; the two different joints were grouted; and the 2.54-cm (1-in) ACP backup fill was placed on both sides of the PCMB. After they were grouted, the joints were covered with wet burlap to aid in curing.

A concrete grout of about a 10-cm (4-in) slump composed of 15 kg (33 lb) of portland cement, 45 kg (100 lb) sand, and 6.8 kg (15 lb) water was used to grout the groove joint. The same mix was used for the dowel connection except that the slump was increased to 15 cm (6 in). Two 10-cm (4-in) cylinders were cast from the mix used to grout each joint. These were cured and tested in compression just before each impact test. The 5-day strength of the cylinders placed in the groove joint was 37 232 kPa (5400 lbf/in^2). The samples from the dowel joints tested 39 576 kPa (5740 lbf/in^2) at 6 days of age.

Crash test 1 was conducted on the groove connection with the 2.54-cm (1-in) ACP located on both sides of the PCMB to prevent lateral displacement of the barrier under the vehicle impact. Because this test proved successful, it was decided to remove the ACP from behind the barrier for crash test 2 on the male-female dowel connection. This test would give an indication of how the doweled connection would behave if the precast sections were used as a temporary barrier with no ACP backup.

VEHICLE CRASH TESTS

Test 1: Grooved Joint Connection

The vehicle used for test 1 was a 2040-kg (4500-lb) 1966 Pontiac. The impact point of the left front fender and the barrier occurred 2.1 m (7 ft) upstream from the groove joint as shown in Figure 2. The actual impact angle was 23.5 deg and the actual impact velocity was 97.4 km/h (60.5 mph). Figure 4 shows the vehicle before and after impact. The vehicle was smoothly redirected and the exit angle was 7 deg. The maximum vehicle roll angle of 18 deg occurred while the vehicle was in contact with the barrier. The vehicle remained upright during the test. The front wheel and steering linkage were damaged and the vehicle was inoperable after the impact. The sequence of the impact is shown in Figure 5.

The average lateral deceleration taken from the high-speed film data was 7.5 g taken over 206 ms. The average longitudinal deceleration over the same period was 1.6 g. The barrier did not roll or slide laterally. Figure 6 shows close-up views of the joint before and after impact. A hairline or shrinkage crack had appeared in the vertical face before impact. There was no evidence that this crack was altered after impact or that any other cracking at the connection occurred during impact. Damage to the precast barrier and joint was nil.

Test 2: Male-Female Joint

The asphalt concrete base was removed from the back side of the PCMB before test 2 to determine whether the barrier had to be stabilized when used as a temporary installation.

The vehicle used for test 2 was a 2060-kg (4540-lb) 1965 Oldsmobile. The impact point of the left front fender occurred 2.1 m (7 ft) upstream from the male-female dowel joint as shown in Figure 2. The actual impact angle was 24.2 deg, and the actual impact velocity was 96.2 km/h (59.8 mph). The vehicle was smoothly redirected and the exit angle was 3 deg. Again the maximum vehicle roll angle of approximately 18 deg occurred while

Figure 1. PCMB cross section.

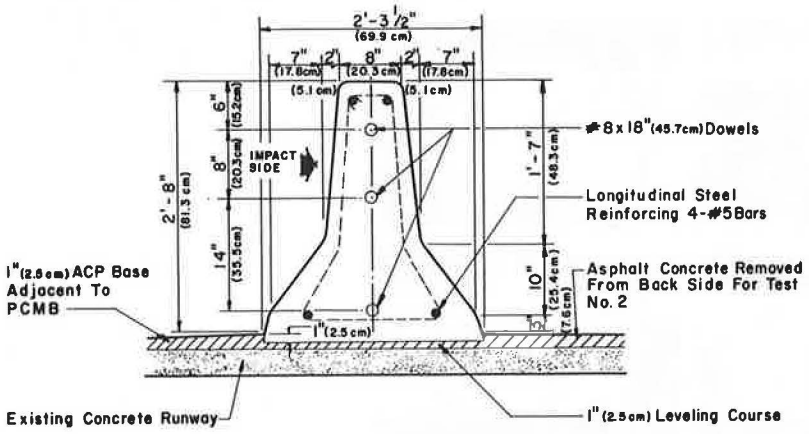

Figure 2. PCMB connection test installation.

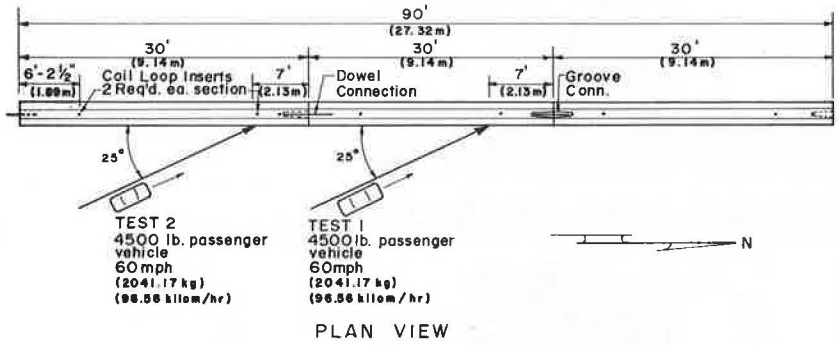

Figure 3. PCMB test connection details.

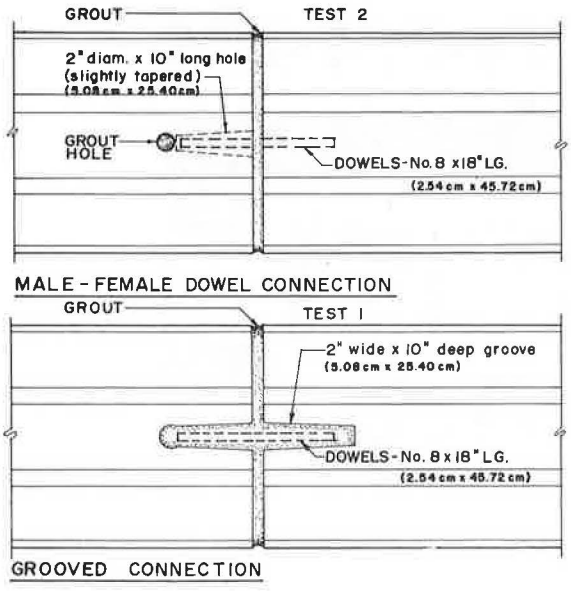

Figure 4. Test vehicle before and after impact.

(a) Before Impact

(b) After Impact

Figure 5. Overhead view of concrete median barrier in test 1.

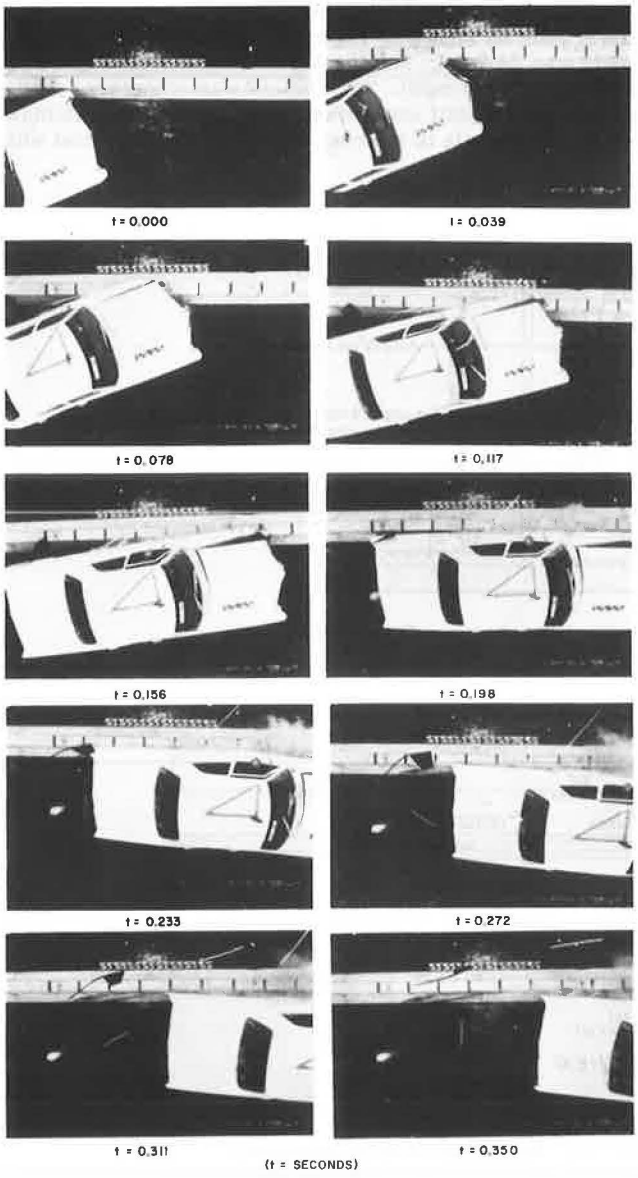

Figure 6. Groove joint before and after test 1.

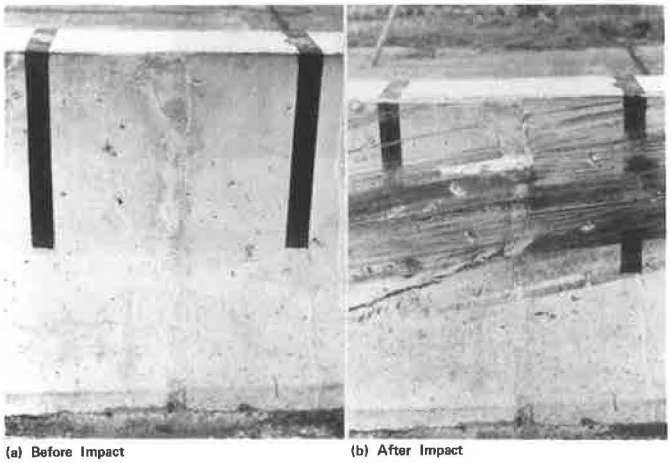

(a) Before Impact (b) After Impact

the vehicle was in contact with the barrier. The vehicle remained upright during the test. The left front wheel and steering linkage were damaged, and the vehicle was inoperable after the impact.

The average lateral vehicle deceleration taken from the film was 6.3 *g* over 223 ms. The average longitudinal deceleration over the same period was 1.1 *g*. The barrier did not roll or rotate during the impact. The precast barrier did displace 34.3 cm (13.5 in) laterally at the connection during vehicle redirection, and significant cracking of the concrete, apparent on both the tension and compression sides of the joint (Figure 7), occurred. The joint held together, however, and smoothly

Table 1. Summary of test data.

Item	Test 1	Test 2
Vehicle year	1966	1965
Vehicle make	Pontiac	Oldsmobile
Mass, kg	2040	2060
Impact angle, deg	23.5	24.2
Initial impact speed, km/h	97.4	96.2
Speed at parallel, km/h	77.2	79.3
Longitudinal distance to parallel, m	4.57	5.02
Permanent barrier displacement, m	0	0.34
Lateral distance to parallel, m	0.55	0.98
Time to parallel, ms	206	223
Average longitudinal deceleration parallel to barrier, *g*	1.6	1.1
Average lateral deceleration normal to barrier, *g*	7.5	6.3
Departure angle, deg	7.0	3.0
Vehicle damage classification		
TAD[a]	FL-5.5	FL-4.5
Society of Automotive Engineers	11FLEW3	11FLEW2

Note: 1 kg = 2.2 lb, 1 km/h = 0.621 mph, 1 m = 3.3 ft.

[a]Traffic Accident Data Project, National Safety Council.

Figure 7. Dowel joint before and after test 2.

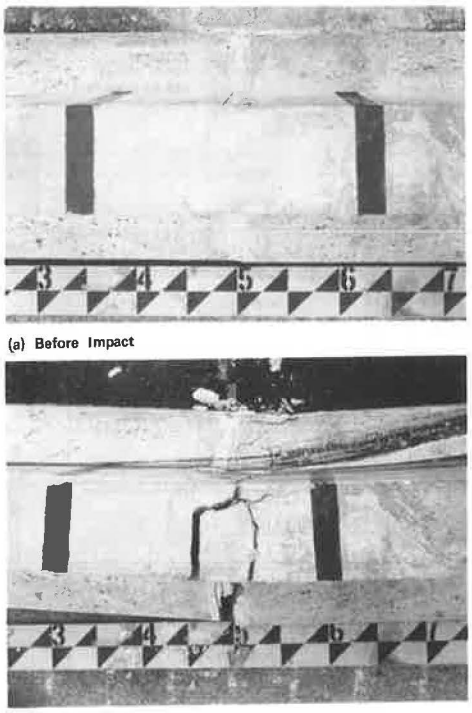

(a) Before Impact

(b) After Impact

redirected the vehicle. The groove joint 9.1 m (30 ft) downstream also was fractured. This allowed the center section to rotate slightly in the horizontal plane between the two joints. The last section downstream from the groove joint (Figure 2) did not move.

DISCUSSION OF TESTS

A brief summary of the test data is given in Table 1. In both tests the vehicle was smoothly redirected and remained upright. The barrier did not rotate in either test.

When the PCMB was supported laterally by the 2.54-cm-thick (1-in-thick) asphalt paving material (test 1), it did not displace laterally and no damage was inflicted on the precast concrete segments or connection. For a permanent installation, the 2.54-cm-thick (1-in-thick) asphalt paving material or some other lateral support should be used so that maintenance or repair cost would be small or nil.

If the PCMB is to be used as a temporary barrier, test 2 indicates that lateral support by the 2.54-cm (1-in) asphalt concrete is not absolutely necessary. However, the barrier can be expected to displace laterally under vehicle impact approximately 0.3 m (1 ft), and significant cracking of the concrete will occur at the segment joints. Under low-speed or low-angle impacts or both, the lateral displacement and cracking of the concrete would probably be minimal.

One can conclude from these two tests that the PCMB will function as designed when the 9.1-m (30-ft) sections are connected by either of the two connections used and backed up with 2.54 cm (1 in) of ACP. This type of installation is recommended for permanent installations. If the PCMB is used as a temporary installation, either connection should be acceptable; however, considerable maintenance can be anticipated if the ACP or some other backup is not used to prevent sliding.

CONCLUSIONS

Past experience has shown that the CMB is an economical and effective traffic barrier. Investigation into the use of a precast concrete median barrier stemmed from the interest involved in using a barrier to be prefabricated concurrently with roadway construction. This more effective usage of work force as well as early project completion and acceptance could provide measurable potential savings to both the contractor and the state. When one installs this barrier on existing facilities, it is frequently desirable to precast the concrete median barrier so that the units can be quickly installed during low traffic volume periods. The 9.1-m-long (30-ft-long) sections with grouted dowel connections and the 2.54-cm (1-in) ACP fill material behind the barrier proved to be an effective barrier in redirecting 2040-kg (4500-lb) vehicles impacting at 96.6 km/h (60 mph) and 25 deg.

If the 2.5-cm (1-in) ACP or some other backup device is not used to prevent lateral sliding, then the doweled connections tested here appear to be adequate; however, considerable maintenance can be anticipated after high-speed, high-angle impacts. This type of installation (without backup device) should only be used as a temporary barrier.

Four No. 4 longitudinal reinforcing bars are adequate for handling and lifting requirements provided that the sections are cast right side up. Where the units will be cast bottom side up (for simpler form design and removal), four No. 5 longitudinal bars are recommended provided two pickup points located approximately 1.9 m (6.21 ft) from each end are used.

The recommendations for reinforcing steel are intended to produce added safety during installation and reduced maintenance when in service. These concrete sections could have been designed as plain, unreinforced concrete members.

ACKNOWLEDGMENTS

This study was conducted under a cooperative program between the Texas Transportation Institute and the Texas Department of Highways and Public Transportation. It was sponsored by the Texas Department of Highways and Public Transportation and the Federal Highway Administration. Liaison was maintained through John F. Nixon of the Texas Department of Highways and Public Transportation. The crash tests and evaluation were carried out by personnel of the Highway Safety Research Center of the Texas Transportation Institute.

REFERENCES

1. J. D. Michie and M. E. Bronstad. Location, Selection, and Maintenance of Highway Traffic Barriers. NCHRP, Rept. 118, 1971.
2. L. C. Lundstrom, P. C. Skeels, B. R. Englund, and R. A. Rogers. A Bridge Parapet Designed for Safety. HRB, Highway Research Record 83, 1965, pp. 169-187.
3. R. D. Young, E. R. Post, and H. E. Ross, Jr. Simulation of Vehicle Impact With Texas Concrete Median Barrier: Test Comparisons and Parameter Study. HRB, Highway Research Record 460, 1973, pp. 61-72.
4. E. R. Post, T. J. Hirsch, G. G. Hayes, and J. F. Nixon. Vehicle Crash Test and Evaluation of Median Barriers for Texas Highways. HRB, Highway Research Record 460, 1973, pp. 97-113.
5. H. E. Ross, Jr. Impact Performance and a Selection Criteria for Texas Median Barriers. Texas Transportation Institute, Texas A&M Univ., College Station, Research Rept. 140-8, April 1974.

Abridgment

Impact Design of Crash Cushions for Nonstationary Barriers

F. W. Jung and A. M. Billing, Ontario Ministry of Transportation and Communications

Nonstationary traffic barriers such as sign trucks with crash cushion attachments can be designed by using barrier resistance charts and acceleration-time diagrams.

Simple equations for both methods were derived and results were compared with more complex computer simulations to illustrate the usefulness of the simple equations. In particular, an equation for a movable barrier resistance chart was derived from the general differential equation, and usage of the chart is discussed and exemplified.

The acceleration-time diagram method is in the form of sets of simple equations based on two (or more) steps of constant crushing forces, and the method can be applied in this form for design purposes.

Feasibility of the methods with regard to angular impacts can be shown by means of a few computer simulation results. The equations for drawing the barrier resistance chart and for calculating the crushing time of the first constant part of the chart are shown in Figure 1 where

- S = stroke or crushing distance of first constant part,
- X = stroke or crushing distance beyond S for m,
- T = crushing time pertaining to S for m,
- m = mass of impacting car,
- m_1 = mass of smallest car to be protected,
- M = mass of sign truck,
- a_m = permissible deceleration of impacting car,
- V = impact velocity, and
- F_1, F = resisting force of ideally shaped barrier material.

Area under the chart represents dissipated impact energy. If resisting forces of actual materials are lower, the strokes (S or X) must be correspondingly larger.

Figure 1. Barrier resistance chart.

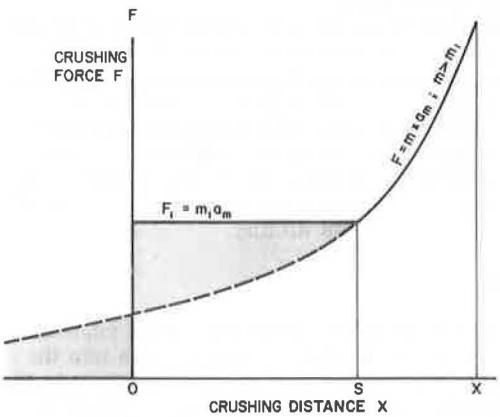

$$S = \frac{M}{m_1 + M} \times \frac{V^2}{2 a_m}$$

$$X = \left[\ln \left(\frac{m}{m_1} \right) - \ln \frac{m + M}{m_1 + M} + \frac{M}{m + M} \right] \times \frac{V^2}{2 a_m}$$

$$T = \frac{KV}{F_1} \left[1 - \sqrt{1 - \frac{2 F_1 S}{K V^2}} \right] ; \quad K = \frac{Mm}{M + m}$$

ACKNOWLEDGMENT

Copies of the paper can be obtained from the Research and Development Division, Ontario Ministry of Transportation and Communications, 1201 Wilson Avenue, Downsview, Ontario, Canada M3M 1J8.

Publication of this paper sponsored by Committee on Safety Appurtenances.

Abridgment

Full-Scale Tests of a Modified Collapsing-Ring Bridge Rail System

C. E. Kimball, M. E. Bronstad, and J. D. Michie, Southwest Research Institute, San Antonio, Texas
J. A. Wentworth and J. G. Viner, Federal Highway Administration

A need exists for a bridge rail system that not only can withstand impacts by large vehicles such as buses and trucks but also does not impart high accelerations to impacting smaller vehicles. Accordingly, a concept known as the collapsing-ring bridge rail system (CRBRS) has been developed that appears to be capable of fulfilling that need. A paper discussing 10 tests of the CRBRS is available from the Transportation Research Board (TRB) (1). This paper presents information on subsequent design modifications and testing. A significant improvement in barrier performance resulted from these modifications. For the first time in history, a 31 751-kg (70 000-lb) vehicle was used to evaluate a traffic barrier.

BACKGROUND

The design premise of the CRBRS is to dissipate vehicle impact energy by collapsing, thick-walled steel rings. As shown in Figure 1, the CRBRS has been designed as a three-stage barrier.

1. Reduction in impact severity, compared with that for conventional nondeflecting bridge rail designs, was sought for vehicles in the weight range of 907 to 1814 kg (2000 to 4000 lb) when they impact the system at 96.6 km/h (60 mph) and 25 deg through the plastic deformation of the collapsing ring as shown in Figure 1a.
2. Redirection of vehicles involved in impacts as severe as an 11 340-kg (25 000-lb) school bus impacting the railing at 96.6 km/h (60 mph) and 20 deg together with having the outer railing system elements behave as a conventional nondeflecting bridge rail as shown in Figure 1b was desired.
3. Controlled dynamic displacement of the outer rail system was desired to permit containment in impacts as severe as those involving an 18 144-kg (40 000-lb) intercity bus or an 18 144-kg (40 000-lb) tractor-trailer truck at 96.6 km/h (60 mph) and 15 deg, as shown in Figure 1c.

As discussed in the earlier TRB paper (1), results of the initial 10-test program of the CRBRS revealed that leaning of the backup posts as they pivoted about the outside baseplate bolt attachment caused heavy vehicles to reach high roll angles during stage 3 (severe) impacts as shown in Figure 1. To eliminate this pivoting, the Federal Highway Administration incorporated the following design changes as shown in Figure 2:

1. Post baseplate thickness was increased from 1.27 cm (½ in) to 2.54 cm (1 in).
2. Two 2.86-cm-diameter (1⅛-in-diameter) outside holes in the W 30.48 × 182.88-cm (W 12 × 72-in) stub beams were slotted.

In addition, to strengthen the system the top rail size was increased from TS 15.2 × 15.2 × 0.47 cm (TS 6 × 6 × 0.187 in) to TS 20.3 × 15.2 × 0.63 cm (TS 8 × 6 × 0.250 in). Thus lateral translation of the system was facilitated because the posts were released from the slotted stub beam when the front bolts failed in tension.

TEST RESULTS

Results of the four-test series are summarized in Table 1. Where applicable, results of previous similar tests with the original design are shown for comparison. Comparisons are made for vehicle exit angle, exit speed, and maximum average vehicle accelerations.

Test 11 was a repeat of test 9, which was the most severe (in terms of barrier damage) of the initial series. Test 12 provided data on performance of CRBRS when impacted by a very heavy [31 751-kg (70 000-lb)] vehicle. Test 13 was performed with no repair of barrier damage sustained in test 12. Test 14 was a repeat of test 10. Further details of the entire test program are available elsewhere (2).

Test 11

The GMC Scenicruiser bus was ballasted to 18 144 kg (40 000 lb) with 2721 kg (6000 lb) in the passenger compartment and 1905 kg (4200 lb) in the cargo compart-

Publication of this paper sponsored by Committee on Safety Appurtenances.

ments (in test 9 all ballast was contained in the cargo compartments). The bus impacted the front rail at 86.7 km/h (53.9 mph) and a 15.1° angle. As shown in Figure 3, impact occurred approximately 0.9 m (3 ft) upstream of post 6. The bus completely collapsed the rings in the impact zone and rolled toward the rail, and the rear of the bus impacted the outer rail system. The redirected bus reached a maximum roll of 8 deg (toward the rail) as shown in Figure 3 before returning to an upright position. Maximum 50-ms average accelerations were 1.2 longitudinal g and 2.1 lateral g; maximum permanent deflections of the three box beam rails were 49.5 cm (19.5 in) on the top rail, 49.3 cm (19.4 in) on the mid rail and 88.9 cm (35.0 in) on the front rail. The inboard (traffic side) baseplate bolts (2 per post) of posts 3 through 10 failed in tension, and the posts were displaced

Figure 1. Collapsing-ring energy absorption concept.

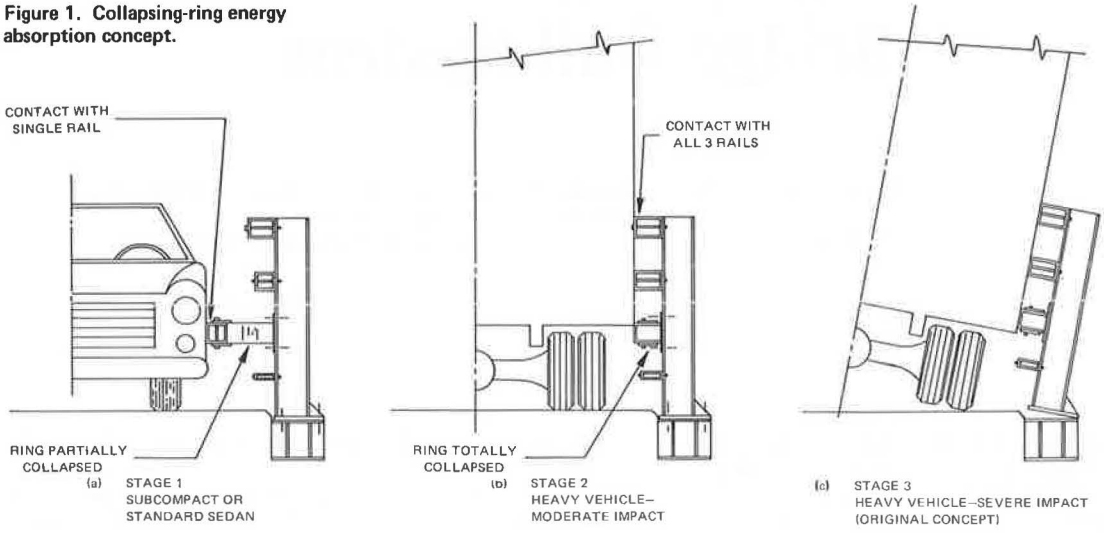

Figure 2. Modifications made to CRBRS for tests 11 through 14.

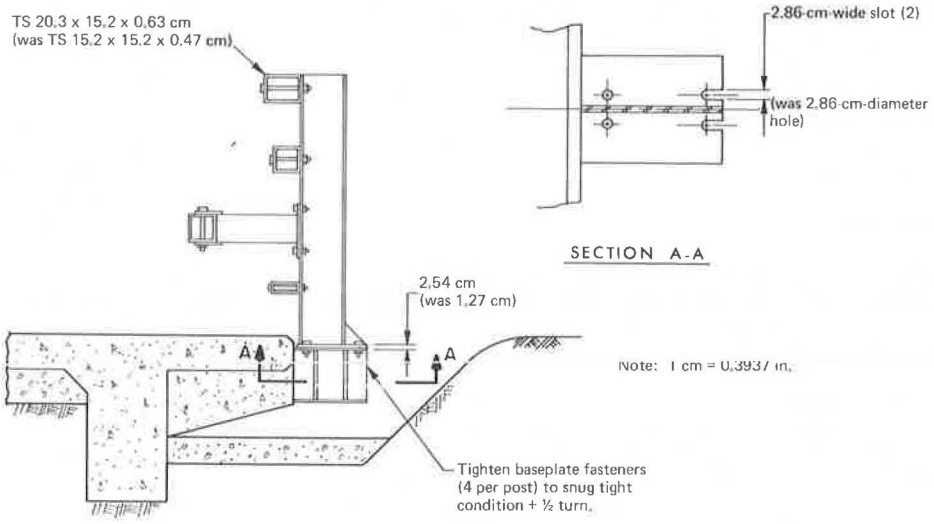

Table 1. Summary of vehicle crash results.

Test Number	Vehicle Weight (kg)	Vehicle Description	Vehicle Impact Conditions		Vehicle Exit Conditions		Max Avg. Vehicle Acceleration[a]		Max Beam Rail Deflections	
			Speed (km/h)	Angle (deg)	Speed (km/h)	Angle (deg)	Longitudinal (g)	Lateral (g)	Dynamic (cm)	Permanent (cm)
11	18 160	Intercity bus	86.7	15.1	80.0	7.9	-1.2	2.2	121.9	88.9
9[b]	18 160	Intercity bus	87.4	19.1	68.9	13.2	-1.4	2.6	153.4	137.2
12[c]	31 780	Tractor-trailer truck	71.4	10.0	69.2	3.0	-3.0	5.0	30.0	24.9
13	1 998	Standard sedan	99.8	22.7	82.4	7.1	-5.3	7.7	53.3	48.3
14	18 160	Tractor-trailer truck	91.7	15.6	83.2	3.0	-1.1	7.8	145.8	135.6
10[b]	18 160	Tractor-trailer truck	88.7	19.0	74.7	11.0	-3.6	8.9	121.9	58.9

Note: 1 kg = 2.2 lb, 1 km/h = 0.621 mph, 1 cm = 0.3937 in.

[a]Maximum acceleration over 50-ms duration obtained from high-speed cine.
[b]Original design test.
[c]Cine analysis not performed for test 12 because of data camera malfunction; values shown are from speed trap, tire mark measurements, or accelerometers.

Figure 3. Comparison of vehicle roll in tests 9 and 11.

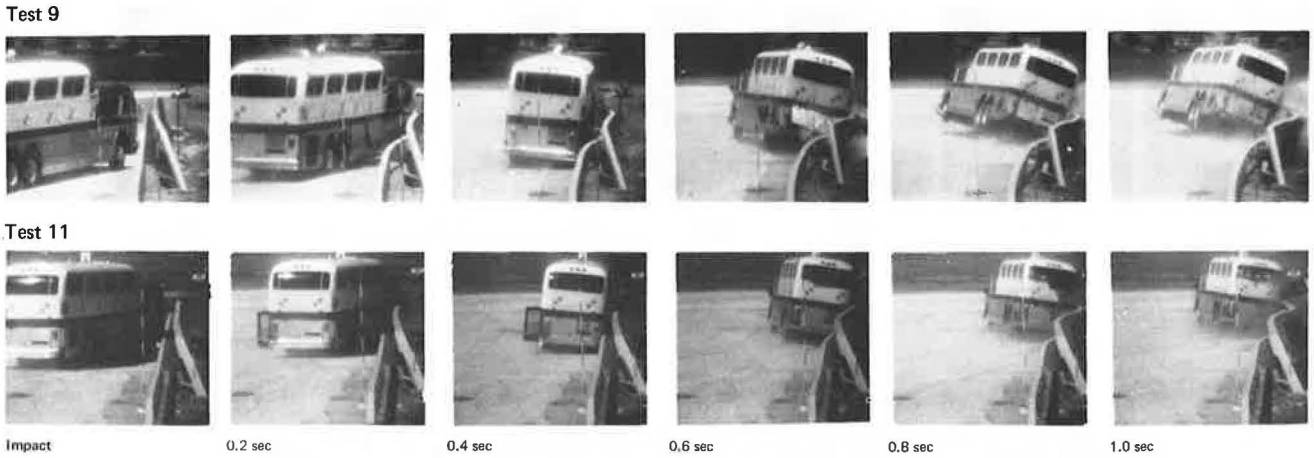

Figure 4. Summary of results for full-scale crash test 12.

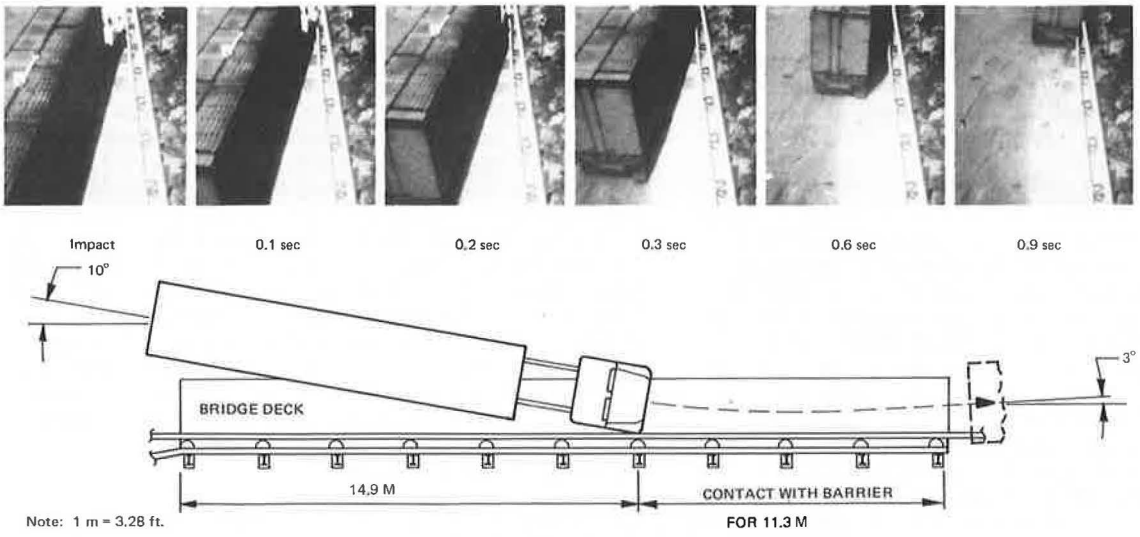

Figure 5. Summary of results for full-scale crash test 13.

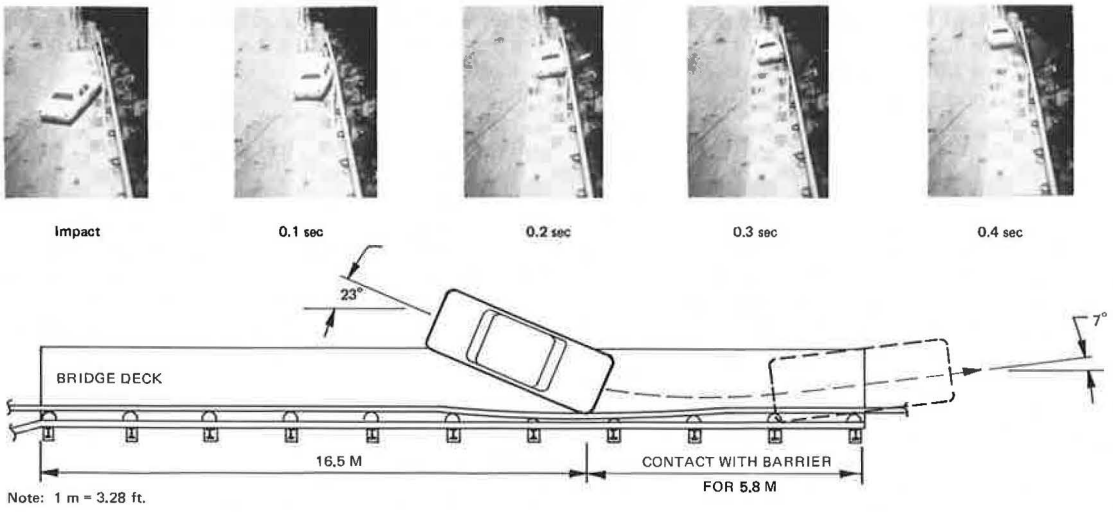

Figure 6. Summary of results for full-scale crash test 14.

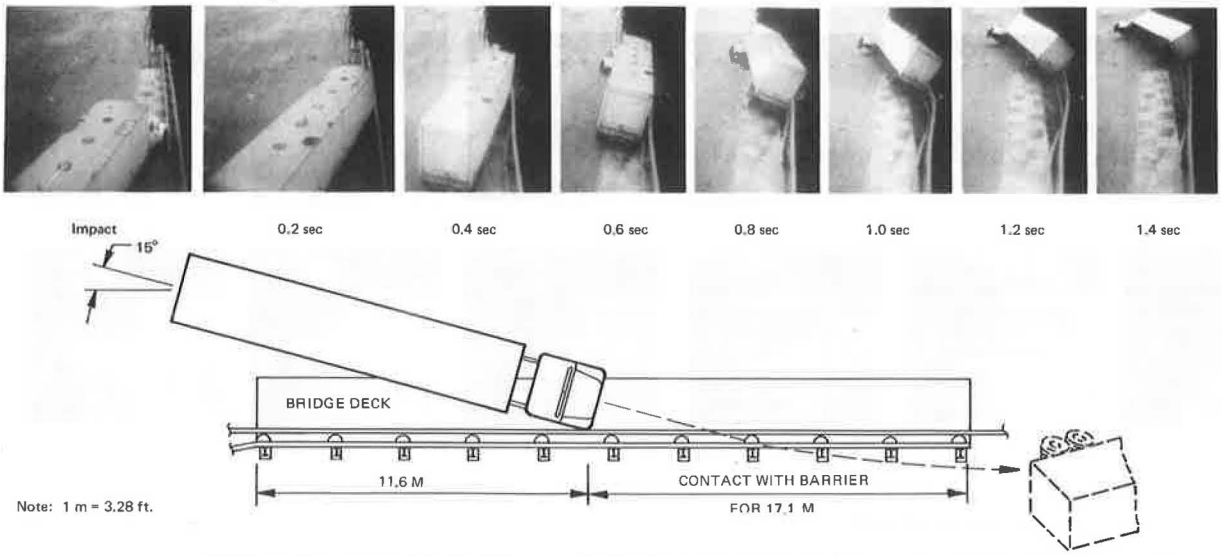

laterally (as designed); maximum baseplate displacement was 54.9 cm (21.6 in). The vehicle was drivable following the test and returned from the test site to Southwest Research Institute under its own power.

Test 12

The 31 751-kg (70 000-lb) tractor-trailer truck containing 21 319 kg (47 700 lb) of ballast consisting of 45-kg (100-lb) bags of sand evenly distributed on the trailer floor impacted the front rail at post 7 with a speed of 71.4 km/h (44.4 mph) and an impact angle of 10 deg. As shown in Figure 4, the truck partially collapsed the rings in the impact zone and rolled toward the rail, and the trailer contacted the top rail continuously between posts 7 and 10. Then the redirected truck returned to an upright position and was braking to a stop when the tractor veered to the right about a hundred meters downstream of the bridge deck. This severe turn caused the trailer to overturn onto its left side; the tractor remained upright as the frame twisted 90 deg. Maximum accelerations were 5.0 longitudinal g and 3.0 lateral g; maximum permanent deflections were 24.6 cm (9.7 in) on the front rail and 1.27 cm (0.5 in) on the top rail. Inspection of the inboard baseplate bolts (two per post) revealed that those of post 8 had failed in tension and those of posts 5 through 10 were loose, which indicates that some elongation had occurred. No lateral displacement of the post baseplates was observed.

Test 13

The 1996-kg (4400-lb) Ford Custom Sedan impacted the damaged front rail (installation damage of test 12 was not repaired) 0.9 m (3 ft) upstream of post 8 at a speed of 99.8 km/h (62.0 mph) and a 22.7-deg angle as shown in Figure 5. The vehicle completely collapsed the ring on post 8 and was smoothly redirected. Maximum 50-ms average accelerations were 5.3 longitudinal g and 7.7 lateral g; maximum permanent deflections were 2.3 cm (0.9 in) on the top rail, 3.8 cm (1.5 in) on the mid rail, and 48.3 cm (19.0 in) on the front rail. The inboard baseplate bolts of post 9 failed in tension (those of post 8 had failed in the previous test), and posts 7, 8, and 9 were displaced laterally. Maximum displacement was 26.7 cm (10.5 in).

Test 14

The 18 144-kg (40 000-lb) tractor-trailer truck containing 9072 kg (20 000 lb) of ballast evenly distributed on the trailer floor impacted the front rail midway between posts 5 and 6 at a speed of 91.7 km/h (57 mph) and a 15.6-deg angle and initiated a slight roll toward the barrier as it was redirected. This roll continued as the trailer impacted the two upper rails which caused the entire rig to roll onto its right side as shown in Figure 6. Maximum 50-ms average accelerations were 1.1 longitudinal g and 7.8 lateral g. The inboard baseplate bolts of posts 3 through 11 failed in tension and those posts were displaced laterally; maximum displacement was 135.6 cm (53.4 in). In addition, the front rail and guardrail and guardrail posts downstream of the bridge deck failed.

DISCUSSION OF RESULTS

Analysis of these four additional tests (tests 11 through 14) revealed six things.

1. The modified or translating basepost design was effective in reducing heavy vehicle roll angles. A comparison of the modified and original designs revealed that the vehicles reached a maximum roll angle of 20° and 8° for tests 9 and 11 respectively.
2. Although the end results of tests 10 and 14 were similar (vehicle rollover), the rollover that occurred during test 14 was much less violent and is attributed partially to an unanchored end. A downstream end anchor similar to that at the upstream end is recommended.
3. The modified post provides forgiving stroke when less than the total 45.7-cm (18-in) stroke of the ring is available for energy absorption. This was demonstrated in test 13 when the vehicle impacted a partially deflected, previously damaged barrier and caused no significant increase in vehicle accelerations over those recorded in similar tests.
4. The CRBRS can restrain articulated vehicles weighing up to 31 751 kg (70 000 lb) in 72.4-km/h (45-mph), 10-deg collisions and 18 144 kg (40 000 lb) in 88.5-km/h (55-mph), 14-deg impacts.
5. Successful redirection of an 18 144-kg (40 000-lb) intercity bus in an 86.9-km/h (54-mph) impact at 15 deg was demonstrated. This vehicle was able to be started and driven away from the test site.
6. System repair costs were less for the modified

CRBRS because the same posts were used for all four tests (no post damage was sustained) and only rail sections and rings required replacement.

REFERENCES

1. C. E. Kimball, M. E. Bronstad, J. D. Michie, J. A. Wentworth, and J. G. Viner. Development of a New Collapsing-Ring Bridge Rail System. TRB, Transportation Research Record 566, 1976, pp. 31-43.
2. C. E. Kimball, M. E. Bronstad, J. D. Michie, J. A. Wentworth, and J. G. Viner. Development of a New Collapsing Ring Bridge Rail System. Federal Highway Administration, Rept. FHWA-RD-76-39, Jan. 1976.

Abridgment

Test Evaluation of Tubular Thrie Beam for Upgrading Concrete Bridge Railing

C. E. Kimball, E. O. Wiles, and J. D. Michie, Southwest Research Institute, San Antonio, Texas

Many existing bridge railings were designed and installed before the recent emphasis on vehicle containment and redirection safety. Under a program sponsored by the Federal Highway Administration (FHWA), we have investigated the safety performance of existing bridge railing systems and have developed retrofit designs that will improve the safety performance of the more prevalent installations. The retrofit design described and evaluated in this paper is believed applicable to a large percentage of those concrete baluster installations that do not have curbs or walkways projecting beyond the face of the concrete railing.

DESIGN FEATURES

The primary element of the design is a new beam rail element known as the tubular Thrie beam. It is fabricated by welding two Thrie (or triple corrugated) beams together as shown in Figure 1. The beam is joined to and blocked out from the concrete baluster rail by 15.24-cm-diameter (6-in-diameter) collapsing rings spaced at 2.54 m (8.33 ft); no attempt was made to space the rings to the concrete post in the test installation. Dimensions of the 15.24-cm-diameter (6-in-diameter), 317-cm-thick (0.125-in-thick) by 55.9-cm-long (22-in-long) rings were established by the equation

$$\text{Dynamic ring energy absorbed} = 4.8\ \sigma_o W t^2 \qquad (1)$$

that was empirically established from another FHWA program (1). In this equation, a design energy of 677 909 kJ (60 000 in·lb) was used with a static initial yield stress σ_o of 248 MPa (36 kip/in^2) and ring width W of 55.9 cm (22 in); required ring thickness t in centimeters was determined.

The tubular Thrie beam was extended 2.54 m (8.33 ft) upstream from the bridge end and transitioned to a single Thrie beam that was structurally anchored.

Publication of this paper sponsored by Committee on Safety Appurtenances.

There are four principal attributes of the retrofit design.

1. The 50.8-cm-wide (20-in wide) tubular Thrie section provides a large contact area with the impacting vehicle, which ensures probable contact with the vehicle hard points and minimizes knifing of the beam into the car structure and snagging potential. Also mounting height for optimum contact with a range of vehicles is less critical.
2. The collapsing rings and relatively stiff beam reduce the intensity and distribute impact forces over an increased length of existing bridge railing, which permits upgrading of otherwise understrength installations.
3. The design is somewhat flexible in its adaptation to existing installations.
4. The design encroaches only 30.5 cm (12 in) into existing bridge deck space, which is a most important consideration for narrow bridges.

Although an upstream terminal was not evaluated, the tubular Thrie beam design is considered an integrated bridge railing that is made up of terminal, approach railing, transition, and bridge railing. Baluster rail and retrofit are shown in Figure 2.

TEST PROGRAM

Five tests were performed by using test procedures outlined in National Cooperative Highway Research Program Report 153 (2). Two base-line tests (tests 3 and 4) were performed with the concrete baluster rail with no retrofit. The tubular Thrie beam system was then installed, and two tests (tests 5 and 6) were performed by using the same conditions of tests 3 and 4. Test 7 was a test of the transition from the tubular Thrie beam to a single Thrie that was used as the approach guardrail to the bridge. A summary of test results is given in Table 1.

Test 3

The 2041-kg (4500-lb) 1972 Ford Galaxie impacted the

concrete baluster rail at 97.0 km/h (60.3 mph) and a 30.0-deg angle. As shown in Figure 3, the vehicle impacted the installation approximately 4.3 m (14 ft) upstream of the end post, broke posts 8 and 9 (posts are numbered consecutively beginning at the upstream end), and caused the rail member downstream of posts 7 and 8 to form a plastic hinge that allowed partial penetration of the vehicle through the rail. Maximum 50-ms average accelerations were 10.7 longitudinal g and 12.3 lateral g.

Test 4

The 966-kg (2130-lb) Toyota Corona impacted the concrete baluster rail at 91.7 km/h (57.0 mph) and a 15.5-deg angle. As shown in Figure 4, the vehicle impacted the installation 7.0 m (23 ft) upstream of the end post and

Figure 1. Tubular Thrie beam retrofit.

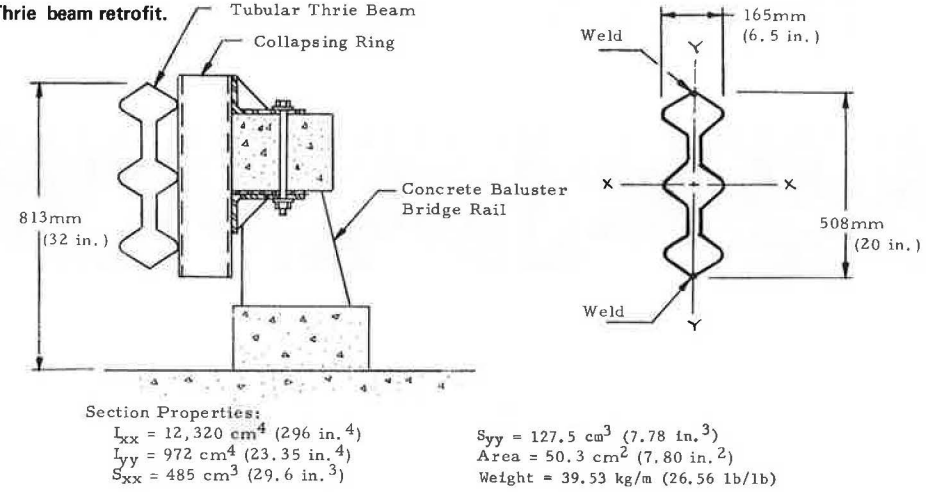

Figure 2. Concrete baluster rail with tubular Thrie beam retrofit.

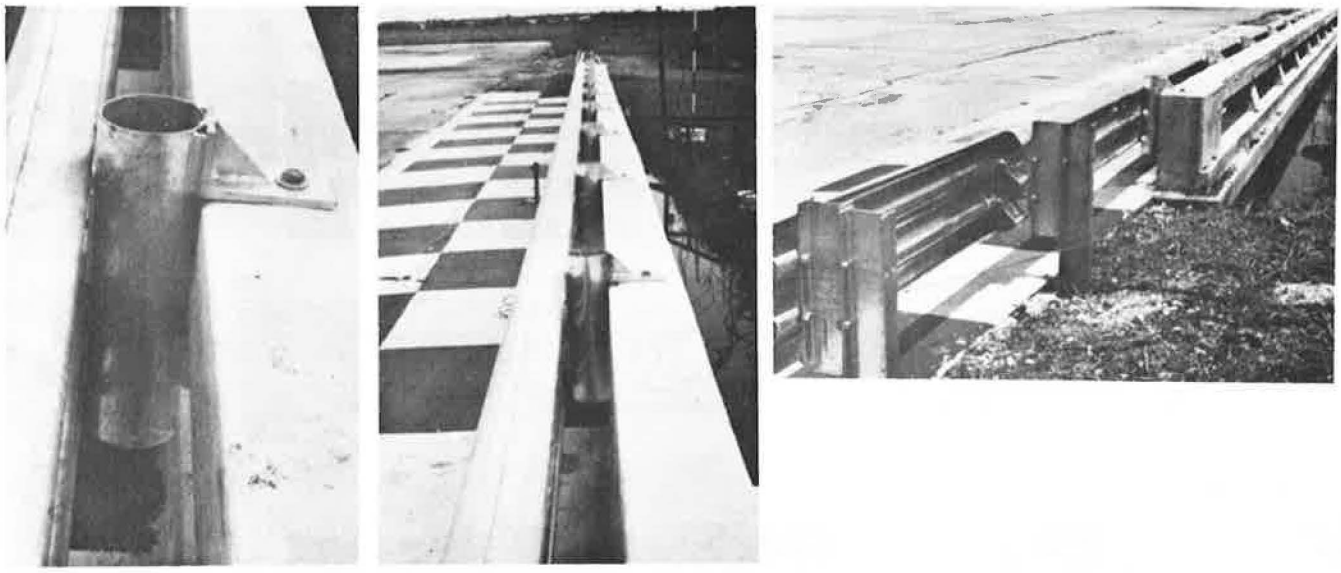

Table 1. Summary of findings.

Test Number	Vehicle Mass (kg)	Impact Speed (km/h)	Impact Angle (deg)	Vehicle Exit Conditions		Max Avg. Vehicle Accelerations[a]		Max Permanent Rail Deflection (cm)
				Angle (deg)	Speed (km/h)	Longitudinal (g)	Lateral (g)	
3	2041	97.0	30.0	2.0	49.6	10.7	12.3	–
4	966	91.7	15.5	5.8	74.0	6.7	8.6	–
5	1021	93.3	17.1	6.8	86.9	4.1	8.4	1.27
6	2041	97.5	25.0	6.0	82.0	5.9	11.7	12.7
7	2132	96.7	25.0	10.0	77.2	5.0	10.0	54.9

Notes: 1 kg = 2.205 lb. 1 km/h = 0.621 mph. 1 cm = 0.3937 in.

[a]Maximum acceleration over 50-ms duration obtained from accelerometers or high-speed cine.

was smoothly redirected. Maximum 50-ms average accelerations were 6.7 longitudinal g and 8.6 lateral *g*.

Test 5

Test 5 was the initial test of the tubular Thrie beam retrofit system. The vehicle used was a 1021-kg (2250-lb) 1971 Ford Pinto, and impact conditions were 93.3 km/h (58.0 mph) and a 17.1-deg angle. As shown in Figure 5, the vehicle impacted midway between rings 5 and 6 (rings are numbered consecutively beginning at the upstream end) and was smoothly redirected. Maximum 50-ms average accelerations were 4.1 longitudinal *g* and 8.4 lateral *g*; maximum permanent rail deflection was 1.27 cm (0.5 in). The vehicle was driven back to the impact area after the test.

Test 6

The 2041-kg (4500-lb) 1973 Mercury Monterrey impacted the tubular Thrie beam installation at 97.5 km/h (60.6 mph) and a 25-deg angle. As shown in Figure 6, the vehicle impacted midway between rings 5 and 6, partially collapsed those rings, and was smoothly redirected.

Figure 3. Summary of test 3 results.

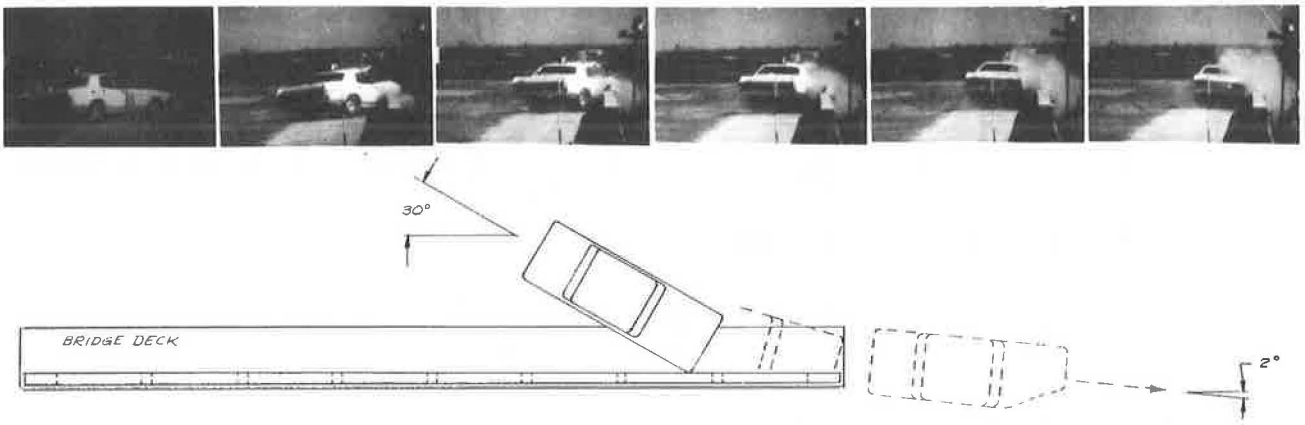

Figure 4. Summary of test 4 results.

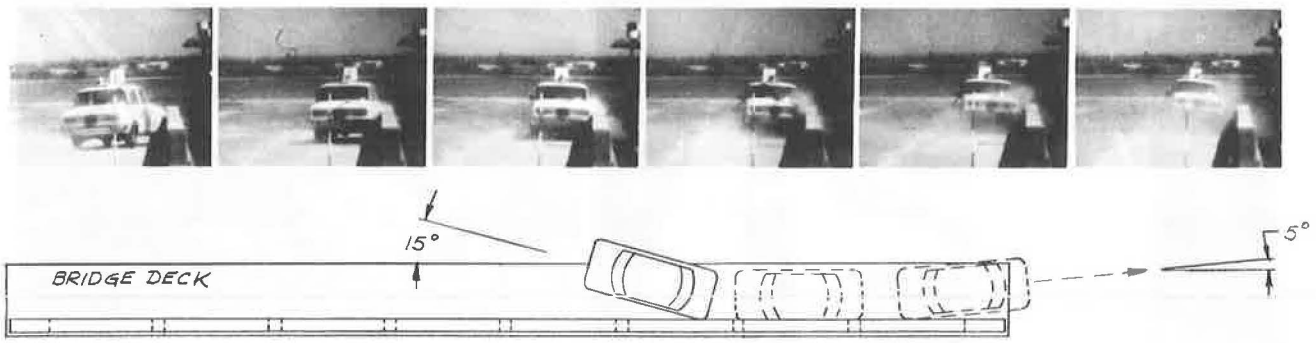

Figure 5. Summary of test 5 results.

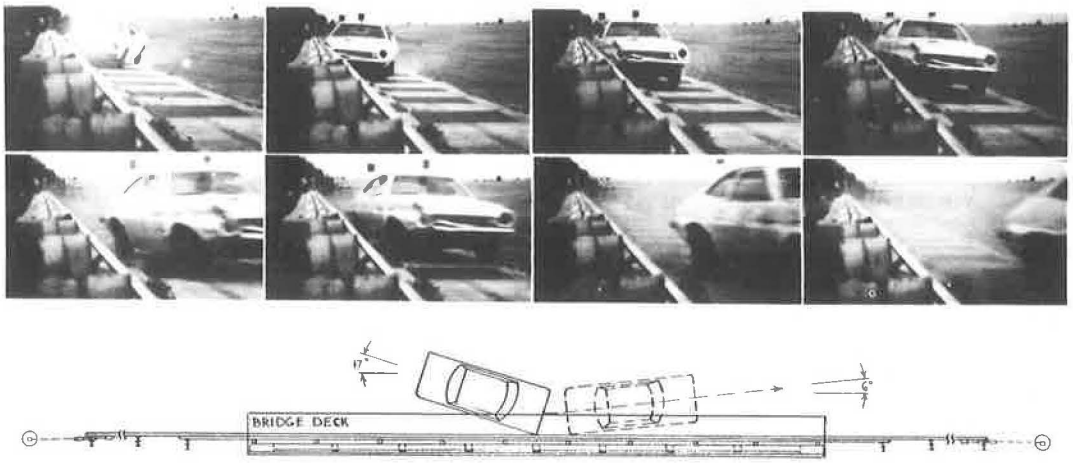

Figure 6. Summary of test 6 results.

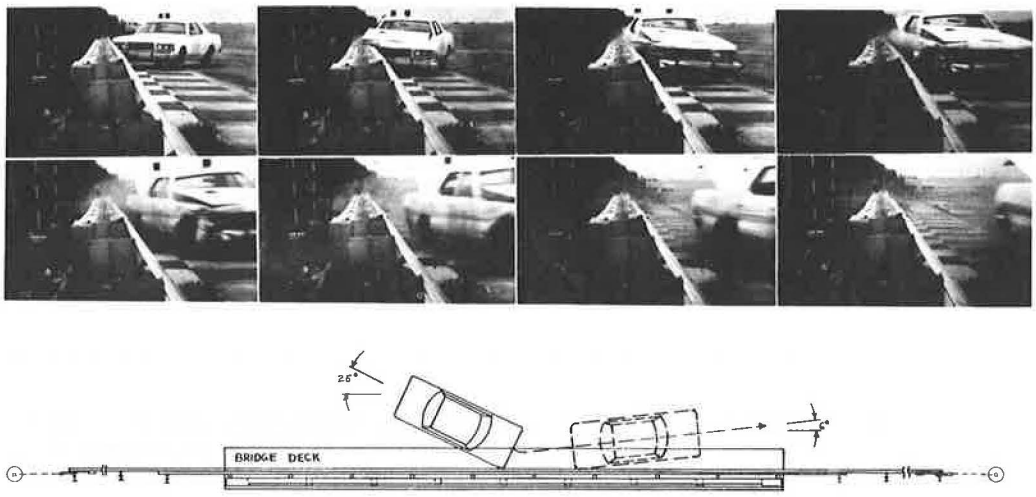

Figure 7. Summary of test 7 results.

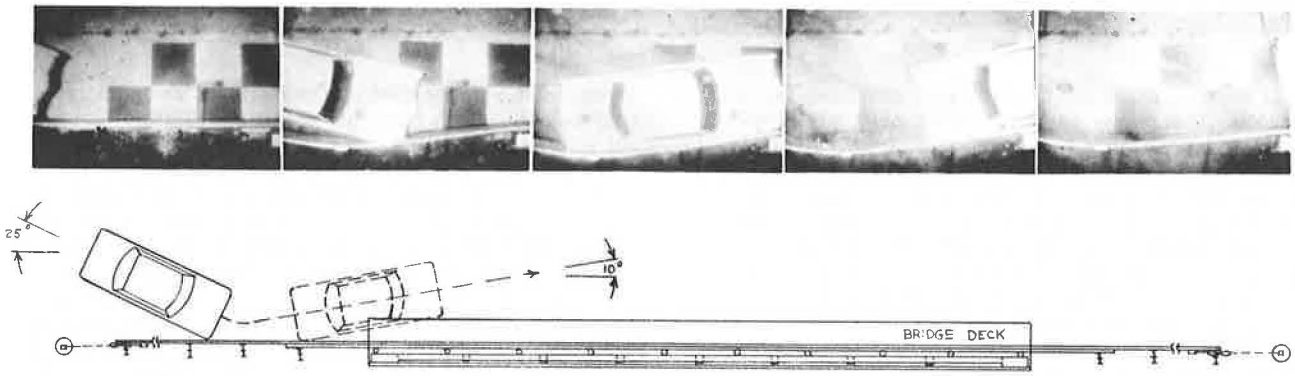

Maximum 50-ms average accelerations were 5.9 longitudinal *g* and 11.7 lateral g; maximum permanent rail deflection was 12.7 cm (5.0 in). The vehicle was driven back to the impact area after the test.

Test 7

The 2132-kg (4700-lb) 1969 Cadillac Sedan deVille impacted the single Thrie beam rail in the transition area at 96.7 km/h (60.1 mph) and a 25-deg angle. As shown in Figure 7, the vehicle impacted the rail 1.4 m (4.6 ft) upstream of the second guardrail post off the bridge deck and was smoothly redirected. Maximum 50-ms average accelerations were 5.0 longitudinal g and 10.0 lateral *g*; maximum permanent rail set was 54.9 cm (21.6 in) after reaching a maximum dynamic deflection of 111.2 cm (43.8 in). The vehicle was driven back to the impact area after the test.

CONCLUSIONS

Analysis of data taken from these tests revealed that

1. The tubular Thrie beam increases the strength of the bridge rail;
2. Damage to the vehicle is greatly reduced [all three vehicles tested with the tubular Thrie beam (tests 5, 6, 7) were drivable after the tests];
3. The single Thrie beam to tubular Thrie beam provides a continuous effective guardrail to bridge rail transition; and
4. The tubular Thrie beam and collapsing ring system is an effective retrofit system that minimally encroaches into the bridge deck.

From these findings and results, we believe that the tubular Thrie beam retrofit design is suitable for in-service performance demonstration.

REFERENCES

1. N. Perrone. Thick-Walled Rings for Energy-Absorbing Bridge Rail Systems. Federal Highway Administration, Rept. FHWA-RD-73-49, Dec. 1972.
2. M. E. Bronstad and J. D. Michie. Recommended Procedures for Vehicle Crash Testing of Highway Appurtenances. NCHRP, Rept. 153, 1974.

Abridgment

Dynamic Tests of Breakaway Lighting Standards by Using Small Automobiles

R. F. Prodoehl, J. P. Dusel, Jr., and J. R. Stoker, Division of Structures and Engineering Services, California Department of Transportation

The triangular steel multidirectional slip base for use on lighting standards was first developed and successfully tested in 1967 by the Texas Transportation Institute (TTI) (1). In 1968, the California Division of Highways performed a series of full-scale dynamic impact tests to evaluate the effectiveness of various types of breakaway devices used on 8.7-m-high (28.5-ft-high) lighting standards with 3.6-m-long (12-ft-long) mast arms, and, in two of the tests, a modified version of the original multidirectional slip base was used. Under the conditions of the 1968 California test, the modified multidirectional slip base proved to be an extremely effective breakaway device when impacted at both high and low speeds by a large automobile and was considered superior to the other designs tested in that series (2).

Since the developmental slip base tests performed by TTI and the California Division of Highways, changes have occurred in slip base and lighting standard design, and the size and weight of the average passenger vehicle have decreased. Lighting standard design changes include larger diameter, thicker walled standards with longer mast arms. Changes in slip base design include use of a keeper plate to prevent base "walking" during heavy wind loads, smaller diameter high-strength slip base clamping bolts, higher clamping bolt tensions, and use of hot-dip galvanized slip base parts. The effects of these changes on the performance of the slip base, especially when impacted by a small automobile, were unknown.

RESEARCH SUMMARY

The objective of this project was to determine the effectiveness of the slip base currently used by the California Department of Transportation on long-masted (type 31) steel lighting standards when subjected to full-scale impact tests by small automobiles. Impact test procedures as specified by the National Cooperative Highway Research Program (3) were followed throughout this project.

Before full-scale impact tests were performed, a study was performed to determine the torque-tension relationship for 22.2-mm-diameter (7/8-in-diameter) galvanized A325 slip base clamping bolts. A curve showing this relationship was developed and used to establish the average applied torque values required to attain the specified design bolt tensions (clamping forces). After the preliminary bolt torque-tension investigation, two impact tests (tests 311 and 312) were conducted. In each test a Ford Pinto weighing 1027 kg (2265 lb) and a slip base assembly on a 10.7-m-high (35-ft-high), 450-kg (992-lb) California Department of Transportation type 31 steel lighting standard were used. The length of the mast arm was 9.1 m (30 ft). The impact speed of the vehicle and the tension in the slip base clamping bolts were important factors in both tests. A higher clamping force is required where longer mast arms are employed to prevent separation of the slip base plates that can occur because of wind loads.

The operation of the slip base and trajectory of the lighting standard were observed at both low, 7.8-m/s (17.5-mph), and medium, 15.4-m/s (34.5-mph), vehicle impact speeds. Strain gauges in each of the three slip base clamping bolts enabled individual bolt tensions, 88.1 kN (19 800 lb) and 67.2 kN (15 100 lb) for crash tests 311 and 312 respectively, to be measured just before each impact test. In both tests, the vehicle and dummy driver were instrumented with accelerometers at critical points so that motion and deceleration data could be recorded and used to determine impact severity. Time intervals between recorded electrical impulses from tape switches mounted on the ground at known distances were used to calculate vehicle speed at various instants during the impact tests.

Table 1 gives a summary of the results of impact tests 311 and 312. The Transportation Laboratory of the California Department of Transportation has written a detailed report (4) of the research performed.

Publication of this paper sponsored by Committee on Safety Appurtenances.

Figure 1. Slip base used with type 31 lighting standard in crash tests 311 and 312.

1. 22.2-mm diameter ASTM A325 galvanized clamping bolts (total 3 per slip base) instrumented with strain gages.
2. 22.2-mm diameter HS anchor bolts (total 3 per slip base) cut flush with top of ASTM A564 Grade 2H galvanized nuts to allow top base plate to slip.
3. 12.7-mm thick steel plate washers (2 per clamping bolt, total 6 per slip base).
4. Surface of foundation beneath slip base clamping bolt heads relieved to provide minimum 3.2-mm clearance.
5. Hardened flat washers (1 per clamping bolt - 1 per anchor bolt, total 6 per slip base).
6. .102-mm galvanized steel keeper plate (one per slip base).

Note: 1mm = .0394 in.

Table 1. Summary of results from impact tests 311 and 312.

Item	Test 311	Test 312
Desired velocity of vehicle, m/s	9.2	17.9
Initial velocity of vehicle, m/s (average over a 1.22-m interval before impact)	7.8	15.4
Final velocity of vehicle, m/s (average over a 0.61-m interval after impact)	4.8	12.2
Change in momentum of vehicle during impact, kN·s	3.065	3.318
Time duration of vehicle contact with pole, s	0.181	0.069
Time required for slip base separation, s	0.055	0.028
Front end deformation of vehicle, mm (measured at bumper height)	432	470
Longitudinal deceleration at the center of gravity of vehicle, m/s^2 (50-ms average)	48.5	47.6
Vehicle kinetic energy at impact, kJ	31.3	122.1

Note: 1 m/s = 2.237 mph, 1 m = 3.281 ft, 1 kN·s = 0.000 225 lbf, 1 mm = 0.0394 in, 1 m/s^2 = 0.102 g, 1 kJ = 0.000 738 ft·lbf.

CONCLUSIONS

The following four conclusions are based on results from full-scale tests 311 and 312 of a Ford Pinto automobile impacting a type 31 lighting standard.

1. The triangular steel slip base currently used by the California Department of Transportation on its types 30 and 31 lighting standards is an effective breakaway device when impacted by small automobiles. Even with the heavier pole, the base slips with a relatively low loss in vehicle momentum at both low and moderate vehicle impact velocities, thus offering minimal breakaway resistance at impact.
2. Higher tensions [up to 88.1 kN (19 800 lb)] in the slip base clamping bolts that were almost twice those previously specified by California DOT did not adversely affect the slip characteristics of the base tested.
3. When a small vehicle having a roof impacts a current type 31 lighting standard with a slip base, neither the initial car-pole impact nor the trajectory and final position of the lighting standard are expected to create serious hazards or injuries to either occupants of the impacting vehicle or passengers of vehicles in adjacent traffic lanes.
4. Damages to the small vehicle in both impact tests were limited to the front end and were less than anticipated. Total costs of completely repairing the Pinto following impact test 311 were approximately $730.

RECOMMENDATIONS

The use of the current California DOT slip base design on types 30 and 31 lighting standards as shown on drawings ES-30A and ES-30B of Standard Plans (5, pp. 241 and 242) should be continued with minor modifications as shown below and in Figure 1:

1. Torques on each of the three slip base clamping bolts should be increased to 203 N·m (150 ft·lb) to ensure a long service life by reducing bolt fatigue;
2. The thickness of the rectangular plate washers used at the top and bottom of each slip base clamping bolt should be increased from 7.9 mm (5/16 in) to 12.7 mm (1/2 in) and minimum steel requirements should conform to the requirements of ASTM A 108;
3. A maximum manufacturing tolerance of ±3.2 mm (±1/8 in) should be specified for the 356-mm (14-in) slip base clamping bolt circle diameter of both the upper and lower slip base plates to avoid adverse bending and yielding of plate washers.

ACKNOWLEDGMENTS

This research was accomplished in cooperation with the Federal Highway Administration. The contents of this report reflect the views of the Transportation Laboratory, California Department of Transportation, which is responsible for the facts and the accuracy of the data presented herein, and do not necessarily reflect the official views or policies of the state of California or the Federal Highway Administration.

REFERENCES

1. T. C. Edwards. Multi-Directional Slip Base for Break-Away Luminaire Supports. Texas Transportation Institute, Texas A&M Univ., College Station, Research Rept. 75-10, Aug. 1967.
2. E. F. Nordlin, W. H. Ames, and R. N. Field. Dynamic Tests of Five Breakaway Lighting Standard Base Designs. Materials and Research Department, California Division of Highways, Research Rept. M&R 636408, Oct. 1968.
3. M. E. Bronstad and J. D. Michie. Recommended Procedures for Vehicle Crash Testing of Highway Appurtenances. NCHRP, Rept. 153, 1974.
4. E. F. Nordlin, R. F. Prodoehl, J. P. Dusel, J. R. Stoker. Dynamic Tests of Breakaway Lighting Standards Using Small Automobiles. California Department of Transportation, Rept. CA-DOT-TL-6490-1-75-47, Dec. 1975.
5. Standard Plans. California Department of Transportation, Jan. 1975.

Simplified Analysis of Change in Vehicle Momentum During Impact With a Breakaway Support

Raymond P. Owings and Clarence Cantor, ENSCO, Inc., Springfield, Virginia

The impact of an automobile with a breakaway support for a sign or luminaire can be divided into three phases. By using simplifying assumptions, one can determine the contribution to change in vehicle momentum (ΔMV) by each phase. The first phase involves the crushing of the automobile with negligible motion of the support. The second phase considers the contribution to ΔMV by base fracture. The third phase considers the contribution to ΔMV by the acceleration of the pole. The results of this analysis are that vehicle change in momentum can be approximated by an equation that has provided valuable insight into the effect of vehicle stiffness, breakaway force level, base fracture energy, pole inertial properties, and vehicle impact speed on ΔMV. This knowledge has facilitated the subsequent development of practical laboratory acceptance test criteria to promote safer sign and luminaire supports.

The performance of a breakaway support for a sign or luminaire is a function of the change in vehicle momentum (ΔMV) produced during impact with the support. The reason for this is that immediately after impact the velocity of an unrestrained occupant relative to the vehicle interior is about the same as the change in velocity of the vehicle. Current Federal Highway Administration (FHWA) and American Association of State Highway and Transportation Officials (AASHTO) criteria (1, 2) set a limit of 4890 N·s (1100 lbf·s) for acceptable ΔMV in full-scale tests.

In order to develop practical laboratory acceptance test criteria, ENSCO conducted a study for FHWA that involved analysis, computer simulation, laboratory tests, full-scale tests, and the correlation of all results. This study has enabled the development of practical laboratory methods of testing breakaway supports to ensure their effectiveness. Owings, Cantor, and Adair, in a paper in this Record, give some of the background on laboratory acceptance testing. The simplified analysis of this paper forms part of that background.

Publication of this paper sponsored by Committee on Safety Appurtenances.

ANALYSIS OF IMPACT

The following simplified analysis provides a better understanding of the phenomenon of impact by an automobile with a sign or luminaire support. One major assumption in the analysis is that the support pole can be considered a rigid body. Other assumptions will be described when they are introduced. The essential validity of these assumptions, with regard to vehicle change in momentum, is confirmed by the good correlation of predicted results from this analysis with those of computer-simulated, laboratory, and full-scale tests as shown by Owings, Cantor, and Adair in a paper in this Record.

If one neglects tire-roadway forces, the momentum change experienced by a vehicle during impact is given by

$$\Delta MV = \int_0^{t_3} F_c \, dt \qquad (1)$$

where

t_3 = time to loss of contact between vehicle and fractured support and
F_c = force exerted by the support on the vehicle.

To facilitate the evaluation of this impulse integral, the impact is divided into three phases. The first phase, from $t = 0$ to $t = t_1$, is characterized by the crushing of the automobile with negligible motion imparted to the support. The second phase, from $t = t_1$ to $t = t_2$, involves the contribution to ΔMV provided by the fracture of the base. The third phase, from $t = t_1$ to $t = t_3$, considers the contribution to ΔMV that is inherent in the momentum imparted to the support.

Figure 1 shows the geometry of impact; Figure 2 shows the three phases of impact. During the first phase of the impact, the work done in crushing the automobile is equal to the change in kinetic energy of the automobile and can be expressed as

$$\int_0^{x_1} F_c \, dx = 0.5M (V_0^2 - V_1^2) \qquad (2)$$

where

X_1 = maximum crush deformation of the automobile,
M = mass of the impacting vehicle,
V_0 = impact speed, and
V_1 = speed at the end of the first phase of the impact.

Equation 2 can be rewritten as

$$\int_0^{X_1} F_c\,dx = M\Delta V_1 V_0/\beta \tag{3}$$

where

$\Delta V_1 \equiv V_0 - V_1$, and
$\beta \equiv [1 - (\Delta V_1/2V_0)]^{-1}$.

But the contribution to ΔMV during the first phase is simply

$$I_1 = \int_0^{t_1} F_c\,dt = M\Delta V_1 \tag{4}$$

Combining equations 3 and 4 yields

$$I_1 = \beta/V_0 \int_0^{X_1} F_c\,dx = \beta E_c/V_0 \tag{5}$$

where $E_c \equiv \int_0^{X_1} F_c dx$ = crush energy.

The value of β is always greater than unity. For moderate velocity change during the first phase, however, β is close to unity and may be regarded as more or less constant. For example, if V_0 = 32.2 km/h (20 mph) and if ΔV_1 = 9.7 km/h (6 mph), then β = 1.18. A representative value of β, for the range of acceptable impacts, is 1.1. Thus the contribution to ΔMV by the first phase can be considered proportional to the energy of vehicle crush (up to breakaway force level F_1) and inversely proportional to impact speed V_0. (Although β is treated as a constant for establishing the basic trends in the first phase of impact, the exact relationship of I_1 versus E_c can be determined by using the exact definition of β.)

For a linear force-deformation characteristic, E_c can be expressed as

$$E_c = 0.5(KX_1^2) = 0.5(F_1^2/K) \tag{6}$$

where

K = vehicle stiffness and
F_1 = breakaway force level of base.

In this case, equation 5 can be expressed as

$$I_1 = \beta F_1^2/2V_0K \tag{7}$$

For a nonlinear force-deformation characteristic, a parameter ω can be introduced as defined in Figure 3. In this case,

$$E_c = 0.5(\omega KX_1^2) = 0.5[\omega(F_1^2/K)] \tag{8}$$

where

$K \equiv F_1/X_1$ = equivalent vehicle stiffness and
F_1 = breakaway force level of base.

Thus equation 5 can be expressed as

$$I_1 = \beta\omega F_1^2/2V_0K \tag{9}$$

This illustrates how a large breakaway force level and low vehicle stiffness can increase the contribution to ΔMV during the first phase.

As shown in Figure 2, the contribution to ΔMV by the second phase (base fracture) is

$$I_2 = \int_{t_1}^{t_2} F_b\,dt \tag{10}$$

which can be rewritten as

$$I_2 = \int_{t_1}^{t_2} F_b\,d\delta/\dot{\delta} \tag{11}$$

where δ = base displacement relative to foundation. At the beginning of base separation ($t = t_1$), the displacement velocity $\dot{\delta}$ is zero and, from physical considerations, cannot change abruptly. (A step function change in $\dot{\delta}$ together with finite inertia of the support would require an infinite force.) After base separation (at $t = t_2$), $\dot{\delta}$ will be close to vehicle velocity V_2, which in turn is some large fraction of the initial impact speed V_0 (if one assumes a relatively small ΔV). This can be expressed as

$$\dot{\delta}(t_2) = \gamma V_0 \tag{12}$$

An average value for γ, over a range of acceptable impacts, is 0.8.

A reasonable form for $\dot{\delta}$, from $t = t_1$ to $t = t_2$, would be a linearly increasing function of time; that is,

$$\dot{\delta} = \gamma V_0\,[(t - t_1)/(t_2 - t_1)], \qquad t_1 \leq t \leq t_2 \tag{13}$$

or

$$\dot{\delta} = \gamma V_0\,(\tau/\tau_m), \qquad 0 \leq \tau \leq \tau_m \tag{14}$$

where

$\tau \equiv t - t_1$ and
$\tau_m = t_2 - t_1$.

Integrating equations 13 and 14 results in

$$\delta(\tau) = (\gamma V_0/2\tau_m)\,\tau^2 + C_1 \tag{15}$$

Because $\delta(0) = 0$, the integration constant $C_1 = 0$. Thus

$$\delta(\tau) = (\gamma V_0/2\tau_m)\,\tau^2, \qquad 0 \leq \tau \leq \tau_m \tag{16}$$

At base separation ($\tau = \tau_m$), maximum displacement can be expressed as

$$\delta_m = (\gamma V_0/2)\,\tau_m \tag{17}$$

By using equations 16 and 17, one can express τ as

$$\tau = (2/\gamma V_0)\sqrt{[\delta_m \delta(\tau)]} \tag{18}$$

Substituting equations 17 and 18 into equations 13 and 14 yields

$$\dot{\delta}(\tau) = \gamma V_0 \sqrt{\delta(\tau)/\delta_m} \tag{19}$$

The integral I_2 of equation 11 can now be expressed in

terms of displacements. Thus

$$I_2 = \sqrt{\delta_m}/\gamma V_0 \int_0^{\delta_m} F_b(\delta)d\delta/\sqrt{\delta} \tag{20}$$

To evaluate equation 20 requires knowledge of the base breakaway characteristic $F_b(\delta)$. In general, $F_b(\delta)$ has a maximum value F_1 at $\delta = 0$, and the value of F_b decreases to zero when $\delta = \delta_m$. One reasonable form for the breakaway characteristic is a linearly decreasing function; that is,

$$F_b(\delta) = F_1[1 - (\delta/\delta_m)], \quad 0 \leq \delta \leq \delta_m \tag{21}$$

Substituting equation 21 into equation 20 and performing the integration yield finally

$$I_2 = (4/3)(F_1\delta_m/\gamma V_0) \tag{22}$$

Because, for this particular base characteristic, BFE = $0.5 F_1\delta_m$, this is equivalent to

$$I_2 = 8/3[(BFE)/\gamma V_0] \tag{23}$$

The result for I_2, as expressed in equation 23, can be shown to be not very sensitive to the form of the assumed base characteristic. For example, assume that the base had a characteristic that remains constant up to breakaway; that is,

$$F_b(\delta) = F_1, \quad 0 \leq \delta \leq \delta_m \tag{24}$$

Then substituting this characteristic in equation 20 and performing the integration yield

$$I_2 = 2(BFE)/\gamma V_0 \tag{25}$$

Thus the drastic change from a triangular to a square wave characteristic only changes the coefficient in equation 23 from 8/3 to 2, which is a change of only 25 percent in the momentum associated with the base fracture phase. Because the triangular characteristic is much closer to a typical base characteristic than the square wave is, equation 23 will be used for studying the contribution to ΔMV of base fracture.

Let us now turn to I_3, the contribution to ΔMV required for acceleration of the support. Figure 2 shows that

$$I_3 = \int_{t_1}^{t_3} (F_c - F_b)dt \tag{26}$$

The force $F_c - F_b$ is the net force acting on the pole, at an approximate distance D_o below the center of gravity, which accelerates the pole in both translation and rotation. The equations of motion are

$$F_c - F_b \equiv F_p = M_p \ddot{X}_{cg} \tag{27}$$

and

$$F_p D_0 = I_p \ddot{\theta} \tag{28}$$

where

M_p = mass of support and
I_p = moment of inertia of support about its center of gravity.

At time t_3 (when the support and automobile lose contact), the bottom of the support has attained a velocity that is denoted by V_3. From kinematics,

$$V_3 = \dot{X}_{cg} + D_0\dot{\theta} \tag{29}$$

From equations 27 and 26,

$$\dot{X}_{cg} = 1/M_p \int_{t_1}^{t_3} F_p\,dt = (1/M_p)I_3 \tag{30}$$

From equations 28 and 24,

$$\dot{\theta} = D_0/I_p \int_{t_1}^{t_3} F_p\,dt = (D_0/I_p)I_3 \tag{31}$$

Substituting equations 30 and 31 into equation 29 yields

$$V_3 = I_3[(1/M_p) + (D_0^2/I_p)] \tag{32}$$

Because $I_p = M_pR^2$ where R = radius of gyration of the support about its center of gravity, equation 32 can be written as

$$V_3 = I_3[(R^2 + D_0^2)/M_pR^2] \tag{33}$$

or

$$I_3 = M_pV_3[R^2/(R^2 + D_0^2)] \tag{34}$$

The velocity V_3 of the support bottom will be greater than the vehicle velocity V_2 at base separation because of the presence of some elasticity in vehicle crush and pole deformation. The vehicle velocity V_2 will be less than the initial impact velocity V_0 although, for an acceptable impact, V_2 will be fairly close to V_0. From empirical data on typical impacts with breakaway supports, it is estimated that V_3 can be expressed as

$$V_3 = \alpha V_0 \tag{35}$$

where $\alpha \approx 1.1$. The actual value of α will vary depending on the elasticity of the impact, the severity of the impact, and the mass of the vehicle. However, the use of a constant, representative value for α has permitted the development of simplified predictive techniques for ΔMV, which have subsequently proved quite reliable.

Thus the final expression for I_3 becomes

$$I_3 = M_p\alpha V_0[R^2/(R^2 + D_0^2)], \quad \alpha \approx 1.1 \tag{36}$$

Unlike I_1 and I_2, the momentum change I_3 is proportional to initial impact speed V_0. The integral I_3 is also proportional to support mass M_p and to the support inertial ratio

$$r \equiv R^2/(R^2 + D_0^2) \tag{37}$$

The value of r will generally lie between 0.25 and 0.5 as shown by the following. First, consider the case of a long, slender member of length L with uniform mass distribution. In this case, the radius of gyration is $R = L/\sqrt{12}$. $D_0 = 0.5L$, and the value of r becomes

$$r \triangleq R^2/(D_0^2 + R^2) = 0.25 \tag{38}$$

Next, consider the mass to be distributed as two point masses, each 0.5M, located at the ends of the support. In this case, the moment of inertia is given by

$$I = 2(0.5M)(L/2)^2 = ML^2/4 \tag{39}$$

Then R = L/2. Because D_0 is again equal to L/2, we have

$$r = R^2/(R^2 + D_0^2) = 0.5 \quad (40)$$

The value of r ranges between 0.25 and 0.5 for cases ranging from uniform mass distribution to equally lumped masses at the end points.

Note that the support inertial ratio r inherently determines the ratio of support center of gravity velocity to base velocity as shown by the following. Eliminating I_3 between equations 34 and 31 yields

$$\dot{\theta} = D_0 V_3/(R^2 + D_0^2) \quad (41)$$

Substituting this into equation 29 and solving for $\dot{X}_{cg}$ yield

$$\dot{X}_{cg} = rV_3 \quad (42)$$

or

$$\dot{X}_{cg}/V_3 = r \quad (43)$$

Thus the support inertial ratio r determines the form of the support trajectory after breakaway in addition to affecting the inertial contribution to ΔMV. A lower value of r implies less motion of the support center of gravity relative to the base after breakaway.

In summary, the expression for the total momentum change is given by

$$\begin{aligned}\Delta MV &= I_1 + I_2 + I_3 \\ &\approx [\beta\omega(F_1^2/2KV_0)] + \left\{8/3[(BFE)/\gamma V_0]\right\} \\ &\quad + (M_p\alpha V_0)\,[R^2/(R^2 + D_0^2)]\end{aligned} \quad (44)$$

From equation 44, for a given vehicle and support, the relationship between momentum change and impact speed is of the form

$$\Delta MV \approx (a/V_0) + bV_0 \quad (45)$$

where

$a = (\beta\omega F_1^2/2K) + \{8/3\,[(BFE)/\lambda]\}$ and
$b = M_p\alpha[R^2/(R^2 + D_0^2)]$.

Thus for high impact speeds, the inertia of the pole is the dominant term in producing momentum change. For low-speed impacts, the breakaway force F_1, the automobile stiffness K, and the base fracture energy are dominant.

Equation 45 allows us to estimate whether impact of a support is more severe at the high end of a given speed range or at the low end. Figure 4 shows two situations. In Figure 4a, the constants a and b are such that vehicle crush and base breakaway effects dominate and the impact is more severe at low speeds. (This is the case with most luminaires.) In Figure 4b, the inertial characteristics dominate and the impact is more severe at the higher speeds. (This is the case for certain massive sign supports.)

The constants a and b are recognized to be not truly constant because they involve parameters β, γ, and α, which are a function of certain velocities during the various phases of impact. However, for a range of breakaway support performance that includes that of any acceptable support, the variation in these "constants" does not produce significant errors in predicted ΔMV. Fairly good correlation has been obtained with results from computer-simulated, laboratory, and full-scale tests by using average or representative values for the parameters β, γ, and α. The selected values of these parameters have been 1.1 for β, 0.8 for γ, and 1.1 for α.

APPLICATION OF RESULTS

The results of this simplified analysis have been used to gain a better understanding of the impact phenomenon and to predict ΔMV for a given breakaway support and impacting vehicle. Comparison of these predicted results with those of computer-simulated, laboratory, and full-scale tests has shown generally good agreement. This agreement has confirmed the essential validity of equation 45 through the speed range of interest for breakaway support performance. This analytic tool permitted the development of rational and practical laboratory methods for testing breakaway supports as discussed by Owings, Cantor, and Adair in a paper in this Record.

Assume that a breakaway support must perform satisfactorily over a designated speed range of impacting vehicles. Then an examination of equation 45 reveals that the critical (worst) performance occurs either at the low impact speed V_L or at the high impact speed V_H. Thus a check of breakaway performance at both ends of the speed range is sufficient to validate support performance throughout the whole speed range. Furthermore, it will be shown that the results of one low-speed test can be used to predict the high-speed performance with reasonable accuracy (assuming repeatable vehicle crush and breakaway base characteristics). Thus one low-speed test can serve as a check of support performance over the entire speed range of interest.

Let the measured ΔMV at the low impact speed be designated as $(\Delta MV)_L$. Then from equation 45,

$$(\Delta MV)_L = (a/V_L) + bV_L \quad (46)$$

Designating the predicted ΔMV at the high speed as $(\Delta MV)_H$,

$$(\Delta MV)_H = (a/V_H) + bV_H \quad (47)$$

Solving for a in equation 46, and substituting the result into equation 47 yield

$$(\Delta MV)_H = [(V_L/V_H)\,(\Delta MV)_L] + b\,[V_H - (V_L^2/V_H)] \quad (48)$$

Recall that

$$b \triangleq M_p\alpha[R^2/(R^2 + D_0^2)] \quad (49)$$

and $\alpha \approx 1.1$. If the pole inertial parameters and the low-speed test results $(\Delta MV)_L$ are known, then equation 48 can be used to predict the high-speed performance of the breakaway system under evaluation.

The mass M_p and the center of mass D_0 can be easily determined by a weight measurement at each end of a horizontally aligned support. The radius of gyration R about the center of mass can be determined in several ways. One simple way is to suspend the support from either top or bottom and measure its natural period T for a small angle oscillation (<10 deg). Then

$$T = 2\pi\sqrt{I_1/gD_1M_p} \quad (50)$$

where

I_1 = moment of inertia of support about suspension point,
g = acceleration of gravity, and
D_1 = distance from suspension point to center of mass.

We have

$$I_1 = M_p(R^2 + D_1^2) \tag{51}$$

Substituting equation 51 into equation 50 and solving for R yield

$$R = \sqrt{D_1[(gT^2/4\pi^2) - D_1]} \tag{52}$$

The selected speed range for acceptable breakaway support performance is 32.2 to 96.6 km/h (20 to 60 mph). Then equation 48 becomes the following (1 m/s = 3.28 ft/s):

$$(\Delta MV)_H = 1/3\,(\Delta MV)_L + b(23.8\ m/s) \tag{53}$$

where

$b \equiv M_p \alpha r$ and
$\alpha \approx 1.1$.

As previously shown, the value of r for nearly all supports lies in the range of 0.25 to 0.5. If we use the larger value in equation 53, together with the largest acceptable value of 4890 N·s (1100 lbf·s) for $(\Delta MV)_L$, we obtain the following (1 N·s = 4.45 lbf·s and 1 m/s = 3.28 ft/s):

$$(\Delta MV)_H = (4890\ N{\cdot}s/3) + 0.55\ M_p\ (23.8\ m/s) \tag{54}$$

Setting $(\Delta MV)_H$ = 4890 N·s (1100 lbf·s) in equation 54 and solving for M_p yield 250 kg (550 lb or 17.1 slugs). Thus, if a support is less than 250 kg (550 lb) and has satisfied the acceptance criteria in a 32.2-km/h (20-mph) test, it will perform satisfactorily in a 96.6-km/h (60-mph) impact.

Figure 1. Impact geometry and definitions.

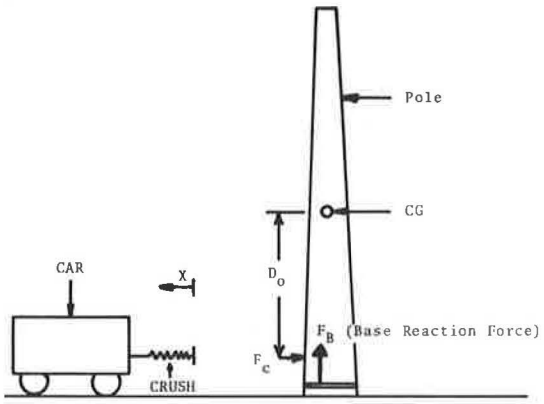

Figure 2. Separation of impact into phases.

PHASES OF IMPACT

1. Crushing of automobile with insignificant motion of structure being impacted.
2. Activation and completion of the breakaway failure mechanism.
3. Acceleration of structure by impacting vehicle.

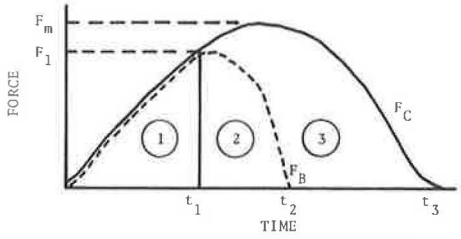

EXPRESSION FOR MOMENTUM CHANGE

$$\Delta MV = \int_{t_1}^{t_3} F_c\,dt$$

$$= \int_0^{t_1} F_c\,dt + \int_{t_1}^{t_3} F_b\,dt + \int_{t_1}^{t_3} (F_c - F_b)\,dt$$

$$= \int_0^{t_1} F_c\,dt + \int_{t_1}^{t_2} F_b\,dt + \int_{t_1}^{t_3} (F_c - F_b)\,dt$$

$$\triangleq I_1 + I_2 + I_3$$

Figure 3. Vehicle crush characterization.

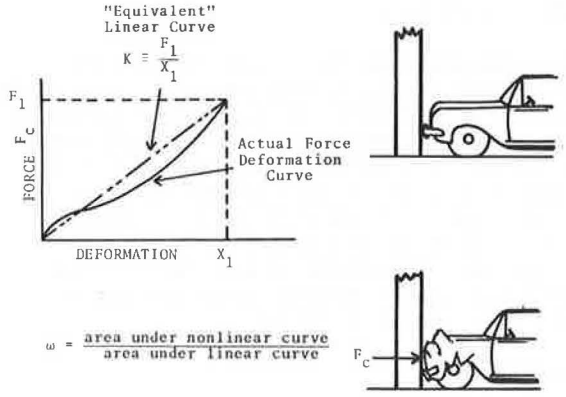

Figure 4. Characteristic variations of ΔMV with speed.

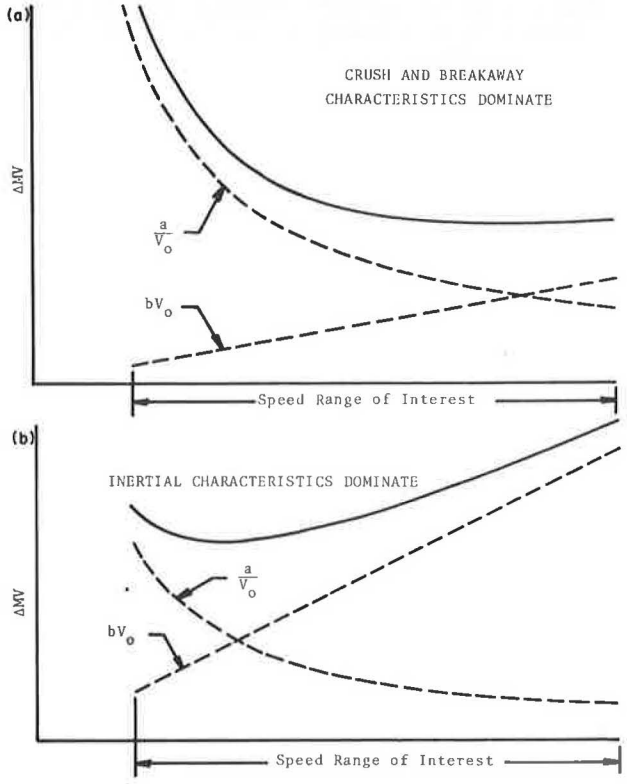

If, in the future, the allowable ΔMV is reduced to 3340 N·s (750 lbf·s) [which is listed as a desirable goal by the AASHTO specifications (2)], then the support mass that could cause excessive ΔMV in a high-speed impact would be reduced accordingly. Following the same procedure as above, we obtain 170 kg (375 lb or 11.6 slugs) as the value of support mass above which $(\Delta MV)_u$ may become excessive.

Because most current luminaire supports are less than 170 kg (375 lb), there is generally no problem associated with ΔMV produced in a 96.6-km/h (60-mph) impact with a luminaire support provided the measured ΔMV in the 32.2-km/h (20-mph) test is satisfactory. However, breakaway sign supports can be heavier and should be checked for $(\Delta MV)_u$ by using equation 51.

Thus the results of this simplified analysis have been very useful in guiding the development of practical laboratory acceptance test criteria for breakaway sign and luminaire supports. These criteria, and the studies leading to their development, are summarized by Owings, Cantor, and Adair in a paper in this Record.

ACKNOWLEDGMENTS

This work was performed by ENSCO, Inc., for the Federal Highway Administration as part of a study under contract DOT-FH-11-8118. We gratefully acknowledge the guidance and support provided by Douglas Chisholm, contract manager, Federal Highway Administration; John Viner, head of the Protective Systems Group, Federal Highway Administration; and James Rudd, manager of highway programs at ENSCO. Of the many ENSCO personnel contributing to this study, James Adair deserves special recognition for his valuable support in all phases of the study.

REFERENCES

1. Application of Highway Safety Measures: Breakaway Luminaire Supports. Federal Highway Administration, Circular Memorandum, June 5, 1968.
2. Standard Specifications for Structural Supports for Highway Signs, Luminaires, and Traffic Signals. AASHTO, 1975.

Abridgment

Laboratory Acceptance Testing of Breakaway Supports for Signs and Luminaires

Raymond P. Owings, Clarence Cantor, and James W. Adair, ENSCO, Inc., Springfield, Va.

Two Federal Highway Administration (FHWA) acceptance standards currently exist for breakaway luminaire supports, and none exist for breakaway sign supports. The first is the acceptance criterion set by FHWA in June 1968 (1) that is based on full-scale vehicle impact tests with a luminaire support. The specified limit on change in vehicle momentum (ΔMV) was set at 4890 N·s (1100 lbf·s). The second set of FHWA acceptance criteria was issued in November 1970 (2) and was based on the use of the simpler rigid pendulum (or drop weight) test. The specified limit on ΔMV in these tests was set at 1780 N·s (400 lbf·s), which was based on test data then available and on some preliminary correlation of these data with previous full-scale test data. Recently, the American Association of State Highway and Transportation Officials (AASHTO) presented specifications covering the performance of breakaway supports for both sign and luminaire supports (3). These specifications were based on full-scale tests and set a maximum limit for ΔMV of 4890 N·s (1100 lbf·s) with a desirable limit of 3340 N·s (750 lbf·s). The AASHTO criteria take into account possible worst case situations by specifying a 1020-kg (2250-lb) test vehicle and requiring satisfactory performance over a speed range of 32.2 km/h (20 mph) to 96.6 km/h (60 mph).

A need still exists for a simple and reliable laboratory test procedure and associated criteria that will ensure safe performance by a breakaway sign or luminaire support. The study recently completed by ENSCO for FHWA has addressed this problem in a comprehensive manner. This study involved

1. Analysis and computer simulation of vehicle impacts with breakaway sign and luminaire supports;
2. Design and construction of a pendulum impact test facility that incorporates simulated vehicle crush and a controlled foundation-soil interface;
3. Impact testing of breakaway supports at this facility;
4. Specification of full-scale vehicle impact tests;
5. Correlation of computer-simulated, laboratory, and full-scale tests;
6. Development of foundation design guidelines and laboratory acceptance test criteria that will ensure satisfactory performance of breakaway supports.

The analytical portion of the study is described by Owings and Cantor in a paper in this Record. In brief, this analysis divided the impact into distinct phases to gain insight into the effect of vehicle stiffness, breakaway force level, base fracture energy, pole inertial properties, and vehicle impact speed on ΔMV. With simplifying assumptions, the results of this analysis were

$$\Delta MV \simeq \frac{a}{V_o} + bV_o \qquad (1)$$

where

- a = constant dependent on vehicle crush and breakaway base characteristics,
- V_o = vehicle impact velocity, and
- b = constant dependent on pole inertial properties.

Computer simulations were performed to gain further understanding of the impact phenomenon and to provide a basis for correlation with subsequent laboratory and full-scale impact tests. The vehicle in the computer model was represented by a single degree-of-freedom, spring-mass system. The spring characteristics, representing the force-deformation characteristics of the vehicle, could be modeled as linear or nonlinear and with partial restitution because vehicle crush is mostly inelastic. The sign or luminaire support was simulated by means of the finite element method for a linear elastic frame. The dynamic response of the foundation in soil was represented by two linear differential equations with constant coefficients—one for translation and one for rotation. The breakaway base was modeled by a specified force-displacement characteristic in which the force (and moment) decays to zero at a given maximum base displacement. When this maximum displacement is

Publication of this paper sponsored by Committee on Safety Appurtenances.

reached, the support and foundation subsystems are completely decoupled. The interaction of the vehicle with the support was accomplished through an iterative procedure that matched the force levels at each time step. Details of the computer simulation model can be found elsewhere (4).

As part of the study, a pendulum impact test facility was designed and constructed to permit controlled testing of breakaway sign and luminaire supports and to facilitate correlation with computer-simulated and full-scale tests. The facility was designed for a maximum speed of 40.2 km/h (25 mph) because previous analysis had shown that vehicle crush and base breakaway characteristics have the most critical effect on ΔMV at low impact speeds. The pendulum mass can be adjusted between 1020 kg (2250 lb) and 2040 kg (4500 lb), which simulates the range of vehicles from subcompacts to full-sized automobiles. Vehicle crush characteristics can be simulated by a presettable honeycomb assembly attached to the front of the pendulum mass. In addition, the facility contains a soil pit to house the foundation for the breakaway support. This permits evaluation of foundation-soil interaction during impact and its effect on ΔMV. The facility contains independent sets of instrumentation for measuring ΔMV during impact, namely a high-speed camera, accelerometers mounted on the pendulum mass, and electronic transducers that measure the speed of the pendulum mass before and after impact. Details of the facility design can be found elsewhere (5).

A series of 27 tests of breakaway supports was conducted at this impact test facility. All tests were conducted at an impact speed of 32.2 km/h (20 mph). Both rigid-faced and crushable-faced pendulum tests were included in this series. The purpose of the rigid-faced tests was to examine the importance of the inertial characteristics of the impacted structure in determining ΔMV. These characteristics determine the constant b of equation 1. The results were almost exactly as predicted by the analysis. The crushable-faced tests included tests of slip base luminaire supports in which the bolt torque was varied and several tests of "identical" shoe base supports. The slip base tests exhibited low ΔMV that increased with bolt torque as expected. The shoe base test results varied considerably because of the variable modes of failure associated with this base. In general, the laboratory test results confirmed the validity of the analytical and computer simulation models.

Finally, a series of seven full-scale tests were specified by ENSCO and carried out at the Texas Transportation Institute. The tests were conducted with compact and full-sized automobiles at impact speeds from 32.2 km/h (20 mph) to 96.6 km/h (60 mph). The breakaway supports included slip base and shoe base luminaire supports and slip base sign supports. The test results were about as expected, showing moderate ΔMV for the slip base supports and high ΔMV for the shoe base supports. More important, the full-scale test results correlated very well with results of computer-simulated and laboratory tests and with results predicted by the analytic model of equation 1. This correlation is discussed in more detail elsewhere (6).

The foregoing work accomplished two main objectives of the study.

1. An understanding of the entire impact phenomenon was achieved. Specifically, the individual effects of vehicle stiffness, breakaway force level, base fracture energy, pole inertial properties, and vehicle impact speed on ΔMV were determined.
2. Good correlation was obtained between the results of analysis, computer simulation, laboratory testing, and full-scale testing.

This understanding and correlation enabled the development of simple laboratory test procedures and acceptance criteria that would ensure satisfactory performance by a breakaway support under field conditions. The recommended laboratory test procedure involves impact testing of the actual breakaway support at 32.2 km/h (20 mph) with a crushable-faced, 1020-kg (2250-lb) mass. A standard crush characteristic is obtained by use of three stacked, aluminum honeycomb segments of specified crush pressure ratings to achieve a generally linear force-deformation characteristic that extends to 133 450 N (30 000 lbf) at 50.8 cm (20 in). The selected impact speed, mass, and crush characteristic represent a conservative set of impact conditions with respect to their effect on ΔMV.

The low-speed performance of the support is considered satisfactory if either of the following conditions is met:

1. The measured ΔMV in the first test is less than 3340 N·s (750 lbf·s) (only one test would then be required) and
2. The measured ΔMV in the first and second tests of identical supports are both less than 4890 N·s (1100 lbf·s).

When a support has satisfied the low-speed criteria, its high-speed performance at 96.6 km/h (60 mph) would be calculated on the basis of its inertial properties together with its measured low-speed ΔMV (Owings and Cantor, in a paper in this Record, give more information on this). This calculation is considered to be valid because the inertial properties of the pole predominate at high impact speeds and these properties can be quite accurately measured. If the calculated ΔMV for high-speed impact is less than 4890 N·s (1100 lbf·s), the support would be considered acceptable. Thus one or two simple laboratory impact tests, together with an extrapolation to check high-speed performance, are sufficient to qualify a given support over the entire speed range of interest. (An examination of equation 1 will reveal that peak ΔMV can only occur at the minimum or maximum speed in the range of interest.) Further details of the laboratory acceptance test procedures and criteria can be found elsewhere (7).

One final item considered in the study was the effect of foundation size on breakaway support performance. An acceptable support, if mounted on an inadequate foundation, could still produce unacceptable levels of ΔMV during impact because of foundation motion. The computer simulation studies and the testing at the impact test facility revealed that a cylindrical foundation 0.61 m (2 ft) in diameter and 1.83 m (6 ft) long would result in negligible increase in ΔMV. Thus this size is recommended as the minimum foundation for breakaway sign and luminaire supports to be compatible with satisfactory impact performance. Of course, other factors, such as wind loading, may necessitate a larger foundation (3).

REFERENCES

1. Application of Highway Safety Measures: Breakaway Luminaire Supports. Federal Highway Administration, Circular Memorandum, June 5, 1968.
2. Application of Highway Safety Measures: Breakaway Luminaire Supports. Federal Highway Administration, Notice, Nov. 16, 1970.
3. Standard Specifications for Structural Supports for Highway Signs, Luminaires, and Traffic Signals. AASHTO, 1975.

4. Simulation Model. ENSCO, Inc., Springfield, Va., task E rept. on safer sign and luminaire supports, Part 1, 1974.
5. Impact Test Facility Operations Manual. ENSCO, Inc., Springfield, Va., task I rept. on safer sign and luminaire supports, Feb. 1975.
6. Correlation of Full-Scale, Laboratory, Analytical and Computer Simulated Results. ENSCO, Inc., Springfield, Va., task K rept. on safer sign and luminaire supports, March 1976.
7. Laboratory Acceptance Testing for Sign and Luminaire Supports. ENSCO, Inc., Springfield, Va., task F rept. on safer sign and luminaire supports, Feb. 1976.

Design Practices for Paved Shoulders

R. G. Hicks, Department of Civil Engineering, Oregon State University
Richard D. Barksdale, School of Civil Engineering, Georgia Institute of Technology
Donald K. Emery, Georgia Department of Transportation

This paper presents the results of a study to develop improved methodology for designing paved shoulders adjacent to portland cement concrete pavements. A survey of 1975 shoulder practices was conducted as a part of National Cooperative Highway Research Program Project 14-3. The results indicate that most shoulder pavement sections are underdesigned. Truck traffic encroaching on the shoulder, together with water entering the longitudinal joint, and severe climatic conditions are the most important causes of early shoulder deterioration. A major recommendation is that the shoulder in the vicinity of the joint be structurally designed to withstand the wheel loadings from encroaching truck traffic. Alternate designs are developed for a range of traffic, soil, and environmental conditions by using the American Association of State Highway Officials Interim Guide for Design of Pavement Structures. These structural sections should be supplemented with subsurface drainage or sealed longitudinal shoulders based on environmental conditions or subgrade conditions or both.

The highway system in the United States is composed of a large number of portland cement concrete (PCC) pavements having asphalt concrete shoulders. The resulting joint formed between the pavement and shoulder has proved to be one of the weakest parts of the pavement-shoulder system (1, 2). Although the rate of deterioration of the pavement and shoulder at the joint varies widely with respect to locality, materials used, and construction practices, the basic mechanisms of joint deterioration are generally the same. If the transverse and longitudinal pavement-shoulder joints are not completely sealed, surface water will infiltrate into the subbase, subgrade, and shoulder. This water, together with repeated traffic loads, can cause the subbase material to be pumped from beneath the concrete slab and beneath the shoulder resulting in faulting of the slab (3, 4) and cracking or settlement of the asphalt concrete shoulder (5, 6, 7) or both. In the northern parts of the United States, infiltration of water beneath the pavement can lead to frost heave, cracking, and early deterioration of the shoulder.

Because pavement and shoulder deterioration is often related to the infiltration of water into the subbase and the underlying subgrade, attempts have been made to prevent infiltration by sealing the longitudinal joints. However, it has generally been conceded that watertight pavement-shoulder joints cannot last the life of the pavement. Therefore, consideration should be given to (a) minimizing the amount of water passing through the joint and (b) designing a stronger pavement-shoulder structure by using, for example, concepts of drainage and base treatment to minimize the effects of water that does eventually pass through the joint. This paper deals primarily with one aspect of the project—developing structural shoulder designs to resist deterioration due to encroaching traffic. The complete findings of this study (including improved drainage and joint sealing) are given elsewhere (8).

CURRENT DESIGN PRACTICES

When considering the structural design of pavement shoulders, one must carefully consider the functions of the shoulder. One purpose of a shoulder is to provide a safe all-weather refuge for vehicles that must leave the main traffic stream (1). Paved shoulders reduce the amount of infiltration of surface runoff and provide some degree of lateral support of the pavement.

Asphalt Concrete Shoulder Sections

The performance of the shoulder with or without a sealed longitudinal joint depends to a considerable degree on the structural strength and design of the shoulder and how it acts with the pavement. During their early development, paved shoulder sections used on Interstate pavements tended to be relatively thin. As the detrimental effects of traffic loading and the environment became apparent, considerably heavier shoulder sections gradually gained relatively widespread use.

Table 1 gives a summary of typical shoulder sections used in 1975 and how they performed. The information reported is based on field inspections made in 15 states and on a questionnaire mailed to each state highway organization. In Table 1, Arkansas, Colorado, Delaware, Iowa, Maryland, Manitoba, Mississippi, Nebraska,

Publication of this paper sponsored by Committee on Shoulder Design.

Table 1. Current asphalt concrete shoulder sections.

State	Surface Course		Base Course		Subbase	
	Material	Thickness (cm)	Material	Thickness (cm)	Material	Thickness (cm)
Alabama	AC	~2.5	AC	~7.6	Select soil	11.4
Arizona	AC	10.2	AB	12.7	ASB	10.2 to 15.2
California	AC	7.6 to 14.0	AB	15.2	ASB	Variable
Connecticut	AC	7.6	SSB	15.2	Not specified	15.2 to 57.2
Georgia	AC	3.8	CTB	15.2	Select borrow	
Florida	AC	2.5	SA	12.7	Sand-clay	15.2
Idaho	AC	9.1	AB	21.3	ASB	6.1
Illinois	AC	3.8	CTB	16.5	ASB	10.2
			LTB	16.5		
			ATB	16.5		
Indiana	ST		ATB	15.2	ATSB	10.2
Kentucky	AC	5.1	AB	Variable		
Kansas		22.9 tapered	AB	10.2	LTS	15.2
Louisiana	AC	20.3 to 25.4	AC	8.9	LTS	
Maine	AC	7.6	AB	22.9	ASB	22.9
Michigan	AC	3.8	ATB	16.5 to 19.1	ASB	35.6
Missouri	AC	5.1	ATB	12.7	ASB	12.7 to 17.8
			CTB	12.7		
Minnesota	AC	3.8 to 5.1	AB	7.6	ASB	22.9 to 27.9
New York	AC or ST	~2.5	Emulsion-stabilized gravel	7.6	ASB	43.2
North Carolina	ST or AC	2.5	AB	20.3	ASB	10.2
North Dakota	AC	10.2	ATB	10.2	LTS	
		5.1	Emulsion or cutback treated	15.2		
Ohio	AC	7.6	ATB	12.7 to 15.2	ASB	15.2
Oregon	AC	Full pavement depth	CTB	10.2 to 15.2	LTS	15.2
					CTS	
Pennsylvania	AC or ST	10.2	AB	15.2	ASB	30.5
South Carolina	AC		ATB			
South Dakota	AC	5.1	ATB	15.2	AC	5.1
			LTB	15.2		
Texas	AC	20.3	ATB	10.2	LTS	
Utah	AC	7.6	AB	15.2	ASB	20.3
Washington	AC	5.1	AB	7.6	ASB	17.8
West Virginia	PM	7.6	AB	15.2	ASB	15.2
Wisconsin	AC	7.6	AB	15.2	ASB	38.1

Note: 1 cm = 0.394 in.

Nevada, New Jersey, New Mexico, Virginia, Wisconsin, and Wyoming did not provide sufficient information, and Alberta, British Columbia, and Vermont had little or no experience with PCC pavements. Also the following codes appear in Table 1:

Code	Definition	Code	Definition
AB	Aggregate base	LTB	Lime-treated base
AC	Asphalt concrete	LTS	Lime-treated subgrade
ASB	Aggregate subbase	PM	Penetration macadam
ATB	Asphalt-treated base	SA	Sand asphalt
ATSB	Asphalt-treated subbase	SSB	Salt-stabilized base
CTB	Cement-treated base	ST	Surface treatment

Full-Depth Asphalt Concrete

Eleven states indicated that they have used full-depth asphalt concrete shoulder sections varying from about 17.8 to 25.4 cm (7 to 10 in) in depth. Arizona and California are considering use of full-depth sections in the future. Illinois, Texas, North Dakota, Louisiana, Michigan, and Ohio were visited to evaluate the field performance of full-depth asphalt concrete shoulders. Use of full-depth shoulders is found to eliminate or greatly reduce cracking near the longitudinal joint and limit separation at the joint to approximately 3.2 mm (⅛ in).

A comprehensive study in Illinois (9) showed that a full-depth bituminous aggregate shoulder section performed better than either cement-aggregate or a pozzolanic aggregate base shoulder. The bituminous aggregate base tapered in thickness from 20 cm (8 in) at the pavement to 15.2 cm (6 in) at the outer edge. A 3.8-cm (1½-in) bituminous concrete surfacing was placed over a 13.9-cm-thick (5½-in-thick) cement aggregate base and over a 16.5-cm (6½-in) pozzolana-aggregate base. In the sections having cement and lime-fly ash bases, longitudinal cracks were found to form approximately 20.3 to 50.8 cm (8 to 24 in) from the joint; random cracks occurred in between. A significant amount of the deterioration observed in the lime-fly ash and cement-aggregate bases was found to be caused by the loss of durability due to freeze-thaw cycles and the presence of brine. The bituminous aggregate bases performed well.

In Michigan (10), considerable settlement of the shoulder occurred and longitudinal cracks usually formed during the first year or two about 15.2 to 30.5 cm (6 to 12 in) from the edge; the shoulder problem was similar to that observed in Illinois. The shoulder section consisted of 3.81 cm (1½ in) of asphalt concrete with an 11.4-cm (4½-in) gravel base. Select stone extended from the main-line pavement 0.6 m (2 ft) under the shoulder. Because of the poor performance of this shoulder section, the following stronger shoulder sections are now used in Michigan:

1. A deep asphalt concrete section equal to the slab thickness at the inside edge and tapering to 16.5 cm (6½ in) at the outside edge placed over a 35.6-cm (14-in) sand subbase and
2. Concrete shoulders conforming to the main-line slab thickness and tapering to 15.9 cm (6¼ in) at 0.9 m (3 ft) from the outside edge and remaining constant to the edge of the shoulder.

The performance of these two sections has been a considerable improvement over the thinner granular base sections.

Full-depth bituminous pavement shoulders in North Dakota are found to perform quite well considering the presence of expansive soils and a very severe climate.

Transverse temperature cracks do occur in the shoulder because of the extreme temperature variations. The shoulders used in North Dakota consist of 10.2 cm (4 in) of asphalt concrete over a 10.2-cm (4-in) liquid or emulsified asphalt-treated base. Important factors contributing to the good performance in North Dakota appear to be the use of a continuously reinforced concrete pavement bituminous stabilized base, and sealed longitudinal pavement-shoulder joints. The sealed longitudinal joints are generally well maintained, and the system appears to be relatively effective in keeping surface water from beneath the pavement. By means of an increase in density requirements from American Association of State Highway and Transportation Officials (AASHTO) [formerly American Association of State Highway Officials (AASHO)] T-99 to T-180, most of the shoulder settlement problems formerly existing in the granular base section have been eliminated.

Texas uses thick asphalt concrete sections consisting of 20.4 cm (8 in) of asphalt-stabilized material over a 10.2-cm (4-in) asphalt-stabilized subbase. The upper 15.2 cm (6 in) of the subgrade beneath this section is frequently treated with lime. Local materials are used extensively in the asphalt-stabilized bases and subbase. Several districts in Texas seal the longitudinal joint to try and keep water from expansive clay subgrades. Use of the deep asphalt sections has greatly minimized the problem although transverse and vertical movements up to approximately 6.35 mm (¼ in) are still found to occur at the joint. Considerably larger movements are caused by expansive clay subgrades.

Cement-Treated Bases

From the survey, five states indicated that they use a cement-stabilized base under an asphalt concrete surface course. All of these states except Oregon use a relatively thin asphalt concrete surfacing varying from 3.81 to 5.08 cm (1½ to 2 in) in thickness. Oregon uses an asphalt concrete surface equal in thickness to that of the PCC slab. Of the states in which field inspections were made, only Georgia continues to use cement-stabilized bases on Interstate pavements. Illinois, Pennsylvania, and Louisiana have discontinued their use on at least Interstate pavements because of poor performance. Field inspections in Illinois, Pennsylvania, Louisiana, Georgia, and Texas showed that their cement-stabilized bases tend to pump, which causes faulting of the main-line slab. Erosion of base material also results in settlement and subsequent cracking and deterioration of the shoulder and main-line slab in the vicinity of the transverse joint. In many instances, a depression forms in the shoulder immediately adjacent to the longitudinal joint and is followed by cracking in this area. The pumping problem is particularly severe in both Georgia and Louisiana where the average annual rainfall is about 127 to 139 cm (50 to 55 in). Georgia uses a 15.2-cm-thick (6-in-thick) cement-treated base with a 3.8-cm (1½-in) asphalt concrete surfacing. The base is usually a cement-treated aggregate overlaying a layer of select borrow material. In Louisiana, extensive use is made of local soils for the cement-stabilized bases for shoulders constructed on primary highways. These shoulders consist of 3.8 to 5.2 cm (1½ to 2 in) of asphalt concrete over a 20.3-cm (8-in) soil and cement base. Louisiana now uses 20.3 cm (8 in) of asphalt concrete over an asphalt concrete base on Interstate pavements.

Granular Bases

Twelve states reported the use of aggregate bases or subbases. Of these twelve, field inspections were conducted in Arizona, California, Minnesota, Ohio, Pennsylvania, and Utah. In general, shoulders constructed with typically 3.8 to 5.1 cm (1½ to 2 in) of asphalt concrete and 15.2 cm (6 in) of granular base have performed poorly at least partly because this section in most instances is grossly underdesigned. Furthermore, sections having deep granular bases have been found to experience settlement problems. Maximum settlements of typically 2.5 to 3.8 cm (1 to 1½ in) appear to be caused primarily by a combination of factors, including some or all of the following: (a) low compaction, (b) use of frost susceptible material, (c) poor gradation or small maximum size aggregate or both, and (d) use of low-quality uncrushed gravel aggregate often having an excessive amount of fines.

In California, the shoulder sections in the valley areas were observed to perform quite well. A relatively small amount of separation at the longitudinal joint [approximately 3.20 to 6.35 mm (⅛ to ¼ in)] and some surface cracking and faulting were observed in the shoulder although the severity is much less than that found in states such as Illinois and Michigan. Some problems with faulting of the main-line pavement are also experienced in the valley areas where there is a mild climate and average annual rainfall of only 38.1 to 50.8 cm (15 to 20 in). Extension of the stabilized subbase under the main-line pavement 0.3 m (1 ft) beyond the edge has been found to significantly reduce the shoulder problems in the valley areas. In contrast, pavements in the mountain areas (near Donner Pass where the winters are quite severe) exhibited extensive shoulder cracking near the longitudinal joint similar to that found in Michigan, Illinois, and Minnesota. California uses 7.6 to 14 cm (3 to 5½ in) of asphalt concrete surfacing over a 15.2-cm (6-in) aggregate base.

Deep granular bases and subbases are used in Minnesota, New York, Ohio, Pennsylvania, and Utah and vary from approximately 25.4 to 45.7 cm (10 to 18 in) in thickness. New York uses approximately 10.2 cm (4 in) of asphalt-treated surfacing, Minnesota uses 3.81 cm (1½ in), and the other states use 7.6 cm (3 in) of asphalt concrete. Maximum settlements from approximately 1.3 to 3.8 cm (½ to 1½ in) have been found to occur in these shoulders, which are underlaid by deep layers of granular materials. Shoulder sections with granular bases are found to perform reasonably better in Ohio than in other states using this type of section. The better performance may be at least partly due to sloping the pavements so that water flows to the inside rather than the outside shoulder. The most serious problem in Ohio appeared to be associated with frost heave during the first winter, which leads to longitudinal cracking about 0.3 m (1 ft) from the edge of the pavement. In the future Ohio plans to use full-depth asphalt concrete shoulders tapering from the PCC slab thickness at the shoulder joint to 15.2 cm (6 in) at the outer edge. In New York, settlement of the shoulder appears to be the most severe type of distress although some cracking also occurs. In Minnesota and Utah, both settlement and cracking of the shoulder near the longitudinal joint are found to be important. Because of current shoulder deterioration, Minnesota plans to use a 10.2-cm (4-in) asphalt concrete surfacing in the future and wait until the shoulder settlement has occurred before sealing the longitudinal joint. Some of the excessive settlement experiences in Minnesota could be caused by compacting the granular materials to only 100 percent of AASHTO T-99 density. Utah and Georgia currently plan to use concrete shoulders on future Interstate pavements.

Pennsylvania has studied the performance of the following four bases: (a) bituminous concrete, (b) soil cement, (c) bituminous soil, and (d) lime fly ash.

Shoulder sections using the asphalt concrete base course have been found to give the best performance and are currently used by Pennsylvania. This section consists of 10.2 cm (4 in) of asphalt concrete, 15.2 cm (6 in) of aggregate base, and a variable thickness subbase. The required subbase thickness, which is typically 30.5 cm (12 in), is determined from frost considerations by using the U.S. Army Corp of Engineers method.

PCC Shoulders

Portland cement concrete shoulders adjacent to main-line concrete pavements have been constructed for the past 12 years. Between 1970 and 1974, approximately 4.77 million m^2 (5.7 million yd^2) of concrete shoulder contracts have been awarded in a total of 21 states (11, 12). The states that have planned or constructed PCC shoulders are shown in Figure 1. Figure 1 is patterned after data in the California Highway Design Manual (16). Table 2 gives a summary of the different shoulder sections used or planned by the various states. Only sections constructed in Illinois, Texas, and Michigan have had traffic for a sufficient length of time to fully evaluate their performance.

In Illinois, the PCC shoulders are found to perform as well as or better than asphalt concrete sections. From the comprehensive study performed in Illinois, five significant conclusions were reached (13):

1. A plain concrete shoulder 15.2 cm (6 in) thick gives good performance.
2. The shoulder should be tied to the main-line pavement by 76.2-cm-long (30-in-long) tie bars spaced 76.2 cm (30 in) on center.
3. Spacing of transverse joints of about 6.1 m (20 ft) is desirable for control of the intermediate cracking.
4. Use of a 15.2-cm (6-in) granular subbase under the concrete shoulder is found to reduce the amount of shoulder cracking by approximately 50 percent. However, the cracks that did develop in the sections not underlaid by a subbase remained closed and did not significantly affect shoulder performance.
5. Sealing the longitudinal edge joint did not improve shoulder performance.

Several states have also followed the recommendations of the Illinois study, and others have increased the slab thickness to equal that of the main-line pavement. The Federal Highway Administration (14) has recommended use of either a straight or tapered concrete shoulder having a minimum thickness of 15.2 cm (6 in). They also recommended a stabilized base. Further, when the inside and outside shoulders are integrally placed in one pass of a slip-form paver with a 7.32-m-wide (24-ft-wide) main-line pavement, a longitudinal joint should be placed between the main-line pavement and the shoulder. When the jointed main-line pavement is used, steel reinforcement is not required in the shoulder. For continuously reinforced pavements, the same percentage of longitudinal steel should be used in the shoulder as is used in the main-line pavement.

E. C. Lokken (11) has prepared recommendations that follow reasonably closely to those of Illinois.

SHOULDER ENCROACHMENT STUDY

Truck encroachment appears to be a major cause of observed cracking and settlement in the vicinity of the shoulder joint. The term encroachment is restricted to continuous movements of truck traffic and does not apply to movements for stopping. Despite the apparent relationship between traffic loading and shoulder distress, little has been done to develop a formal approach for designing structural shoulder sections. Early studies concerned with transverse placement of trucks used the data only for the design of the main-line pavement.

The objectives of this study were twofold: (a) to determine, on the basis of actual observations, the amount and extent of shoulder encroachment by trucks and (b) to develop criteria that pavement designers can use to arrive at an optimal structural design of the paved shoulder. This study consists of summarizing observations of transverse truck placement on rural freeways with free-flow characteristics. All observations relate to rural freeways and should not be considered applicable to other types of facilities.

Procedure

For the study performed in Georgia (15), trucks were selected at random and followed by observers for 16.1 km (10 miles). Those trucks not completing a full 16.1-km (10-mile) trip were dropped from the analysis. Records were made of the time on the shoulder to determine the longitudinal distance for each encroachment. Estimates of transverse encroachment with respect to the shoulder joint were made based on the dimensions obtained for different types of trucks at several terminals in the Atlanta, Georgia, area.

A total of 205 trucks were followed for the 16.1-km (10-mile) distance in nine states. Sixty percent of the trucks followed were on PCC main-line paving, and 40 percent were on asphalt concrete main-line paving. A comparison in truck classification between the randomly selected samples and two continuous count stations in Georgia was made to ensure a representative sample. As shown by the data given in Table 3, the comparison is reasonably close except for the two-axle, single-unit trucks.

Results

Table 4 gives a summary of information on outside shoulder encroachments by type of shoulder. Sixty-five percent of all trucks encroached on the shoulder sometime during the 16.1-km (10-mile) study length. The percentage was similar for asphalt concrete and bituminous surface treatment shoulders, which indicates that rough-textured shoulders do not necessarily discourage encroachment on the shoulder. A total of 677 encroachments were observed, or an average of approximately 3.3 encroachments/vehicle for the 16.1-km (10-mile) study length.

Table 5 gives a summary of the number of outside shoulder encroachments by type of truck; Table 6 gives encroachments by type of terrain. The results indicate that certain types of trucks and terrain are more likely to contribute to a higher incidence of shoulder encroachments. For example, 83 percent of the four-axle, multiple units encroached on the shoulder an average of 4.7 encroachments/vehicle. Although 60 percent of the three-axle, multiple units encroached, they did so an average of 8.5 times. Types of terrain also had a significant effect on the number of encroachments. The higher incidence of horizontal curves in rolling and hilly terrain appears to have contributed to the high encroachment ratio.

The following tabulation gives a summary of frequency, time, longitudinal distance, and transverse placement of encroachments (1 km = 0.621 mile; 1 m = 3.28 ft):

Figure 1. States having concrete shoulder projects by end of 1974.

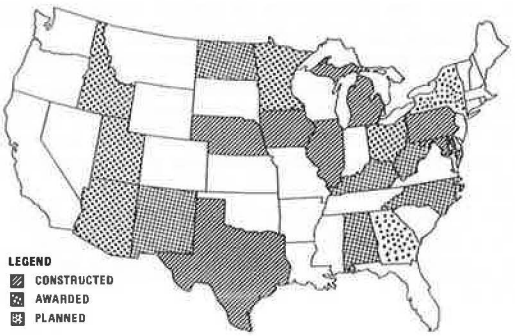

Item	Outside Shoulder	Median Shoulder
Avg. encroachments per truck in 16.1 km	3.30	0.25
Avg. time on shoulder per encroachment, s	4.5	3.4
Avg. longitudinal distance on shoulder per encroachment, m	117	104.9
Avg. transverse distance on shoulder per encroachment, m	0.18	0.015

For the outside shoulder, average transverse encroachment was 17.7 cm (0.58 ft). Actual distribution for the outside shoulder is shown in Figure 2. A considerable amount of traffic is found to operate on the outside shoulder to a distance of approximately 30.5 cm (12 in) from the longitudinal joint.

Table 2. Summary of PCC shoulder designs.

State	Type of Pavement	Slab Thickness (cm)	Base		Tie Bars	
			Type	Thickness (cm)	Size Number	Spacing (cm)
Alabama	Continuously reinforced concrete	20.3	Aggregate	15.2		
Georgia	Plain	27.9 taper to 15.2	Subgrade		10.2	76.2
Illinois	Plain	15.2	Subgrade		10.2	76.2
Iowa	Plain	15.2				
Kentucky	Plain, reinforced	12.7 to 17.8				
Maryland	Reinforced	17.8			10.2	76.2
Michigan	Plain	22.9 taper to 15.9	Aggregate	10.2	Hook bolt	101.6
Nebraska	Plain	14.0	Subgrade			
New Mexico	Plain	20.3	Cement stabilized base			
New York	Plain	15.2	Aggregate	20.3 min.		
North Carolina	Plain	17.8				
North Dakota	Continuously reinforced concrete	20.3	Aggregate	5.1	12.9	121.9
Pennsylvania	Plain	15.2	Aggregate	30.5	Hook bolt	
Texas	Continuously reinforced concrete	20.3	Cement stabilized base	15.2	10.2	91.4
Utah	Plain	22.8	Cement stabilized base	12.7	12.7	91.4
West Virginia	Plain	20.3	Cement stabilized base	15.2		

Notes: 1 cm = 0.394 in.
Design details not available on Arizona, Idaho, and Minnesota.

Table 3. Comparison of truck classification from study trucks and two continuous-count stations.

Truck Class	Study Trucks		Station Trucks[a] (%)
	Number	Percent	
2 axle, single unit	45	21.9	13.7
3+ axle, single unit	8	3.9	3.0
3 axle, multiple unit	10	4.9	4.7
4 axle, multiple unit	31	15.1	21.5
5+ axle, multiple unit	111	54.1	57.1
Total	205	100	100

[a]One station on I-85, 129 km (80 miles) northeast of Atlanta, and one station on I-75, 161 km (100 miles) south of Atlanta.

Table 4. Summary of outside shoulder encroachments by type of shoulder pavement.

Item	Asphalt Concrete	Bituminous Surface Treatment	Total
Number of samples	129	76	205
Number of trucks encroaching	83	50	133
Percent of trucks encroaching	64.3	65.8	64.9
Number of encroachments	398	279	677
Avg. encroachments per truck encroaching	4.8	5.6	5.1
Avg. encroachments per truck	3.1	3.7	3.3
Avg. vehicle speed, km/h	—	—	103

Note: 1 km/h = 0.621 mph.

Table 5. Encroachments on outside shoulder by type of truck.

Type of Truck	Trucks in Sample	Trucks Encroaching		Encroachments	Avg. Encroachments per Truck Encroaching	Avg. Encroachments per Truck
		Number	Percent			
2 axle, single unit	45	30	66.7	133	4.4	2.96
3+ axle, single unit	8	3	25.0	21	7	2.63
3 axle, multiple unit	10	6	60.0	51	8.5	5.1
4 axle, multiple unit	31	26	83.9	123	4.7	3.97
5+ axle, multiple unit	111	68	64.0	349	1.6	3.14
All trucks	205	133	64.9	677	5.1	3.30

Design Criteria for Shoulders

The data on shoulder encroachment can be used to develop a design traffic number in terms of percent of main-line traffic. For example, consider the traffic conditions existing on I-75 at Perry, Georgia, and the previously observed 3.3 outside shoulder encroachments per truck for 16.1 km (10 miles) (1 km = 0.621 mile):

Item	Calculation
1973 avg. annual daily traffic	22 966
Design trucks, %	19.5
Design trucks, one way	2239
Outside shoulder encroachments per day in 16.1-km segment	7389
Total encroachment distances in 16.1-km segment, km	865
Encroachments for given point	54
Trucks encroaching on shoulder, %	2.4

On the average, each of these encroachments resulted in a traveled distance of 117 m (384 ft) on the shoulder. For this example, there are 54 encroachments each day by the 2239 trucks, or 2.4 percent of the trucks that use the outside shoulder. Because the truck wheels are concentrated primarily within about 30.5 cm (12 in) of the longitudinal joint, use of the full percentage of truck traffic for structural design appears justified.

STRUCTURAL DESIGN STUDY

Structural shoulder pavement designs have gradually developed more through experience than from rational pavement design analyses. Apparently only California uses a formal design procedure for shoulders (16). In California, shoulder sections are designed for 1 percent of the main-line traffic index (TI); TI is 5 [approximately 10^4 equivalent 80.1-kN (18-kip) axle loads]. The results of the encroachment of main-line truck traffic onto the shoulder presented in this paper, however, have shown that 1 percent encroachment is low for at least some traffic flow conditions. This study indicates that, for free-flow traffic conditions in at least rural areas of the South, shoulder pavement within 0.3 m (1 ft) of the joint should be designed for at least 2 to 2.5 percent of the truck traffic.

The purpose of the study presented in this section is to determine, by using an AASHO procedure (17), shoulder sections designed for the anticipated traffic. Both asphalt and PCC shoulder designs were developed for 1, 2.5, and 5 percent shoulder encroachment.

Asphalt Concrete Shoulder Design

The required structural number (SN) of the shoulder section was calculated by using the AASHO equation for flexible pavements (17). A computer solution of the equation was used for the variables given in Table 7 for terminal serviceability indexes (P_t) of 2.5 and 3.0. To illustrate for flexible shoulders the structural sections required by the AASHO equation (17), three alternative sections were

Figure 2. Distribution of outside shoulder encroachments.

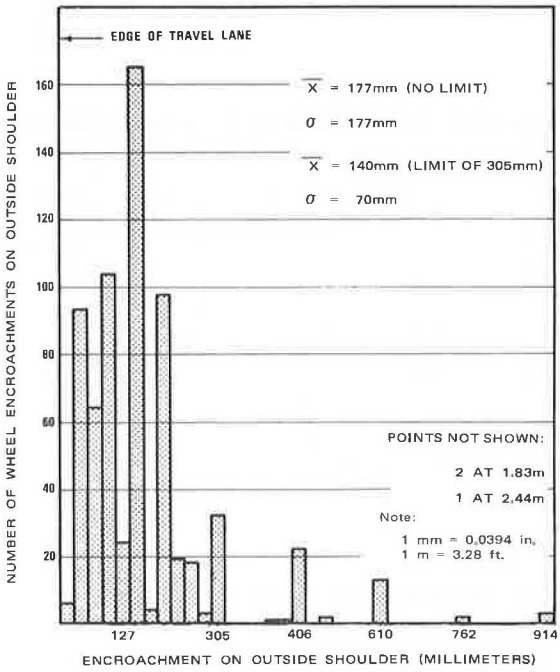

Table 6. Encroachments on outside shoulder by type of terrain.

Type of Terrain	Total Trucks	Trucks Encroaching	Encroachments	Avg. Encroachments per Truck Encroaching	Avg. Encroachments per Truck
Flat	67	43	190	4.42	2.84
Rolling	134	87	480	5.52	3.58
Hilly	4	3	7	2.33	1.75
All terrain	205	133	677	5.09	3.30

Table 7. Structural numbers for flexible pavements.

Traffic Number	P_t	Regional Factor 0.5			Regional Factor 1.0			Regional Factor 5.0		
		SS 3	SS 5	SS 10	SS 3	SS 5	SS 10	SS 3	SS 5	SS 10
10^6	2.5	4.11	2.86	1.27	4.69	3.31	1.45	6.06	4.61	1.95
	3.0	5.56	3.50	1.28	6.25	4.45	1.47	7.84	6.15	2.02
10^5	2.5	2.54	1.84	0.76	2.92	2.09	0.90	4.11	2.85	1.27
	3.0	2.85	1.90	0.76	3.64	2.20	0.90	5.56	3.50	1.28
10^4	2.5	1.65	1.18	0.38	1.88	1.36	0.48	2.54	1.84	0.76
	3.0	1.68	1.20	0.38	1.94	1.38	0.48	2.54	1.90	0.76
10^3	2.5	1.05	0.70	—	1.21	0.83	0.16	1.65	1.19	0.38
	3.0	1.01	0.70	—	1.22	0.38	0.16	1.69	1.20	0.38

Note: SS = soil support.

Table 8. Examples of design thickness for flexible shoulder.

Shoulder Traffic Number	Equivalent Main-Line Traffic Number	Truck Usage of Inside Edge of Shoulder (%)	Material	Thickness (cm)		
				Conventional	Cement-Stabilized Base	Full-Depth Asphalt Concrete
1×10^4	1×10^6	1	AC	7.6	5.1	7.6
	4×10^5	2.5	ATB	–	–	5.1
	2×10^5	5	CTB	–	12.7	–
			AB	10.2	–	–
			Total	17.8	17.8	12.7
1×10^5	1×10^7	1	AC	10.2	7.6	7.6
	4×10^6	2.5	ATB	–	–	14.0
	2×10^6	5	CTB	–	15.2	–
			AB	21.6	–	–
			ASB	–	10.2	–
			Total	31.8	33.0	21.6
1×10^6	1×10^8	1	AC	12.7	12.7	7.6
	4×10^7	2.5	ATB	–	–	29.2
	2×10^7	5	CTB	–	15.2	–
			AB	45.8	–	–
			ASB	–	30.5	–
			Total	58.4	58.4	36.8

Notes: 1 cm = 0.394 in.
$a_1 = 0.44$ for AC; $a_2 = 0.30$ for ATB; $a_2 = 0.20$ for CTB; $a_2 = 0.14$ for AB; $a_3 = 0.11$ for ASB.

Table 9. Design slab thicknesses in centimeters for a rigid pavement with a terminal serviceability index of 2.5.

Traffic Number	Modulus of Elasticity (6 Pa)	FS[a] = 2.8 MPa[b]			FS[a] = 4.8 MPa[b]			FS[a] = 6.9 MPa[b]		
		SR[c] = 0.41 MPa	SR[c] = 0.69 MPa	SR[c] = 2.76 MPa	SR[c] = 0.41 MPa	SR[c] = 0.69 MPa	SR[c] = 2.76 MPa	SR[c] = 0.41 MPa	SR[c] = 0.69 MPa	SR[c] = 2.76 MPa
10^6	6.9	24.1	23.4	18.3	16.8	15.2	–[d]	21.2	10.2	–[d]
	29.0	25.7	25.2	23.4	19.1	18.3	15.5	14.5	14.0	10.4
	41.4	25.9	25.7	23.9	19.3	18.8	16.5	15.0	14.5	11.9
10^5	6.9	15.0	13.5	–[d]	9.4	–[d]	–[d]	–[d]	–[d]	–[d]
	29.0	17.3	16.8	13.7	11.9	11.2	–[d]	9.4	8.9	–[d]
	41.4	17.8	17.3	19.7	12.2	11.7	8.9	9.7	9.1	–[d]
10^4	6.9	7.9	–[d]	–[d]	–[d]	–[d]	–[d]	–[d]	–[d]	–[d]
	29.0	10.9	10.4	–[d]	7.9	7.1	–[d]	6.1	4.8	–[d]
	41.4	11.2	10.7	–[d]	8.1	7.6	–[d]	6.6	5.8	–[d]

Note: 1 cm = 0.394 in. 1 Pa = 0.000 145 lbf/in^2.
[a]FS = flexural strength. [b]Working stress = 75 percent of flexural strength. [c]SR = subgrade reaction. [d]Did not converge.

Table 10. Required concrete shoulder thickness with and without a 15.2-cm subbase.

Shoulder Traffic Number	Equivalent Main-Line Traffic Number	Truck Usage of Inside Edge of Shoulder (%)	Shoulder Slab Thickness (cm)	
			On Subgrade	On Subbase
1×10^4	1×10^6	1	7.6	–
	4×10^5	2.5		
	2×10^5	5		
1×10^5	1×10^7	1	12.7	–
	4×10^6	2.5		
	2×10^6	5		
1×10^6	1×10^8	1	19.1	15.2
	4×10^7	2.5		
	2×10^7	5		

Note: 1 cm = 0.394 in.

studied. The thickness of the asphalt concrete surface is fixed at 7.6 cm (3 in) for the conventional asphalt concrete shoulder section; the asphalt surface is fixed at 5.1 cm (2 in) for cement-treated base sections; cement-treated base thicknesses are fixed at 15.2 cm (6 in). The full-depth asphalt concrete sections had a surface course thickness of 7.6 cm (3 in). The calculated thickness of the remaining layers is determined by using the AASHO equation (17):

$$SN = a_1D_1 + a_2D_2 + a_3D_3 \quad (1)$$

where

a_1, a_2, and a_3 = layer coefficients and
D_1, D_2, and D_3 = layer thickness.

Examples of design thickness for flexible shoulders are given in Table 8 for a regional factor of 1.0, soil support of 3.0, and a P_t of 2.5. The material codes used in Table 8 are the same as those used in Table 1. Consider, for example, the results given in Table 8 for a main-line design traffic of 4×10^6 equivalent 80.1-kN (18-kip) axle loads and a 2.5 percent truck usage of the inside edge of the shoulder. For these design considerations, a 7.6-cm (3-in) asphalt concrete surfacing and 14-cm (5½-in) asphalt-treated base would be required. The theoretically equivalent aggregate and cement-treated base sections from the AASHO procedure (17) are also given in Table 8 and could be used as alternate designs. The 21.6-cm (8½-in) full-depth asphalt concrete shoulder section required for a main-line traffic of 4×10^6 axle loadings compares favorably with the shoulder designs now used by Illinois, North Dakota, Texas, and Louisiana that were gradually developed through field experience. For higher design traffic volumes, stronger shoulder sections than those currently used would be required, which is also illustrated by the data given in Table 8.

PCC Shoulder Design

The required design slab thickness obtained by using the AASHO rigid pavement equation (17) is given in Table 9 for the indicated range of variables and a terminal serviceability index of 2.5. The AASHO rigid pavement equation (17) was solved by using a computer. The concrete slab was assumed to be supported either directly on a subgrade having a Winkler modulus of 1661 kg/dm^3 (60 lb/in^3) or by a 15.2-cm (6-in) high-quality subbase with an overall effective Winkler modulus of 11 072 kg/dm^3 (400 lb/in^3).

Table 10 gives a summary of the required slab thickness by using the rigid equation with and without a 15.2-cm-thick (6-in-thick) high-quality subbase. From this table, a 19.1-cm-thick (7½-in-thick) slab is required when placed directly on the subgrade and a 15.2-cm-thick (6-in-thick) slab is required for a 15.2-cm (6-in) high-quality subbase for a main-line design traffic of 4×10^7 axle loadings and a shoulder encroachment of 2.5 percent. These theoretically required slab thicknesses are quite similar to sections currently used by many states as shown by the data given in Table 2. In Table 10, $P_t = 2.5$, modulus of elasticity of concrete = 29 GPa (4.2×10^6 lbf/in^2), and flexural concrete strength = 4.8 MPa (690 lbf/in^2).

DESIGN IMPLICATIONS

The field observations have shown that shoulder distress is primarily concentrated within approximately 61 cm (24 in) of the longitudinal pavement-shoulder joint. Longitudinal cracking of shoulders having relatively thin structural sections in areas of severe winters is likely to occur during the first winter that traffic is on the pavement. For similar shoulders constructed in the fall and left untrafficked through the first winter, little or no cracking develops. Furthermore, the distribution of truck traffic found to encroach on the shoulder very closely coincides with the usual location of primary shoulder cracking. These findings indicate that a significant part of the structural damage occurring near the longitudinal joint is the result of the application of heavy truck traffic to the edge of the shoulder. In general, cracking of the outer two-thirds of the shoulder is not a significant problem. Premature cracking in the vicinity of the outside edge of the shoulder for asphalt concrete surface thicknesses less than about 5.1 cm (2 in) in several instances is found to be the result of the surface thickness being significantly less than the specified value.

SHOULDER DESIGN PROCEDURE

The shoulder in the vicinity of the longitudinal joint should be structurally designed to carry the anticipated truck traffic. Little information is currently available on the actual usage by truck traffic of the shoulder in the vicinity of the longitudinal joint. The California Department of Transportation currently uses 1 percent of the main-line traffic for shoulder design. This study indicates, however, that, for at least rural Interstate pavements in the Southeast, truck encroachment on the shoulder due to wandering is about 2.4 percent. The mean distance of encroachment is about 17.8 cm (7 in), and almost all of the encroachments are within approximately 61 cm (24 in) of the pavement edge. In the absence of more reliable usage data, shoulders in rural areas with free-flowing traffic characteristics should probably be designed for at least 2 to 2.5 percent of the main-line truck traffic. No data were collected for truck encroachments in heavily congested urban areas.

Use of the AASHO equations (17) and 2.5 percent truck encroachment is found to give realistic structural shoulder sections based on observed field performance for both flexible and rigid pavements. The AASHO equations (17) are used in this study for illustration only; other suitable design methods could be used, depending on established practice and experience. Design methods developed for the main line, however, should only be used until suitable procedures are available for the shoulder.

When 2 to 2.5 percent of the main-line truck traffic is encroaching on the shoulder, the AASHO equations (17) show that many currently used asphalt concrete shoulder sections are underdesigned in the vicinity of the longitudinal pavement-shoulder joint. Use of full-depth asphalt concrete and PCC shoulder sections has greatly reduced distress near the longitudinal joint. These sections generally satisfy or almost satisfy the theoretically required structural numbers given by the AASHO equations (17). These theoretical results help to at least partially explain the good performance of portland cement and full-depth asphalt concrete shoulders and the relatively poor performance of weaker conventional or cement-stabilized shoulder sections.

After studying these results, we recommend that the structural shoulder section be designed for the expected amount of truck traffic due to encroachment by using currently accepted design methods. In general, construction of shoulders with sufficient structural strength to carry the expected traffic should greatly reduce the amount of distress currently experienced at the longitudinal joint. Problems with excessive water, shoulder settlements, expansive clay subgrades and frost-susceptible bases, subbases, or subgrades should be provided for separately.

Because virtually all truck encroachment apparently occurs within 61 cm (24 in) of the longitudinal joint, the potential exists for significant savings in construction costs if a shoulder design having a variable structural strength is used. Tapered sections or special, variable strength structural shoulder designs can be used to strengthen the shoulder in the critical area of heavy loading.

SUMMARY

The longitudinal pavement-shoulder joint problem is complex and the cause of a considerable amount of shoulder distress. The severity of deterioration of the shoulder in the vicinity of the longitudinal joint appears to be significantly influenced by a number of factors including the following: (a) the strength and type of the structural shoulder section, (b) traffic use of the shoulder, (c) environmental factors, (d) subgrade conditions, and, in some instances, (e) the design features of the main-line pavement.

Most of the distress is located within approximately 61 cm (24 in) of the joint and appears to be directly related to the encroachment of heavy truck traffic on the shoulder. The most important measure to minimize the observed distress is to structurally design the shoulder in the vicinity of the joint by using currently available design methods (for main-line traffic) to carry the truck traffic expected to encroach on the shoulder. In the absence of more reliable data, shoulders in rural areas with free-flowing traffic characteristics should probably be designed for at least 2 to 2.5 percent of main-line truck traffic. Additional investigations are necessary to determine design values of truck encroachment for other conditions. Further, additional work is required in the development of pavement design procedures for shoulders. Until then, procedures developed for main-line pavements, such as the AASHO equations (17), or other suitable methods should be used.

ACKNOWLEDGMENTS

This paper represents a portion of a study undertaken as a part of the National Cooperative Highway Research Program. This paper has not been reviewed by any of the sponsoring agencies and does not necessarily represent their viewpoints. Practicing engineers and researchers too numerous to acknowledge individually have contributed greatly to various aspects of the project.

REFERENCES

1. M. L. O'Toole. Highway Shoulders: Their Construction and Maintenance Problems. Proc., 58th Michigan Highway Conference, 1973, pp. 38-43.
2. Current Practices in Shoulder Design, Construction, Maintenance and Operation. HRB, Highway Research Circular 142, April 1973, 15 pp.
3. D. C. Spellman, J. R. Stoker, and B. F. Neal. Faulting of Portland Cement Concrete Pavements. Materials and Research Department, California Division of Highways, Research Rept. 635167-2, Jan. 1972, 22 pp.
4. W. Gulden. Pavement Faulting Study, Extent and Severity of Pavement Faulting in Georgia. Office of Materials and Tests, Georgia Department of Transportation, GHD Research Project 7104, Aug. 1972, 83 pp.
5. E. C. Novak, Jr. Study of Frost Action in Class AA Shoulders Near Pontiac. Michigan Department of State Highways, Research Rept. 671, April 1968.
6. Paved Shoulder Problems on Stevenson Expressway. Illinois Division of Highways, Research and Development Rept. 19, July 1967, 22 pp.
7. L. J. McKenzie. Experimental Paved Shoulders on Frost Susceptible Soils. Illinois Division of Highways, Research and Development Rept. 24, Dec. 1969, 51 pp.
8. Improved Pavement-Shoulder Joint Design. NCHRP, Project 14-3.
9. L. J. McKenzie. Experimental Paved Shoulders on Frost Susceptible Soils. Illinois Department of Transportation, Research and Development Rept. 39, March 1972, 77 pp.
10. C. J. Arnold and M. A. Chinati. Experimental Concrete and Bituminous Shoulder Construction Report. Michigan Department of State Highways, Research Rept. R-844, Jan. 1973, 12 pp.
11. E. C. Lokken. What We Have Learned to Date From Experimental Concrete Shoulder Projects. HRB, Highway Research Record 434, 1973, pp. 43-53.
12. Concrete Shoulders: Performance Construction Design Details. American Concrete Paving Association, Oak Brook, Ill., Technical Bulletin 12, 1972, 33 pp.
13. Portland Cement Concrete Shoulders. Illinois Division of Highways, Research and Development Rept. 27, July 1970, 31 pp.
14. Portland Cement Concrete Shoulders. Federal Highway Administration, Notice N 5040, June 5, 1974, 2 pp.
15. D. K. Emery, Jr. Transverse Lane Placement for Design Tracks on Rural Freeways. Office of Road Design, Georgia Department of Transportation, preliminary rept., 1974.
16. Highway Design Manual. California Division of Highways, 1972.
17. Interim Guide for Design of Pavement Structures. AASHO, Washington, D.C., 1972, 125 pp.

State-of-the-Art Review of Paved Shoulders

Josette M. Portigo, Michigan Department of State Highways and Transportation

Paving shoulders of highways was begun by state highway agencies to eliminate maintenance and safety problems brought about by increasing traffic densities and axle loads. Not all states have established policies concerning the paving of shoulders. In many, the decision to pave the shoulder is still made on an individual project basis and depends on engineering judgment, past experience, and availability of funds. Because paving highway shoulders is a relatively new practice, state agencies have not had sufficient time to accumulate data for cost-benefit analyses on which to base the justification for paving shoulders. The paved shoulder has not solved all maintenance and safety problems and has even generated several. In addition, it requires a higher initial investment than that required for an unpaved shoulder and is therefore not economically feasible for low-volume highways. Nevertheless, it has gained the general acceptance of both highway engineers and motorists. This report discusses all aspects of shoulder paving and presents methods used by state highway agencies to cope with all types of problems that they encounter in paving shoulders in their highway systems.

The term "paved shoulder" applies to any one of a wide range of all-weather highway shoulders including bituminous surface-treated shoulders, bituminous mats on stabilized gravel base, full-depth asphalt shoulders, and portland cement concrete (PCC) shoulders. They are constructed adjacent to main-line pavements of equal or better type. Unless specified otherwise, the term "shoulder," in this paper refers to the shoulder to the right of the traffic lane.

Except on Interstate and federal-aid routes where shoulder requirements are specified, the decision on whether a shoulder should be paved and what type of pavement to be used is, in most cases, the result of balancing engineering judgment and maintenance and accident experience on existing shoulders against economic considerations. Engineering judgment includes considerations of wheel load estimates for shoulder design, effect of types of shoulders on plans for future widening or upgrading and on traffic and maintenance operations, and intangible benefits derived from paving the shoulder.

This report summarizes available information on paved shoulders is based on a review of existing literature. It does not in any way attempt to offer solutions to the problems associated with paved shoulders. It does present different ways in which state highway agencies and other concerned groups have tried to cope with these problems. It is hoped that a knowledge of what has been done and what is being done can serve as a guide to future studies and investigations needed to better understand paved shoulders and to improve their performance.

DEFINITION, FUNCTIONS, AND REQUIREMENTS OF PAVED SHOULDERS

Definition

The American Association of State Highway Officials (AASHO) (1), which is now the American Association of State Highway and Transportation Officials (AASHTO), defines the shoulder as

> the portion of the roadway contiguous with the traveled way for the accommodation of stopped vehicles, for emergency use, and for lateral support of base and surface courses. It varies in width from only about 2 ft or so on minor rural roads, where there is no surfacing or the surfacing is applied over the entire roadbed, to about 12 ft on major roads, where the entire shoulder may be stabilized or have an all-weather surface treatment.

The all-weather surface treatment may consist of a bituminous surface treatment with a minimum thickness of about 2.54 cm (1 in) or a bituminous mat over a stabilized gravel base. The entire shoulder structure may be either an extension or a variant of the main-line paving as are full-depth asphalt shoulders, PCC shoulders, and shoulder areas in full-width paving.

Publication of this paper sponsored by Committee on Shoulder Design.

Functions

The conventional functions of the paved shoulder embodied in the AASHO definition of shoulders are as follows:

1. Accommodation of vehicles for emergency or other use and
2. Lateral support of base and surface courses.

A vehicle stopped on a travel lane for any reason forces moving vehicles to merge into fewer lanes at lower speeds. By providing refuge for stopped vehicles, a paved shoulder helps to maintain the capacity of a highway (2). Studies conducted by Billion (3), Bellis (4), and Bergsman and Shufflebarger (5) identified the reasons for, and frequency of, shoulder occupancy by motorists on urban and rural freeways. Reasons for emergency stops, occurring once per approximately 1900 vehicle-km (1200 vehicle-miles), included tire changing, vehicle checking, running out of gas, and overheating. Leisure or convenience stops, making up three-fourths of the total stops, were made for resting and eating, caring for children and pets, and obtaining bearings. Moskowitz and Schaefer (6) observed that a vehicle leaving the roadway has a good chance of avoiding an accident if sufficient maneuvering room is available. A paved shoulder also serves as a detour for traffic during maintenance or construction operations or after an accident while main lanes are being cleared. Bergsman and Shufflebarger (5) ascribe 6 to 8 percent of the total use of shoulders to accidents.

At the Western Association of State Highway Officials road test conducted in Malad, Idaho, from 1952 to 1954, it was found that, without a paved shoulder, the outer wheel paths of a pavement structure were inferior to the inner wheel paths in their ability to support test loads (7, pp. 203-204). With paved shoulders providing support to the pavement structure, the conditions of interior loading always apply. Treybig, Hudson, and Abou-Ayyash (8) showed in their study with concrete shoulders constructed integrally with the pavement that the maximum deflection caused by an 80.1-kN (18-kip) load about 0.3 m (1 ft) from the edge of an 18 or 20-cm (7 or 8-in) continuously reinforced concrete pavement slab without concrete shoulders was about twice that in the same slab with concrete shoulders.

Other conventional functions of paved shoulders not explicitly embodied in the AASHO definition given at the beginning of this section are

1. Facilitation of water removal from the main-line pavement,
2. Aesthetic value as an aid to driver comfort and freedom from fatigue,
3. Provision of bicycle routes (Hawaii and Michigan are paving some of the shoulders on their primary and secondary systems to accommodate bicycle traffic), and
4. Provision of space for routing traffic during construction and operating space for maintenance equipment.

Innovative uses of paved shoulders, devised in recent years and aimed primarily at increasing travel lane capacity, are as follows (9):

1. Provision of room for slower vehicles to permit passing maneuvers,
2. Extra lane for added capacity during peak periods, and
3. Widening of existing two-lane highways by overlaying travel lanes and both shoulders and remarking with solid double centerline to provide an undivided four-lane highway ("poor-boy design" now in use in Texas).

Requirements

For a paved shoulder to perform its functions as defined, it must meet certain requirements.

1. It must be stable in all kinds of weather to withstand (a) the standing load of a disabled or otherwise stopped vehicle or of maintenance equipment, (b) occasional traffic when the shoulder is used for detours or during maintenance operations, (c) through traffic when the shoulder is used as an extra lane for peak periods in states where this is not prohibited, and (d) the tearing effect caused by a vehicle that leaves the highway at high speed, when a motorist suddenly applies the brakes or attempts to change the direction of the vehicle (10).
2. It must be wide enough to accommodate parked vehicles. Objects on the shoulder that leave a clearance of 0.9 m (3 ft) or less from the pavement edge have been established to constitute a hazard.
3. It must be in such condition that a motorist can safely leave the travel lane at high speed when necessary to avoid or lessen the severity of an accident. This condition further requires the paved shoulder to be (a) continuous (intermittent turnouts at some facilities do not provide the distance needed for decelerating or reentering the traffic stream quickly and safely), (b) flush with the pavement edge [Brittenham, Glancy, and Karrer (11) found shoulder heights uneven with the edge of pavement because of settlement or heave of the shoulder structure at nearly three-fourths of all the accident locations they studied], (c) sloped sufficiently to drain surface water across but not sloped too steeply to constitute a hazard or create driver fear of rolling off, (d) free of ruts and potholes, and (e) skidproof.
4. The paved shoulder must be easy to maintain. Shoulder maintenance requires workers and machines to be working close to traffic, and, in spite of all precautions taken, this is a constant source of danger to the workers as well as to the traveling public passing them.

TYPES OF PAVED SHOULDERS

There are five general types of paved shoulders.

1. The bituminous surface-treated shoulder consists of a gravel shoulder on which coats of liquid bituminous material have been applied; surface mat thickness is at least 2.54 cm (1 in). Regional terminology such as armor coat, inverted penetration, multiple (double or triple) surface treatments, and seal coats all apply to bituminous surface treatments (12).
2. The bituminous aggregate shoulder is usually constructed adjacent to a flexible or a rigid main-line pavement. This shoulder consists of a bituminous mat on top of a gravel base course of variable depth that may or may not be stabilized with a bituminous mixture.
3. For the full-depth asphalt shoulder, asphalt mixtures are employed for all courses and are laid directly above the prepared subgrade (13). It is intended for construction adjacent to better quality roadways that are either flexible or rigid.
4. Shoulder areas of asphalt highways paved full width are built integrally with the pavement; subbase, base, and surface layers are placed across the entire section ditch to ditch. They are not to be confused with conventional shoulders of highways in which an overlay from shoulder edge to shoulder edge gives the surface

the appearance of full-width paving.

5. The PCC shoulder consists of a variable-depth PCC slab placed on a stabilized base or a prepared subgrade. A PCC shoulder can be constructed integrally with the main-line pavement or can be placed after the main-line pavement has hardened. It may be conventionally reinforced, continuously reinforced, or nonreinforced and be with or without tie bars. The PCC shoulder is no longer considered experimental by the Federal Highway Administration (FHWA) as of June 1974.

POLICIES CONCERNING PAVED SHOULDERS

An examination of the responses of state highway agencies to queries sent them concerning their current shoulder policies indicates that

1. Fifteen states have documented policies,
2. Twenty-eight states have no separate policies but have shoulder paving standards (six of these states prefer to make judgment decisions on paving after evaluation of the individual project), and
3. Five states pave shoulders integrally with the main-line pavement.

Whether there is a written policy or not, decisions concerning paved shoulders for new construction are shown, in the responses, to be based on one or on a combination of the following: (a) type of main-line pavement, which is often a function of classification; (b) traffic volumes [average daily traffic (ADT)], vehicles per day, daily hourly volume (DHV), or percentage of commercial vehicles; (c) engineering judgment and overall experience gained from previous construction of a similar type of facility; and (d) availability of funds.

Upgrading existing shoulders by paving involves maintenance and safety experiences, engineering judgment, and availability of funds.

Shoulder paving practices, based on 47 of the responses received for this report, are as follows: 23 states pave all shoulders; 5 states pave according to classification (for example, class 3 and higher freeways and class 1 freeway and expressway facilities); 8 states pave according to traffic volume (2 states use percentage of commercial vehicles as a basis); 6 states pave primary and major highways; and 5 states pave major highways and selected locations. This distribution agrees with that of Heimbach and Vick (14).

The Missouri State Highway Department has developed a set of criteria for paved shoulder types from implementation of a shoulder study by using relative cost and performance of a variety of shoulder designs to determine optimum shoulder designs for a given traffic intensity at particular locations in Missouri (15). The North Carolina Department of Transportation and Highway Safety has completed a study of cost effectiveness of paved shoulders for establishing priority warrants (16). This study concludes that a range of paved shoulder construction costs can be economically justified on the basis of accident cost reductions for two-lane, two-way rural primary highways with ADT volumes of 2000 to 15 000.

SHOULDER DESIGN

Like its main-line counterpart, a shoulder pavement needs to satisfy certain geometric, drainage, and structural requirements. AASHTO policy publications present a comprehensive treatment of design standards for highway shoulders; therefore, only a brief review will be presented here.

Geometric Design Elements

The widths of usable shoulders given here are prescribed by AASHO (1, 48).

For two-lane rural highways with ADT less than 250, desirable width of usable shoulder is 1.8 m (6 ft) [minimum 1.2 m (4 ft)]. For DHV over 400, desirable width is 3.6 m (12 ft) [minimum 3 m (10 ft)]. A reduction of 0.3 or 0.6 m (1 or 2 ft) in difficult terrain is allowed if the normal shoulder width is 1.8 m (6 ft) or more so that the minimum, regardless of terrain, is 1.2 m (4 ft).

For divided highways, the width of usable outside shoulder is 3 m (10 ft) [minimum 2.4 m (8 ft)]. Where truck combinations are high and grading costs are low, 3.4 to 3.6 m (11 to 12 ft) may be considered. On divided highways with three or more lanes in each direction, a full-width median shoulder of 2.4 to 3 m (8 to 10 ft) is desirable to give the driver in distress in the lane nearest the median a place of refuge.

Shoulders must be continuous not only on pavement sections but also across structures.

A cross slope of 4.2 cm/m (½ in/ft) is used by most states; 3.1 or 6.2 cm/m (⅜ or ¾ in/ft) is not uncommon; and occasionally a slope of 8.3 cm/m (1 in/ft) is used. The lower the shoulder type is, the greater the slope will be.

The desirability of providing contrast between the pavement and the shoulder and the methods and problems of achieving the contrast are discussed in the section on field performance.

Design of Drainage

Drainage of surface water from the main-line pavement to the ditch is generally accomplished by providing the shoulder with an impermeable surface combined with the right amount of cross slope. However, excess water may accumulate beneath the surface of the main-line pavement not only by infiltration from the top but also from other conditions such as capillary moisture, trenched pavement design, and hydrogenesis (water formation mechanism). Reducing the accumulation of excess moisture under the surface of the shoulder by design takes three forms. The first is using a granular subbase or equivalent plane layer of sufficient thickness across the full shoulder width to the in slope to interrupt capillary action. The thickness of the interrupting layer varies from 8 to 63 cm (3 to 25 in).

The second method is improving shoulder foundation design to eliminate conditions conducive to swelling, heave, volume change, and settlement. Brakey (17), in reporting on bumps and swells on roads built over shales in dry, rainless regions, believes that conditions of hydrogenesis are present in road subbases in those areas. Colorado's answer to hydrogenesis is the use of full-depth asphalt that is impermeable to air or the use of an impervious asphalt membrane directly on top of the subgrade and underneath a 5-cm (2-in) sand layer. Wyoming uses a 5-cm (2-in) sand blanket on top of an asphalt membrane.

The third method is providing supplementary subsurface drainage. Virginia designs pavement edge drains under the shoulders at low points of vertical curves. Arkansas provides aggregate outlet trenches from outside the shoulder edge at 61-m (200-ft) minimum intervals. Many states used underdrains for both edges of the pavement but provided no details on their use.

Structural Requirements

Two primary considerations used to determine structural requirements are the expected loading and the supporting ability of the subgrade. An additional consideration for the paved shoulder is the percentage of travel lane loading estimated to use the shoulder. As of 1973, only California and Iowa had a design load criterion for paved shoulders. The California Department of Transportation bases its shoulder design on 1 percent of the wheel loads in the adjacent lane with no traffic index less than 5.0. Iowa designs its shoulders on the assumption that the paved strip must carry the heaviest wheel load (18). States that pave full width have their road shoulders built to 100 percent the structural strength of their main-line pavements. In most other states, the general idea is to build higher type of shoulders for higher type of cross sections or systems or higher ADT roads; the shoulders are designed for lighter or fewer wheel loads than those anticipated on the corresponding main-line pavement.

Current structural designs of paved shoulders consist mainly of type and thickness of surface and base. Bituminous mats vary from 4.4 cm (1¾ in) thick to more than 13 cm (5 in) thick in some states and up to 23 cm (9 in) thick in others. Base courses, 15 cm (6 in) or more in thickness, are plant-mixed bituminous base, calcium chloride stabilized based, or dense-graded aggregate base. If a subbase is provided, the purpose is invariably to improve subsurface drainage. Availability of aggregates and climatic conditions have been suggested as factors influencing variations in relative thickness of surfacing and base course of bituminous shoulders (19, p. 100).

The thickness of PCC shoulders found in current designs varies from 20 or 23 cm (8 or 9 in) uniform or tapering from pavement thickness at the inside edge to 15 cm (6 in) at the outer edge. The need for reinforcement in PCC slabs for shoulders has not been established. The Illinois study showed that a 15-cm (6-in) thickness of plain concrete is adequate with 0.8-m (30-in) tiebars spaced 0.8 m (30 in) on centers. The need for tie bars between the shoulder and main-line pavement slabs has not been established. It has also been shown that joint keys can be omitted. The Illinois concrete shoulder study also indicated that fairly close spacing [6 m (20 ft)] of transverse joints is desirable (20).

In an FHWA Notice of June 5, 1974, in which state highway agencies were notified that construction of PCC shoulders adjacent to PCC main-line pavements is no longer experimental, the FHWA laid out design criteria for PCC shoulders concerning slab thickness, base course, joint requirements, reinforcement, and corrugations.

SHOULDER CONSTRUCTION

Standard procedures for the construction of paved shoulders are essentially similar to those for their main-line pavement counterparts; therefore, no more than an occasional reference to either will be made here. The construction of paved shoulders has, in fact, brought out the ingenuity and creativity of engineers and contractors faced with a task for which their standard equipment was suddenly not suitable. The contractor who built the first PCC shoulders in Illinois (the first in the country) in 1965 used an extruder or slip-form paver made in his shop. He also had to devise a float from a 9-m (3-ft) strip of corrugated metal to form the shoulder corrugations and a rig to drill the tie bars into the old concrete (21, 22).

Currently available slip-form paving equipment can be used with either transit-mixed or central-mixed concrete. These pavers can control line and grade electronically, place tie bars to the edge of existing slabs with self-drilling or nondrilling expansion anchors, and lay 12.5 m (41 ft) of paving [(1.5 m (5 ft) for left shoulder, 7.6 m (25 ft) for main line, and 3.3 m (11 ft) for right shoulder] in a single pass. Corrugations are formed by a separate power-driven corrugated roller (23). Asphalt paving contractors have recently devised procedures for grooving 7.6-cm-thick (3-in-thick) asphalt shoulders to create a rumble effect (24).

Most of the states queried expressed no serious problems encountered in the construction of paved shoulders. Those that did have problems indicated the following: (a) difficulty in attaining proper compaction in the shoulder area closest to the main-line pavement; (b) softening of the shoulder subgrade because of exposure to rain and to joint-cutting water; (c) possible relationship between sequencing of shoulder paving and shoulder settlement; and (d) separation at longitudinal joint between PCC pavement and bituminous shoulder.

Inadequate compaction in the area adjacent to the main-line pavement has been identified as a prime cause for the settling of shoulders and of pavement edge failures. Part of the problem is believed to be the inability of equipment to get close enough to the pavement edge to properly compact that area of the shoulder.

Michigan, experimenting with the use of sawed-sealed longitudinal joints between PCC pavements and bituminous shoulders as a means of reducing shoulder surface cracking, found that seal-treated interface joints did not completely prevent longitudinal shoulder cracking although they at least temporarily reduced the total cracking in that project (25). Michigan no longer seals joints of this type. The Pennsylvania Department of Transportation has also eliminated mechanical grooving and sealing between its roadway pavement and shoulder (26). Problems of longitudinal joints are treated in detail elsewhere (49).

FIELD PERFORMANCE

The decision to pave a shoulder, or the choice of shoulder paving, is justifiable on the basis of field performance as evidenced by smoother traffic operations, greater safety, and lower maintenance.

Traffic Operations

Paved shoulders have been demonstrated to affect traffic operations in certain ways.

1. They improve lateral placement of vehicles on the main-line pavement by increasing the "effective width" of the pavement. In a speed-placement study, Taragin found in 1945 (27) that bituminous shoulders at least 1.2 m (4 ft) wide adjacent to 5.5 to 6.1-m (18 to 20-ft) surfaces improved the lateral placement of free-moving vehicles to a greater extent than was obtainable by increasing the surface width to 6.1 to 6.7 m (20 to 22 ft) respectively.
2. They ease driver tension by giving the driver a sense of openness and an ensurance of space for emergency maneuvers. (This is closely connected to item 1 although it is not so easily quantifiable.)
3. They maintain highway capacity by providing an area for stopped vehicles.
4. They increase highway capacity in those parts of the country where the paved shoulder serves as a courtesy lane for slower moving traffic to allow faster moving vehicles to pass or as an auxiliary lane during peak periods.
5. They obtain more uniform traffic speed by allow-

ing motorists to leave the traffic lane at higher rates of speed so that following vehicles do not have to slow down considerably.

Despite the operational advantages gained by paving the shoulders, two kinds of problems have been identified. The first is the tendency of vehicles to encroach on a paved shoulder or to use the paved shoulder as a travel or turning lane. Clearly, this is a problem only on facilities or in states where the use of the shoulder for travel is prohibited or discouraged. This prohibition exists because the shoulder has not been designed to support the same intensity of load as has the main-line pavement. It has, furthermore, been argued that, if the shoulder is intended to serve as a refuge for stopped vehicles, then allowing travel on the shoulder creates a hazard for both traveling and stopped vehicles. The second problem is differentiating the shoulder from the travel lanes. Both problems take on significant dimensions only where paved shoulders are reserved for conventional uses. District engineers admit that much shoulder encroachment is random, is not done on purpose, and is attributed to an increased sense of security afforded by a paved shoulder to a motorist who feels secure enough to drive close to the edge of the travel lane and to occasionally ride on the shoulder area. Except for the Williston study of edge striping in Connecticut (28), most of the shoulder delineation studies have been conducted in the western portion of the country (29, 30, 31, 32, 33). Findings have indicated that less shoulder encroachment was observed when the shoulder was differentiated from the travel lane by contrast in surface appearance, texture, or slope.

Shoulder delineation has been accomplished in many different ways for various shoulder materials and lane materials. (A few of the methods covered in this section were used in connection with delineation studies, but whether they were implemented in later projects is not known.)

Methods When Travel Lane and Shoulder Are of PCC

1. Provide a color difference between travel lane and shoulder (23, 34). A bituminous overlay for the shoulder area also provides effective visual delineation.
2. Paint a 10 to 15-cm (4 to 6-in) continuous stripe on the edge of the pavement either alone or in combination with corrugations, or paint stripes on the corrugated area (35).
3. Use raised markers (a problem in snow-removal areas).
4. Use corrugations.
5. Use burlap drags, shallow corrugations, metal lath impressions, raised ceramic squares, red precast concrete, or ceramic tile jiggle bars, all of which have been tried or used in Texas (36, 37).

Methods When Travel Lane and Shoulder Are of Bituminous Surface

1. Use pavement edge stripes as required for Interstate projects.
2. Use different-colored cover aggregates (usually lighter colored) on the shoulder area. Experiences with this method have not been encouraging; contrast fades with time when cover aggregates are sloughed off or compacted into the bituminous layer.

Methods When Travel Lane and Shoulder are of Different Surfaces

1. Take advantage of built-in delineation when a bituminous shoulder adjoins a PCC pavement. Iowa deepens the contrast by spraying liquid asphalt on the aggregate cover. Chip seals are sometimes used to further increase demarcation.
2. Use pavement edge lines.

Other Methods

1. Render shoulder slope uncomfortable for use in traveling but safe for emergency use (38).
2. Paint diagonal stripes on the shoulder area.
3. Use signs that convey the message not to travel on shoulder. There is no general agreement on the usefulness of these signs by themselves, although they may be used to reinforce other methods.
4. Pave only a 0.6 to 1.2-m-wide (2 to 4-ft-wide) strip adjacent to the pavement and leave the rest of the shoulder as 1.8 to 3 m (6 to 10 ft) of stabilized gravel of adequate strength. The strip will take care of the lateral support function and occasional encroachment, and the gravel area will discourage travel. A main objection to this method is the expense of maintaining both a paved and a gravel surface.

Safety

Safety studies found in the literature relating to shoulders are mainly concerned with the effect, if any, of the width of the shoulder, paved or unpaved, on accident frequency. These studies, conducted by Raff (39), Belmont (40, 41), Head and Kaestner (42), Stohner (43), Billion and Stohner (44), Blensly and Head (45), and Brittenham, Glancy, and Karrer (11), covered a variety of possible accident factors such as design features, traffic volumes, types of shoulders, widths, cross sections, alignment, and bridge approach widths. The findings obtained to determine the relationship between accident experience and shoulder characteristics have not been consistent. One of the conclusions brought out by Heimbach and Vick (14) is that the effect of paved shoulders on accident experience and traffic operations can only be correctly determined when all other roadway and traffic characteristics are examined at the same time.

Responses by state highway agencies to queries concerning the safety of paved shoulders showed general agreement where paved shoulders are compared with gravel, turf, earth, or surface-treated shoulders. No numerical data were received except from the Louisiana Department of Highways, which had conducted an informal accident survey and came out with the following accident figures: 0.22, 0.77, and 1.47 accidents/million vehicle-km (0.36, 1.24, and 2.37 accidents/million vehicle-miles) for asphalt, gravel and shell, and grass shoulders respectively. The following general comments were offered by state highway agencies: Vehicles are reluctant to leave the paved surface and park on a grass shoulder; some head-on collisions have been avoided; additional room is available for overly wide loads to maneuver without cutting ruts along the slab edge; drainage carried completely across the top of the roadway to the in slope has lengthened pavement life and has done away with accidents caused by vehicles dropping off onto a soft shoulder; flow of travel is now smoother; traffic does not seem to follow as close to the painted centerline stripe; accident rates have been lowered; vehicular control is superior to that on a stone surface; driver fatigue and necessity for maintenance forces in the roadway area have been reduced; driver

fear of steering near the travel lane edge has been eliminated; greater separation of opposing traffic flow is now possible; accident potential of exposed shoulder edges has been reduced.

Maintenance

Paved shoulders are the latest in a series of attempts to build an improved shoulder that would eliminate the maintenance problems existing for previous types of shoulders and provide for future increases in traffic volume and axle load. Thus technology has progressed from earth shoulders, to turf or sod shoulders, to gravel or stone shoulders, to surface-treated or bituminous sealed shoulders, and finally to bituminous or PCC paved shoulders. With the high degree of maintenance required for unpaved shoulders, it is not surprising that highway engineers would look to shoulder paving for relief. The fact is, however, that, although paved shoulders have eliminated soft shoulders, blading, reshaping, and replacement of shoulder materials, a new set of operational problems and maintenance problems have moved in, namely, settlement, heaving, cracking, and separation at the longitudinal joint.

From the maintenance point of view, two types of paved shoulders are performing well enough to justify their construction. These are the PCC shoulder adjacent to PCC pavement and the bituminous paved shoulder adjoining flexible pavement or built integrally with it. Included in the second are the "beefed-up" and full-depth asphalt shoulders.

Maintenance requirements on the bituminous shoulders previously mentioned are usually the same as those required for the main-line pavement so that both get the same amount of maintenance, which in some states is scheduled every 5 years.

PCC shoulders are practically maintenance-free. Full-width paving, characterized by the absence of longitudinal joints between the main-line pavement and the shoulder area, reduces the type of maintenance equipment needed and lessens the number of operations required (46). Full-width and full-depth construction is strongly recommended where future shifts of centerline may occur or additional lanes may be constructed. The need for shoulder removal and construction is eliminated at a critical time adjacent to intense traffic.

Problems Generated by Shoulder Paving

Longitudinal joint problems are encountered in bituminous shoulder adjoining PCC pavements. Separation of the shoulder from the pavement at the joint seems typical and is accompanied by vertical displacement, longitudinal cracks about 0.6 m (2 ft) from the pavement edge, and random cracks in the 0.6-m-wide (2-ft-wide) area. Michigan and Minnesota are experiencing these problems. The separation at the joint is followed by entry of water into the base and subgrade, loss of supporting power, deterioration of shoulder surfacing, settlement of the shoulder structure, and development of ridges and bumps. When these problems exist, shoulder paving can hardly be viewed as a maintenance advantage. New York and Minnesota have been investigating the causes of shoulder settlement and cracking (47), and an intensive study of pavement-shoulder joint design under the National Cooperative Highway Research Program is being conducted (49).

Slope erosion is a minor problem occurring on the area where the shoulder meets the in slope. It is due to the increased runoff from both pavement and paved shoulder. If the sod is not maintained in that area, that portion is eroded away after a few heavy downpours. To minimize this problem, Iowa includes a rock fillet at the shoulder edge. Virginia solves this problem by placing a bituminous curb in a protected position under the guardrail to carry the surface water to a paved down drain. Illinois employs a drain of coarse aggregate similar to Iowa's rock fillet.

Vegetation growth is not a serious problem, although it is a chronic nuisance. It is more of a problem in the southern states where longer growing seasons prevail. Some states in the north and south have more problems than others because of the persistence of tougher types of weeds indigenous to their areas. Salt grass is a problem in the more arid parts of Nebraska. Success with this problem has been reported for many combinations of herbicides and modes of application.

Shoulder Upgrading

Because of the increased acceptance of paved shoulders, attention is being directed to the remaining thousands of kilometers of substandard shoulders, gravel, and seeded earth adjoining bituminous and PCC pavements. In the interest of safety, some states, such as New Hampshire, New York, and Michigan, have been upgrading shoulders on a statewide scale. Michigan has just started a program that will stabilize 686 km (426 miles) of substandard shoulders in the primary and secondary systems by using 77 to 136-kg (170 to 300-lb) bituminous mat. Most of the shoulders will be 0.9 m (3 ft) wide. About 97 km (60 miles) will be 2.4 m (8 ft) wide to accommodate bicycle traffic.

SUMMARY

Most states have well-defined policies concerning shoulder paving or have their policies embodied in their design standards and criteria. In general, paved shoulders are justified by

1. Smoother traffic operations. Effective width of the traveled pavement is increased. Uniform traffic speed is obtained. Highway capacity is maintained or increased.
2. Safer traffic operations. Space is provided for emergency maneuvers, vehicle check or repairs, and rest and breaks in long-distance driving. Driver tension is eased by a sense of openness, and driver fear of rolling off the pavement edge is eliminated, thus providing greater separation of opposing traffic flow. Because space is available for routing traffic during maintenance operations, safer working conditions for maintenance forces are possible.
3. Reduced maintenance requirement on shoulder and main-line pavement. Lateral support provided by the shoulder improves the condition and longevity of the main-line pavement. Surface runoff is drained across the shoulder. Continual regrading, reshaping, and replacement of shoulder material are eliminated.

Shoulder design of both bituminous and PCC shoulders is generally an extension or variation of the corresponding bituminous and PCC main-line pavement design, as practiced in the different states with reduced thicknesses for the component courses in the shoulder pavement. Only California and Iowa have criteria for shoulder structural strength. Judgment and past experience with similar types of shoulders enter heavily into shoulder design practices. Geometrics are all guided by AASHTO policy.

Field performance of well-designed paved shoulders has been demonstrated to be generally better than that of unpaved shoulders. Although there have not been

enough recorded data to substantiate claims that a highway with paved shoulders is safer than one with unpaved shoulders, the elements that differentiate the paved from the unpaved can be identified as contributing to greater highway safety. Separation of the bituminous shoulder from the PCC main-line pavement at the longitudinal joint and the attendant shoulder cracking and distress still represent the most troublesome aspect of shoulder paving at the present time.

RECOMMENDED RESEARCH

Both the literature and current practices on paved shoulders have shown the need for study and investigation to arrive at

1. A more or less uniform set of loading criteria for different types of paved shoulders.
2. Comprehensive methods of maintenance accounting that will yield data for a complete maintenance history for a given section with a given type of shoulder.
3. A method of evaluating paved shoulder performance to include in either a pavement feedback system or a shoulder feedback system.
4. An evaluation of effects of various types of paved shoulders on the performance of main-line pavement types.
5. Determining the cause of the separation of bituminous shoulders from PCC main-line pavements.
6. Establishing the relation of paved shoulder to accidents.

CONCLUSION

Highway engineers have recognized the advantages of the paved shoulder, and motorists have responded favorably to it. Some states have already embarked on statewide programs of rehabilitating the shoulders that were built before the benefits of paved shoulders were recognized and accepted. A few states would recommend the paving of shoulders of high-traffic routes and selected locations but doubt that paving is economically feasible for the rest of their state highway networks. Shoulder paving has grown from an art to a technology, but it is still a young technology. There is much to learn and much to do in the years ahead.

ACKNOWLEDGMENT

The information in this paper was compiled by the Michigan Department of State Highways and Transportation in cooperation with the Federal Highway Administration, U.S. Department of Transportation, under contract DOT-FH-11-8194. The work described reflects the views of the author, who is responsible for the facts and the accuracy of the data presented herein. The contents do not necessarily reflect the official views or policies of the Federal Highway Administration.

REFERENCES

1. A Policy on Geometric Design of Rural Highways. AASHO, Washington, D.C., 1965.
2. Highway Capacity Manual—1965. HRB, Special Rept. 87, 1965.
3. C. E. Billion. Shoulder Occupancy on Rural Highways. Proc., HRB, Vol. 38, 1959, pp. 547-575.
4. W. R. Bellis. Shoulder Use. HRB, Bulletin 170, 1958, pp. 51-53.
5. S. E. Bergsman and C. L. Shufflebarger, Jr. Shoulder Use on an Urban Freeway. HRB, Highway Research Record 31, 1963, pp. 1-19.
6. K. Moskowitz and W. E. Schaefer. California Median Study: 1958. HRB, Bulletin 266, 1960, pp. 34-62.
7. The WASHO Road Test. HRB, Special Rept. 22, 1955.
8. H. J. Treybig, W. R. Hudson, and A. Abou-Ayyash. Application of Slab Analysis Methods to Rigid Pavement Problems. Center for Highway Research, Univ. of Texas at Austin, May 1972.
9. J. M. Portigo and G. D. Weaver. State-of-the-Art Review of Paved Shoulders. Paper presented at TRB Summer Meeting, Ann Arbor, Mich., Aug. 1975.
10. S. E. Ridge. Maintenance Costs of Highway Shoulders. HRB, Bulletin 151, 1957, pp. 20-21.
11. T. G. Brittenham, D. M. Glancy, and E. H. Karrer. A Method of Investigating Highway Traffic Accidents. HRB, Bulletin 161, 1957, pp. 30-47.
12. M. Herrin, C. R. Marek, and K. Majidzadeh. State of the Art: Surface Treatments. HRB, Special Rept. 96, 1968.
13. Thickness Design—Full-Depth Asphalt Pavement Structure for Highways and Streets. Asphalt Institute, College Park, Md., 8th Ed., 1969.
14. C. L. Heimbach and H. D. Vick. The Exploration of Economic, Safety, Maintenance and/or Operations on Paved Versus Unpaved Shoulders. North Carolina State Univ. at Raleigh, 1966.
15. L. T. Murray. Shoulder Maintenance Considerations in Missouri. Missouri State Highway Department, Jefferson City.
16. C. L. Heimbach, W. W. Hunter, C. G. Chao, and T. W. Griffin. Investigation of the Relative Cost-Effectiveness of Paved Shoulders on Various Types of Primary Highways in North Carolina for the Purpose of Establishing Priority Warrants. North Carolina State Univ. at Raleigh, 1972.
17. B. A. Brakey. Road Swells: Causes and Cures. Civil Engineering, American Society of Civil Engineers, New York, Dec. 1970, pp. 48-50.
18. H. K. Glidden. Asphalt Shoulder Methods for an Iowa Freeway. Roads and Streets, April 1965, pp. 74-75 and 140-145.
19. Proceedings: Mississippi Valley Conference. 1970.
20. Portland Cement Concrete Shoulders. Illinois Division of Highways, Springfield, 1970.
21. R. F. Nusbaum. Illinois Builds Concrete Shoulders. Roads and Streets, Feb. 1966, pp. 74-84.
22. R. L. Duncan. Illinois Builds Concrete Shoulders. Proc., 57th Annual Road School, Purdue Univ., Lafayette, Ind., 1971, pp. 123-126.
23. G. K. Ray, E. D. Lokken, and E. G. Robbins. Slipform Construction of Highway Appurtenances. Portland Cement Association, 1973.
24. J. A. Burton. Don't Drive on Me. Cook County Highway News, May 1974, p. 4.
25. C. A. Zapata. Evaluation of Sawed-Sealed Longitudinal Joints Between Bituminous Shoulders and Rigid Pavements as a Means of Reducing Longitudinal Shoulder Cracking. Michigan Department of State Highways and Transportation, Lansing, Research Rept. R-683, 1969.
26. Special Report on Paved Shoulders. Task Force 70-2, Pennsylvania Department of Transportation, Harrisburg, final rept., 1971.
27. A. Taragin. Effect of Roadway Width on Vehicle Operation. Public Roads, Vol. 24, No. 6, Oct.-Nov.-Dec. 1945, pp. 143-160.
28. R. M. Williston. Effect of Pavement Edge Markings on Operator Behavior. HRB, Bulletin 266, 1960, pp. 8-27.
29. W. E. Willey. Arizona's Dashed Shoulder Stripe.

Traffic Quarterly, Vol. 9, No. 2, April 1955, pp. 212-219.
30. A. Taragin. Driver Behavior as Related To Shoulder Type and Width on Two-Lane Highways. HRB, Bulletin 170, 1958, pp. 54-76.
31. N. H. Jorol. Lateral Vehicle Placement as Affected by Shoulder Design on Rural Idaho Highways. Proc., HRB, Vol. 41, 1962, pp. 415-432.
32. M. L. Kermit and T. C. Hein. Effect of Rumble Strips on Traffic Control and Driver Behavior. Proc., HRB, Vol. 41, 1962, pp. 469-482.
33. A. J. Schepp and D. R. Lamb. Shoulder Delineation Markings and Lateral Placement of Vehicles. Public Works, April 1965, pp. 118-120.
34. R. M. Callan. Colored Concrete Corrugated Shoulders. Highway Focus, U.S. Department of Transportation, Vol. 5, No. 1, April 1973, pp. 13-16.
35. R. Cahoon. Use of a Rumble Stripe to Reduce Maintenance and Increase Driving Safety. HRB, Special Rept. 107, 1960, pp. 89-98.
36. D. V. Purington. Safety Shoulders of Red Jiggle Bars Provide Haven for Disabled Vehicles on Bridge in Houston, Texas. Better Roads, June 1958, p. 23.
37. Roads Rumble for Safety's Sake. Engineering News Record, Sept. 15, 1966.
38. M. D. Shelby and P. R. Tutt. Vehicle Speed and Placement Survey. HRB, Bulletin 170, 1958, pp. 24-50.
39. M. S. Raff. Interstate Highway-Accident Study. HRB, Bulletin 74, 1953, pp. 18-45.
40. D. M. Belmont. Effect of Shoulder Width on Accidents on Two-Lane Tangents. HRB, Bulletin 91, 1954, pp. 29-32.
41. D. M. Belmont. Accidents Versus Width of Paved Shoulders on California Two-Lane Tangents—1951 and 1952. HRB, Bulletin 117, 1956, pp. 1-16.
42. J. A. Head and N. F. Kaestner. The Relationship Between Accident Data and the Width of Gravel Shoulders in Oregon. Proc., HRB, Vol. 35, 1956, pp. 558-576.
43. W. R. Stohner. Relation of Highway Accidents to Shoulder Width on Two-Lane Rural Highways in New York State. Proc., HRB, Vol. 35, 1956, pp. 500-504.
44. C. E. Billion and W. R. Stohner. A Detailed Study of Accidents as Related to Highway Shoulders in New York State. Proc., HRB, Vol. 36, 1957, pp. 497-508.
45. R. C. Blensly and J. A. Head. Statistical Determination of Effect of Paved Shoulder Width on Traffic Accident Frequency. HRB, Bulletin 240, 1960, pp. 1-23.
46. D. H. Hays. Shoulder Maintenance. Proc., 36th Annual Conference, Western Association of State Highway Officials, Texas, 1957, pp. 169-170.
47. W. P. Moody and E. J. Lange. The Evaluation of Shoulders in Four Counties. New York Department of Transportation, Albany, 1971.
48. Geometric Design Standards for Highways Other Than Freeways. AASHO, Washington, D.C., 1965.
49. Improved Pavement-Shoulder Joint Design. NCHRP, Research Project 14-3.